

Suspended Sediment, Water Quality, and Hydrodynamics of the Petitcodiac River Estuary, New Brunswick (2002 – 2003)

K.J. Curran, T.G. Milligan, G. Bugden, B. Law, and M. Scotney

Science Branch, Maritimes Region
Fisheries and Oceans Canada
Bedford Institute of Oceanography
P.O. Box 1006
Dartmouth, Nova Scotia, B2Y 4A2
Canada

2004

**Canadian Technical Report of
Fisheries and Aquatic Sciences 2516**



Fisheries and Oceans
Canada

Pêches et Océans
Canada

Canada

Canadian Technical Report of
Fisheries and Aquatic Sciences 2516

2004

**Suspended Sediment, Water Quality, and Hydrodynamics of the Petitcodiac
River Estuary, New Brunswick (2002 – 2003)**

by

K.J. Curran, T.G. Milligan*, G. Bugden, B. Law, and M. Scotney

Science Branch, Maritimes Region
Fisheries and Oceans Canada
Bedford Institute of Oceanography
P.O. Box 1006
Dartmouth, Nova Scotia, B2Y 4A2
Canada
*E-mail: milligant@mar.dfo-mpo.gc.ca

© Her Majesty the Queen in Right of Canada, 2004.
Cat. No. FS 97-6/2516E ISSN 0706-6457

Correct citation for this publication:

Curran, K.J., T.G. Milligan, G. Bugden, B. Law, and M. Scotney. 2004.
Suspended Sediment, Water Quality, and Hydrodynamics of the Petitcodiac
River Estuary, New Brunswick (2002–2003). Can. Tech. Rep. Fish. Aquat.
Sci. 2516: xi + 88 p.

TABLE OF CONTENTS

LIST OF TABLES.....	vi
LIST OF FIGURES.....	vii
ABSTRACT/ RÉSUMÉ	xi
1.0 INTRODUCTION	1
2.0 METHODS.....	2
2.1 OVERVIEW	2
2.2 ACOUSTIC DOPPLER CURRENT PROFILER (ADCP) AND OTT CURRENT METER	4
2.2.1 <i>Bridge deployments</i>	4
2.2.2 <i>Vessel-mounted deployments</i>	5
2.3 CONDUCTIVITY, TEMPERATURE, AND DEPTH (CTD), OPTICAL BACKSCATTER (OBS), AND DISSOLVED OXYGEN (DO)	6
2.4 DISCRETE SALINITY AND SUSPENDED PARTICULATE MATTER (SPM).....	6
2.5 DISAGGREGATED INORGANIC GRAIN SIZES (DIGS)	7
2.6 NUTRIENTS (NUTS).....	7
3.0 RESULTS.....	8
3.1 TRANSECT 101 (T101) AT GUNNINGSVILLE BRIDGE.....	8
3.1.1 <i>ADCP velocity and backscatter profiles</i>	9
3.1.2 <i>Salinity, temperature, and density profiles</i>	15
3.1.3 <i>Salinity, OBS, and dissolved oxygen profiles</i>	23
3.1.4 <i>Discrete salinity, SPM, and velocity</i>	31
3.1.5 <i>Discrete salinity and nutrients</i>	33
3.2 TRANSECT 21 (T21) NEAR OUTHOUSE POINT	36
3.2.1 <i>ADCP velocity and backscatter profiles</i>	36
3.2.2 <i>Salinity, temperature, and density profiles</i>	36
3.2.3 <i>Salinity, OBS, and dissolved oxygen profiles</i>	36
3.2.4 <i>Discrete salinity, SPM, and velocity</i>	40
3.2.5 <i>Discrete salinity and nutrients</i>	40
3.3 TRANSECT 11 (T11) NEAR DOVER.....	43
3.3.1 <i>ADCP velocity and backscatter profiles</i>	43
3.3.2 <i>Salinity, temperature, and density profiles</i>	46
3.3.3 <i>Salinity, OBS, and dissolved oxygen profiles</i>	48
3.3.4 <i>Discrete salinity, SPM, and velocity</i>	50
3.3.5 <i>Discrete salinity and nutrients</i>	50
3.4 TRANSECT 1 (T1) NEAR HOPEWELL CAPE.....	53
3.4.1 <i>ADCP velocity and backscatter profiles</i>	53
3.4.2 <i>Salinity, temperature, and density profiles</i>	57
3.4.3 <i>Salinity, OBS, and dissolved oxygen profiles</i>	61
3.4.4 <i>Discrete salinity, SPM, and velocity</i>	65
3.4.5 <i>Discrete salinity and nutrients</i>	66
4.0 DISCUSSION	67
4.1 RIVER VELOCITY AND FLOW DYNAMICS.....	68
4.2 SALINITY, TEMPERATURE, AND DENSITY	70
4.3 SUSPENDED SEDIMENTS	73
4.4 WATER QUALITY	81
5.0 CONCLUSIONS	82

ACKNOWLEDGEMENTS	83
BIBLIOGRAPHY	84
ADDITIONAL REFERENCES	88

LIST OF TABLES

Table 1.	Petitcodiac River field surveys and data collection, 2002 – 2003.	4
Table 2.	Details of Gunningsville Bridge surveys, 2002-2003.	9

LIST OF FIGURES

Figure 1.	Site map of Petitcodiac River study area.	3
Figure 2.	Velocity and acoustic backscatter profiles versus time at the thalweg position of Transect 101, March 26, 2002.	10
Figure 3.	Velocity and acoustic backscatter profiles versus time at the thalweg position of Transect 101, October 9, 2002.	11
Figure 4.	Velocity and acoustic backscatter profiles versus time at the thalweg position of Transect 101, March 20, 2003.	13
Figure 5.	Velocity and acoustic backscatter profiles versus time at the thalweg position of Transect 101, May 14, 2003.	14
Figure 6.	Salinity, temperature, and density profiles versus depth at the thalweg position of Transect 101, March 26, 2002.	16
Figure 7.	Salinity, temperature, and density profiles versus depth at the thalweg position of Transect 101, March 27, 2002.	16
Figure 8.	Salinity, temperature, and density profiles versus time at the thalweg position of Transect 101, October 9, 2002.	17
Figure 9.	Salinity, temperature, and density profiles versus time at the thalweg position of Transect 101, March 19, 2003.	18
Figure 10.	Salinity, temperature, and density versus time at the thalweg position of Transect 101, March 20, 2003.	20
Figure 11.	Salinity, temperature, and density profiles versus time at the thalweg position of Transect 101, May 14, 2002.	21
Figure 12.	Salinity, temperature, and density profiles versus time at the thalweg position of Transect 101, September 12, 2003.	22
Figure 13.	Salinity, optical backscatter, and dissolved oxygen profiles versus depth at the thalweg position of Transect 101, March 26, 2002.	24
Figure 14.	Salinity, optical backscatter, and dissolved oxygen profiles versus depth at the thalweg position of Transect 101, March 27, 2002.	25
Figure 15.	Salinity, optical backscatter, and dissolved oxygen profiles versus time at the thalweg position of Transect 101, October 9, 2002.	26

Figure 16.	Salinity, optical backscatter, and dissolved oxygen profiles versus time at the thalweg position of Transect 101, March 19, 2003.	27
Figure 17.	Salinity, optical backscatter, and dissolved oxygen profiles versus time at the thalweg position of Transect 101, March 20, 2003.	28
Figure 18.	Salinity, optical backscatter, and dissolved oxygen profiles versus time at the thalweg position of Transect 101, May 14, 2003.	29
Figure 19.	Salinity, optical backscatter, and dissolved oxygen profiles versus time at the thalweg position of Transect 101, September 12, 2003.	30
Figure 20.	Discrete salinity, suspended particulate matter, and velocity versus time at the thalweg position of Transect 101.	34
Figure 21.	Discrete salinity and nutrient concentrations versus time at the thalweg position of Transect 101.	35
Figure 22.	Velocity and acoustic backscatter profiles versus time at the thalweg position of Transect 21, May 15, 2003.	37
Figure 23.	Salinity, temperature, and density profiles versus time at the thalweg position of Transect 21, May 15, 2002.	38
Figure 24.	Salinity, optical backscatter, and dissolved oxygen profiles versus time at the thalweg position of Transect 21, May 15, 2003.	39
Figure 25.	Discrete salinity, suspended particulate matter, and velocity versus time at the thalweg position of Transect 21.	41
Figure 26.	Discrete salinity and nutrient concentrations versus time at the thalweg position of Transect 21.	42
Figure 27.	Velocity and acoustic backscatter profiles versus time at the thalweg position of Transect 11, June 12, 2003	44
Figure 28.	Velocity and acoustic backscatter profiles versus time at the thalweg position of Transect 11, September 9, 2003.	45
Figure 29.	Salinity, temperature, and density profiles versus time at the thalweg position of Transect 11, June 12, 2003.	46
Figure 30.	Salinity, temperature, and density profiles versus time at the thalweg position of Transect 11, September 9, 2003.	47

Figure 31.	Salinity, optical backscatter, and dissolved oxygen profiles versus time at the thalweg position of Transect 11, June 12, 2003.	48
Figure 32.	Salinity, optical backscatter, and dissolved oxygen profiles versus time at the thalweg position of Transect 11, September 9, 2003.	49
Figure 33.	Discrete salinity, suspended particulate matter, and velocity versus time at the thalweg position of Transect 11.	51
Figure 34.	Discrete salinity and nutrient concentrations versus time at the thalweg position of Transect 11.	52
Figure 35.	Velocity and acoustic backscatter profiles versus time at the thalweg position of Transect 1, June 13, 2003.	54
Figure 36.	Velocity and acoustic backscatter profiles versus time at the thalweg position of Transect 1, September 10, 2003.	55
Figure 37.	Velocity and acoustic backscatter profiles versus time at the thalweg position of Transect 11, September 11, 2003.	56
Figure 38.	Salinity, temperature, and density profiles versus time at the thalweg position of Transect 1, June 13, 2003.	58
Figure 39.	Salinity, temperature, and density profiles versus time at the thalweg position of Transect 1, September 10, 2003.	59
Figure 40.	Salinity, temperature, and density profiles versus time at the thalweg position of Transect 1, September 11, 2003.	60
Figure 41.	Salinity, optical backscatter, and dissolved oxygen profiles versus time at the thalweg position of Transect 1, June 13, 2003.	62
Figure 42.	Salinity, optical backscatter, and dissolved oxygen profiles versus time at the thalweg position of Transect 1, September 10, 2003	63
Figure 43.	Salinity, optical backscatter, and dissolved oxygen profiles versus time at the thalweg position of Transect 1, September 11, 2003.	64
Figure 44.	Discrete salinity, suspended particulate matter, and velocity versus time at the thalweg position of Transect 1.	66
Figure 45.	Discrete salinity and nutrient concentrations versus time at the thalweg position of Transect 1.	67

Figure 46.	The affect of gate manipulation on the water column salinity, temperature, and density structure at Transect 11, located 16-km downstream of the causeway	72
Figure 47.	Suspended particulate matter and DIGS clearance rates at Transect 11	76
Figure 48.	Density, optical backscatter, acoustical backscatter, and SPM versus time at Transect 1, June 13, 2003.	78
Figure 49.	Downstream and cross-sectional surveys of bottom sediment accumulation versus distance.	80

ABSTRACT

Curran, K.J., T.G. Milligan, G. Bugden, B. Law and M. Scotney. 2004. Sediment, Water Quality, and Hydrodynamics of the Petitcodiac River Estuary, New Brunswick (2002 –2003). Can. Tech. Rep. Fish. Aquat. Sci. 2516: xi + 88 p.

The Petitcodiac River, New Brunswick, is the largest river discharging into the upper Bay of Fundy. The hydrological and geological characteristics of the river were altered dramatically by the construction of a causeway between the City of Moncton and the Town of Riverview in 1968. The construction of the causeway has changed the hydrodynamics and accelerated the deposition of fine sediment in the upper reaches of the river estuary. One of the outcomes has been a reduction in fish passage that impacts some fish species. In an attempt to re-establish fish passage modifications to the causeway have been proposed. These modifications are the subject of an Environmental Impact Assessment (EIA). Despite many studies over the last several decades, a fundamental lack of understanding of the basic dynamics of the system still remains. In 2002 and 2003, members of the Science Branch of Fisheries and Oceans Canada, Maritimes Region, conducted 13 field surveys on the Petitcodiac River Estuary. The objectives of these surveys were: 1) test instrumentation and develop sampling strategies for data collection in the unique conditions found within the Petitcodiac River System; 2) provide data in support of predictive modelling studies being conducted by consultants as part of the EIA; and 3) provide data that would permit the conclusions of the EIA to be evaluated by Fisheries and Oceans Canada in a scientifically-defensible manner. This report outlines the instrumentation deployed and data collected from the Petitcodiac River Estuary during the field surveys. Preliminary analysis of the data is also presented.

RÉSUMÉ

Curran, K.J., T.G. Milligan, G. Bugden, B. Law and M. Scotney. 2004. Sediment, Water Quality, and Hydrodynamics of the Petitcodiac River Estuary, New Brunswick (2002 –2003). Can. Tech. Rep. Fish. Aquat. Sci. 2516: xi + 88 p.

La rivière Petitcodiac, au Nouveau-Brunswick, est la plus grande rivière qui se jette dans la partie supérieure de la baie de Fundy. Ses caractéristiques hydrologiques et géologiques ont été profondément modifiées par la construction d'une chaussée entre Moncton et Riverview, en 1968. La construction de cette chaussée a changé la dynamique du débit de la rivière et accéléré le dépôt de fins sédiments dans le cours supérieur de l'estuaire de la rivière. Elle a notamment restreint le passage du poisson, ce qui a eu des effets sur certains d'entre eux. Des modifications destinées à rétablir le passage du poisson ont été proposées. Elles font l'objet d'une évaluation environnementale (EE). Malgré les nombreuses études effectuées au cours des quelques dernières années, il existe des lacunes fondamentales dans la compréhension de la dynamique de base de ce réseau hydrographique. En 2002 et 2003, des membres du personnel de la Direction des sciences de Pêches et Océans Canada, Région des Maritimes, ont procédé à 13 études sur le terrain dans l'estuaire de la Petitcodiac. Ces études visaient les objectifs suivants : 1) faire l'essai d'instruments et élaborer des stratégies d'échantillonnage en vue de la collecte de données dans les conditions uniques qui caractérisent le réseau hydrographique de la Petitcodiac; 2) fournir des données à l'appui des études de modélisation à des fins prévisionnelles qui sont en train d'être effectuées par des consultants dans le cadre des EE et 3) fournir des données permettant à Pêches et Océans Canada d'évaluer les conclusions des EE d'une manière qui soit défendable sur le plan scientifique. Le présent rapport décrit les instruments utilisés et les données recueillies dans le cadre des études de terrain effectuées dans l'estuaire de la Petitcodiac. On y présente aussi les analyses préliminaires des données.

1.0 INTRODUCTION

Large-scale barriers such as causeways can alter the physical, chemical, and biological conditions in tidal rivers in which they are constructed, resulting in an alteration of the system's natural balance. Subsequently, the health of organisms that occupy and utilize the local habitat for survival also may be affected, such as in the Petitcodiac River (Wells, 1999). The Petitcodiac River is the largest river discharging into the upper Bay of Fundy (Richardson *et al.*, 2002). It has been altered dramatically by the construction of a causeway, which changed the flow dynamics and accelerated the deposition of fine sediment in the upper reaches of the river estuary (Bray *et al.*, 1982; Galay, 1983).

In 1968, the New Brunswick Department of Transportation constructed the Petitcodiac River Causeway between the City of Moncton and the Town of Riverview. The outcome has been a change in the suspended sediment, water quality, and hydrodynamics within the Petitcodiac River Estuary. Prior to causeway construction, the saltwater intrusion associated with waters of the upper Bay of Fundy extended upstream of Moncton to near Salisbury (Schell, 1998). The intrusion formed brackish water that acted as a transition zone for sensitive fish species migrating between the upstream freshwater of the Petitcodiac River and the downstream saltwater of the upper Bay of Fundy (Locke *et al.*, 2003). The saltwater intrusion also provided important nursery habitat for several fish species. At present, the causeway acts as a barrier to the saltwater intrusion, despite the presence of five spill gates. A fishway designed to permit fish passage across the causeway also has been ineffective (Butler, 1969). Since the causeway's construction, elimination and reduction of several fish species within the Petitcodiac River have been observed (Locke, 2003).

In an attempt to re-establish fish passage and improve water quality alteration of the causeway has been proposed. This has resulted in an Environmental Impact Assessment (EIA) of 4 project options to restore fish passage in the Petitcodiac River System and an evaluation of the status quo. Despite many studies over the last several decades, a fundamental lack of understanding of the basic dynamics of the system still remains (Schell, 1998; New Brunswick Department of Supply and Services, 2002). In 2002 and 2003, members of the Science Branch of Fisheries and Oceans Canada, Maritimes Region, conducted 13 field surveys on the Petitcodiac River Estuary. The objectives of these surveys were: 1) test instrumentation and develop sampling strategies for data collection in the unique conditions found within the Petitcodiac River System; 2) provide data in support of predictive modelling studies being conducted by the proponents as part of the EIA; and 3) provide data that would permit the conclusions of the EIA to be evaluated by Fisheries and Oceans Canada in a scientifically-defensible manner. This report outlines the instrumentation deployed and data collected during the field surveys. Preliminary analysis of suspended sediment, water quality, and velocity data from the Petitcodiac River Estuary is also presented.

2.0 METHODS

2.1 OVERVIEW

The Petitcodiac River drains approximately 2300 km², with the watershed located in southeast New Brunswick (Schell, 1998). Typically, the Petitcodiac River flows from its source in a northeast direction and just east of Moncton meanders approximately 90°. It then flows in a south-southeast direction discharging into Shepody Bay of the upper Bay of Fundy (Figure 1). Above the causeway, the Petitcodiac River is joined by five tributaries: the Anagance River; Coverdale River; Little River; North River; and Pollet River. Below the causeway, the Memramcook River joins the Petitcodiac River at Hopewell Cape. In this study, the sampling effort focused on that segment of the Petitcodiac River Estuary below the causeway, from the Gunningsville Bridge to Hopewell Cape.

From March 2002 to September 2003 data was collected from the Petitcodiac River Estuary during thirteen field surveys. In 2002, surveys were performed on March 26, March 27, and October 9 (Table 1). For these surveys, data was collected at a fixed position in the river every 15 – 30 mins. over entire tidal periods. All samples were collected from the Gunningsville Bridge, Transect 101 (T101), located approximately 3-km downstream of the causeway (Figure 1). In 2003, data was collected from the Gunningsville Bridge on March 19, March 20, May 14, and September 12, while data also was collected from three cross-river transects downstream of the causeway (Table 1).

In 2003 cross-river transects running perpendicular to the shore were sampled using a 6.4-m (21-ft) aluminum boat fitted with an Acoustic Doppler Current Profiler (ADCP) and differential GPS. Transects were sampled continuously over an entire tidal cycle, with each transect taking 15 – 30 mins. On May 15, sampling was carried out for part of the tidal cycle at Transect 21 (T21), located 5.5-km from the causeway (Figure 1). On June 12, sampling was carried out at Transect 11 (T11) near Dover, located 16-km from the causeway (Figure 1) and on June 13 at Transect 1 (T1) near Hopewell Cape, located 34-km from the causeway (Figure 1). Transect 11 was reoccupied on September 9 and Transect 1 on September 10 and September 11. Table 1 outlines the date, location, and data collected for each survey.

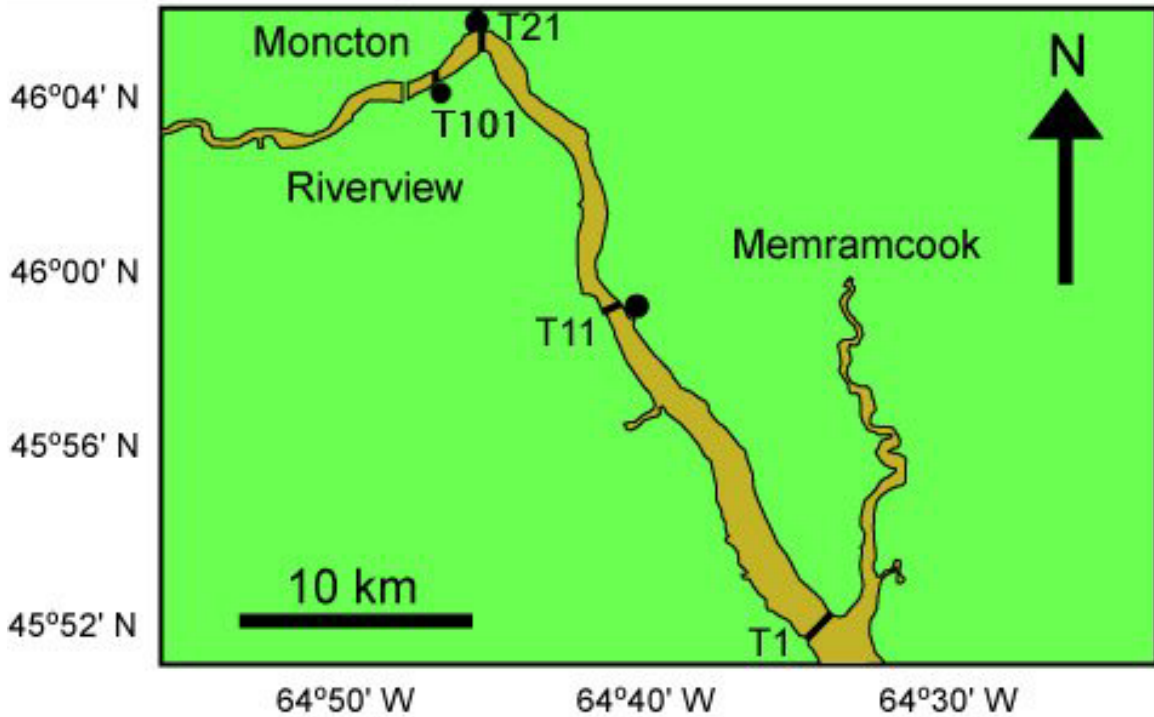
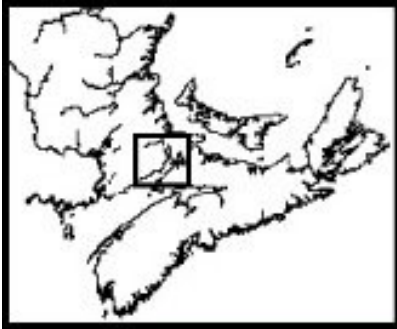


Figure 1. Site map of the Petitcodiac River study area. Sample locations are Transect 101 (T101) at the Gunningsville Bridge, Transect 21 (T21) near Outhouse Point, Transect 11 (T11) near Dover, and Transect 1 (T1) near Hopewell Cape. The filled circles mark the locations of tidal observations and predictions.

Several different instruments were used to collect suspended sediment, water quality, and velocity data during the thirteen field surveys. Briefly, data collected included velocity and acoustical backscatter profiles (ADCP), conductivity, temperature, and depth (CTD) profiles, optical backscatter (OBS) profiles, dissolved oxygen profiles (DO), discrete velocity (OTT), and discrete water samples. Discrete surface water samples were collected using 2-L, plastic sample bottles mounted in a weighted harness. Discrete bottom water samples were collected using a Niskin bottle with a modified trigger mechanism designed for high flow environments. Typically, discrete bottom water samples at Transect 101 were collected 0.5 m above the river bottom only during slack tide, as high tidal velocities made sampling difficult. All discrete water samples were subsampled into pre-labeled, plastic bottles and stored in a cooler for transport to

the laboratory. Subsamples were then analyzed for salinity (SAL), suspended particulate matter (SPM) concentrations, disaggregated inorganic grain sizes (DIGS), and dissolved nutrient concentrations (NUTS). Water level was recorded at Hall's Creek near Moncton by Environment Canada and predicted for Dover (Figure 1).

Table 1. Petitcodiac River field surveys and data collection, 2002 – 2003.

Survey Number	Survey Date	Survey Transect	Profile			Discrete		
			ADCP	CTD/OBS /DO	OTT	SAL	SPM/DIGS	NUTS
1	Mar 26, 2002	T101	x	x		x	x	x
2	Mar 27, 2002	T101		x		x	x	x
3	Oct 9, 2002	T101	x	x		x	x	x
4	Mar 19, 2003	T101		x	x	x	x	x
5	Mar 20, 2003	T101	x	x	x	x	x	x
6	May 14, 2003	T101	x	x	x	x	x	x
7	May 15, 2003	T21	x	x		x	x	x
8	June 12, 2003	T11	x	x		x	x	x
9	June 13, 2003	T1	x	x		x	x	x
10	Sept 9, 2003	T11	x	x		x	x	x
11	Sept 10, 2003	T1	x	x		x	x	x
12	Sept 11, 2003	T1	x	x		x	x	x
13	Sept 12, 2003	T101		x		x	x	x

2.2 ACOUSTIC DOPPLER CURRENT PROFILER (ADCP) AND OTT CURRENT METER

2.2.1 Bridge deployments

The acoustic doppler current profiler (ADCP) uses the characteristics of sound reflected from particles in the water to estimate the velocity and sediment concentration at several depth increments from the instrument's transducer to the river bottom. Two bottom-directed, ADCP instruments were used for profiling at Transect 101 in 2002 and 2003. These were a 300 kHz ADCP mounted in a stabilizing wing and a 600 kHz ADCP mounted in a floating trimaran. The 300 kHz ADCP instrument was suspended in the water column from the bridge. The 600 kHz ADCP only was used for inter-instrument calibration. The pitch and roll of each instrument was logged internally and then used for quality control of the data.

For the 300 kHz ADCP deployment on March 26, 2002, velocity and backscatter were averaged internally every 5-minutes by the instrument. As a result, the data were not quality controlled. For the instrument deployments on October 9, 2002, March 20 and May 14, 2003, the ADCP velocity and backscatter measurements were post-processed by averaging over 5-minute time intervals. This was performed by calculating the mean and standard deviation of data within 5-minute bin ranges. The averaged data was then estimated using only that data that was within two standard deviations of the mean. Post-processing was used

to remove outlier observations that may have influenced the measured velocity. On March 19, March 20, and May 14, 2003, an OTT current meter was used to estimate the surface velocity at Transect 101, as the ADCP instruments only estimated velocity and backscatter at a fixed depth below the surface. The OTT current meter could not determine the direction of the flow however the direction was recorded manually by the field surveyors.

2.2.2 Vessel-mounted deployments

A vessel-mounted, 1200 kHz RD Instruments ADCP was used for cross-river transect surveys. The ADCP was interfaced with a differential GPS for velocity referencing, as the high sediment concentrations within the river prevented bottom tracking. The ADCP velocity and backscatter measurements were averaged in the cross-river direction over specified intervals, depending on the width of the river at a given transect. For example, cross-sectional data from Transect 21, which during the survey varied in width from about 125 m at High Water (HW) to almost dry at Low Water (LW), was formed into averages every 20 m across the river, using 10 m averaging radii around each averaging position. Cross-sectional data from Transect 11, which varied in width from about 500 m at HW to too narrow for transects at LW, was formed into averages every 100 m across the river, using 50 m averaging radii around each averaging position, and data from Transect 1, which varied in width from about 1550 m at High Water (HW) to about 1150 m at LW was formed into averages every 200 m across the river, using 100 m averaging radii around each averaging position. Averaging was used to reduce the tremendous amount of data that was collected by the instrument over entire surveys. The number of cross-sectional averaging positions per transect changed as the river width changed with the tide.

All data was processed by determining the bearing of the transect in the west-east direction across the river. From the thalweg position, the deepest point in the river at the transect, averaging positions were determined on each side of the thalweg to the riverbanks. At each averaging position and the thalweg position, a specified averaging radius circle was used to find all velocity and backscatter measurements positioned within the radius for averaging. For all data positioned within the radius the mean and standard deviation were calculated. The averaged data was then estimated using only that data that was within two standard deviations of the mean. This was done to remove outlier observations that may have influenced the average.

As with all ADCP data, caution should be used in interpreting velocity and backscatter very near the bottom. This is especially true in the Petitcodiac River where the interface between the water column and bottom often is not well defined. Due to limitations with the ADCP instruments used to measure velocity and backscatter, the bottom depth could not be estimated for most transects, likely due to high bottom sediment concentrations. Similarly, in other marine environments sediment concentrations on the order of 10 g l^{-1} have caused

ADCP backscatter to rapidly decrease to 20 – 40 dB, which was explained by the presence of fluid muds (Traykovski et al., 2000).

2.3 CONDUCTIVITY, TEMPERATURE, AND DEPTH (CTD), OPTICAL BACKSCATTER (OBS), AND DISSOLVED OXYGEN (DO)

Conductivity, temperature, and depth (CTD) profiles, optical backscatter (OBS) profiles, and dissolved oxygen (DO) profiles were collected for all surveys using a Seabird SBE 25 CTD equipped with a Seapoint OBS turbidity meter and SBE 23Y dissolved oxygen sensor. The OBS estimates the sediment concentration using reflected light, the OBS voltage being proportional to the sediment concentration within the expected range of the instrument. In other marine environments, however, concentrations on the order of 10 g l^{-1} have caused a non-linear decrease in OBS output towards and below 0 volts as concentrations increased on the order of 100 g l^{-1} (Kineke and Sternberg, 1992). As a result, a rapid decrease in OBS output may reflect a sediment concentration increase on order of $10 - 100 \text{ g l}^{-1}$, rather than a decrease in concentration.

For surveys conducted at Transect 101, CTD, OBS, and DO profiles were collected only when the current velocity was sufficiently low to permit the instrument package to be lowered through the water column. For cross-river surveys, the ability of the boat to move freely with the tidal current enabled collection of CTD, OBS, and DO profiles over entire tidal periods. Density (σ_t) was calculated using salinity and temperature, and is presented as the observed density minus 1000 kg m^{-3} . Because of the very high sediment concentrations, high enough to affect the effective density of the water, apparent inversions in the density calculated from the temperature and salinity were observed. Similar observations were made on the highly turbid Amazon Shelf (Trowbridge and Kineke, 1994). The dissolved oxygen sensor was not calibrated prior to surveying, which may result in sensor drift. Within the survey casts, however, variations in DO are real even if the absolute DO levels are slightly inaccurate. In a series of laboratory experiments, very high sediment concentrations were not observed to affect the operation of the pump system or the temperature/conductivity sensor on the Seabird SBE 25 instrument package.

2.4 DISCRETE SALINITY AND SUSPENDED PARTICULATE MATTER (SPM)

Discrete water subsamples collected for salinity were stored in the laboratory to allow suspended sediment within the bottle to deposit. Salinity was then measured using a Guildline salinometer. Discrete water subsamples collected for suspended particulate matter (SPM) concentration were filtered through $8.0 \mu\text{m}$ Millipore cellulose filters, retaining particles larger than $1 \mu\text{m}$ in diameter (Sheldon, 1972; Kranck and Milligan, 1992). Filters were then dried and weighed for total SPM concentration and processed for disaggregated inorganic grain sizes (DIGS).

2.5 DISAGGREGATED INORGANIC GRAIN SIZES (DIGS)

Disaggregated inorganic grain sizes (DIGS), or the component inorganic grains in suspension, were processed for all discrete water samples at the Particle Dynamics Laboratory, Fisheries and Oceans Canada, Maritimes Region. A subsample of sediment in a measured volume from each discrete water sample was filtered and placed in a low-temperature ashers, then digested with hydrogen peroxide to remove all organic matter and the filter (Milligan and Kranck, 1991). The remaining inorganic component particles were added to a 1% NaCl electrolytic suspension and then processed using a Coulter Multisizer IIe electro-resistance particle size analyzer.

The Coulter Multisizer IIe determines the number and volume of particles in an electrolytic suspension by drawing the suspension through a small aperture of known diameter using a vacuum. As a particle passes through the aperture, a current maintained by two electrodes on either side of the aperture fluctuates due to increased impedance by the passing particle, and is detected as a voltage pulse proportional to the particle's spherical volume. The pulses are sized and counted using predetermined equivalent spherical diameter sizes calibrated with particles of known diameter (Milligan and Kranck, 1991).

All subsamples analyzed were first sonicated using a sapphire-tipped, ultrasonic probe to ensure particle dispersion. The subsamples were then counted using the 400- μm (sizing particles 8 – 200 μm in diameter), 200- μm (sizing particles 4 – 100 μm in diameter), and 30- μm (sizing particles 0.6 – 15 μm in diameter) aperture tubes. The multisizer is equipped with a stir-rod that ensures large particles remain in suspension during processing. The resultant size distributions for each aperture tube were then merged based on a best match of results to create a continuous disaggregated inorganic grain size distribution of the subsample. The DIGS distributions are output as logarithmic concentration versus logarithmic-binned grain size. The concentration is measured in parts per million (ppm), which is the volume units of particles per million volume units of the original sample processed.

2.6 NUTRIENTS (NUTS)

Discrete water subsamples collected for dissolved nutrient concentrations were processed at the Nutrient Laboratory, Fisheries and Oceans Canada, Maritimes Region. Samples were filtered with a 0.45 μm teflon filter before processing to remove sediment. All nutrient subsamples were analyzed for dissolved concentrations of silicate (SiO_2), phosphate (PO_4), nitrate (NO_3), nitrite (NO_2), and ammonia (NH_4). The dissolved nutrient concentrations were analyzed using spectrophotometric methods. Briefly, the dissolved silicate concentration was estimated from the formation of molybdenum blue in the presence of silicomolybdate acidic solution, based on the automated procedure of Strickland and Parsons (1972) (Industrial Method No. 186-72W). The dissolved phosphate

concentration was estimated from the formation of phosphomolybdenum blue complex in the presence of ammonium molybdate acidic solution, based on the automated procedure of Murphy and Riley (1962) (Industrial Method No. 155-71W). Dissolved nitrate and nitrite concentrations were estimated by reducing nitrate to nitrite using a copper-cadmium reactor column (Armstrong et al., 1967; Grasshoff, 1969). Nitrite ions then react with sulfanilamide under acidic conditions, forming a diazo compound that couples with N-1-naphthylethylenediamine dihydrochloride to form a reddish-purple azo dye (Industrial Method No. 158-71W). Last, the dissolved ammonia concentration was estimated from the reaction of ammonia with orthophtaldialdehyde (OPA) and sulfite, based on the automated procedure of K erouel and Aminot (1997).

3.0 RESULTS

Environment Canada acquired water levels at Hall's Creek, near Transect 21, during 2002 and 2003, using ultrasonic instrumentation (Figure 1). The Hall's Creek water level data is used in this study to support observations made at Transect 101 and Transect 21. The unique characteristics of the Petitcodiac River at Moncton, however, make it difficult to observe water levels at this location. Environment Canada has indicated that the data does not meet National Water Survey Standards and may be affected by local noise caused by wind. In addition, what appear to be low water levels in the data may be exposed mud flats and not the actual water level. Despite these challenges, the observed water levels at Hall's Creek are used to provide a more accurate representation of the tidal signal at Transect 101 and Transect 21, where the water level is severely altered, or clipped. Considering this, water levels at Transect 101 and Transect 21 may not agree with depth observations from the instruments used in this study. For Transect 11 and Transect 1, predicted water levels at Dover are used in data analysis. All observations in this study are referenced to Universal Time (UTC).

3.1 TRANSECT 101 (T101) AT GUNNINGSVILLE BRIDGE

In total, seven surveys were performed at Transect 101. In 2002, three surveys were carried out under different causeway gate operations, tidal conditions, and seasons. Details are displayed in Table 2. During the March 26, 2002 survey slack high water was at 1600 h. A lot of ice passed Transect 101 at 1648 h and was flushed from upstream by 1726 h. At 1839 h, the downstream velocity decreased and slack low water was at 1852 h. During the March 27, 2002 survey the tidal bore passed at 1250 h, with high tide at 1530 h. No causeway gates were opened during this survey. On October 9, 2002 low tide was at 1230 h. A 0.25-m wave passed downstream of Transect 101 at 1500 h. The tidal bore passed at 1552 h and a 1 m wave moved upstream. Slack high tide was at 1830 h.

In 2003, four surveys were carried out at Transect 101. Details are again displayed in Table 2. During the survey of March 19, 2003 the tidal bore passed

at 1500 h and slack high tide was at 1800 h. Following gate opening on March 20, 2003, slush moved downstream past Transect 101. The tidal bore passed at 1539 h and slack high tide was at 1800 h. During the survey on May 14, 2003 the tidal bore passed at 1222 h and slack high tide was at 1430 h. Last, during the survey on September 12, 2003 slack low tide was at 1245 h. The tidal bore passed at 1616 h with slack high tide at 1728 h.

Table 2. Details of Gunningsville Bridge Surveys 2002-2003.

Survey Number	Date	Survey Period (UTC)	Tidal Conditions	Gate Operation (UTC)
1	Mar 26, 2002	1600-2000	Ebb Tide	Two Gates Open 1635-1835
2	Mar 27, 2002	1230-1430	Flood Tide	Gates Closed
3	Oct 9, 2002	1300-2030	Tidal Period	One Gate Open 1445-1830
4	Mar 19, 2003	1200-2230	Tidal Period	Gates Closed
5	Mar 20, 2003	1130-2200	Tidal Period	One Gate Open 1326-1453
6	May 14, 2003	1100-2000	Tidal Period	One Gate Open 1032-1339
13	Sept 12, 2003	1400-2000	Flood Tide	Two Gates Open 1924-2027

3.1.1 ADCP velocity and backscatter profiles

For all surveys at Transect 101, a 300 kHz ADCP mounted on a stabilizing wing was deployed. The design of the instrument only permitted velocity and backscatter measurements to be logged at a fixed depth below the instrument's transducer, which was 1.8 m. Because the instrument moved through the water column as the water level changed an instrument depth also had to be added to the transducer depth, which may result in surveys having different initial depth measurements. Again, caution should be used in interpreting velocity and backscatter values from the ADCP very near the bottom, as high bottom sediment concentrations may influence the instrument's measurements.

On March 26, 2002, it was difficult to obtain a continuous ADCP velocity and backscatter record as the instrument was frequently removed from the water to avoid collision with ice. Two causeway gates were opened from 1635 – 1835 h, during ebb to low slack tide. Between 1800 – 1835 h, the downstream velocities at 3.5 m depth were approximately 2 m s^{-1} , which then decreased to 0 m s^{-1} by 1847 h (Figure 2). The backscatter at 3.5 m depth was 193 dB between 1800 – 1835 h and then decreased to 183 dB by 1847 h (Figure 2). At 1912 h, backscatter was 150 dB. Following closure of the causeway gates at 1835 h, a decrease in the downstream velocity and backscatter were observed (Figure 2). This was also observed by field surveyors who noted a substantial decrease in the apparent downstream velocity by 1839 h. At this time, the ebb tide was approaching slack low tide. No ADCP data was collected on March 27, 2002.

On October 9, 2002, one causeway gate was opened from 1445 – 1830 h during flood tide. At 1552 h, the tidal bore passed Transect 101 and the velocity at 2.5 m depth reversed from 0.32 m s^{-1} downstream at 1612 h to 0.13 m s^{-1} upstream

at 1647 h (Figure 3). A maximum upstream velocity of 0.55 m s^{-1} was observed at 2.5 m depth, during flood tide. At 1810 h, the upstream velocity at 2.5 m depth decreased to 0.12 m s^{-1} , while the upstream velocity at 4 m depth was 0.43 m s^{-1} . The upstream velocity at 2.5 m depth approached 0 m s^{-1} at 1832 h, while velocity at 4 m depth did not reach 0 m s^{-1} until 1912 h. At 1957 h, the maximum downstream velocity associated with the ebb tide was 0.86 m s^{-1} , at 2.5 m depth. The maximum downstream velocity at 4 m depth during ebb tide was 0.84 m s^{-1} , at 1942 h. The backscatter at 2.5 m depth increased from 47 dB at 1632 h to 189 dB at 1647 h, as the upstream velocity increased during flood tide (Figure 3). Backscatter was low throughout the water column at the beginning of the flood tide and decreased with depth during slack high tide. Backscatter between 180 – 205 dB were observed during flood and slack high tide, and then decreased during the ebb tide to 120 dB by 2012 h.

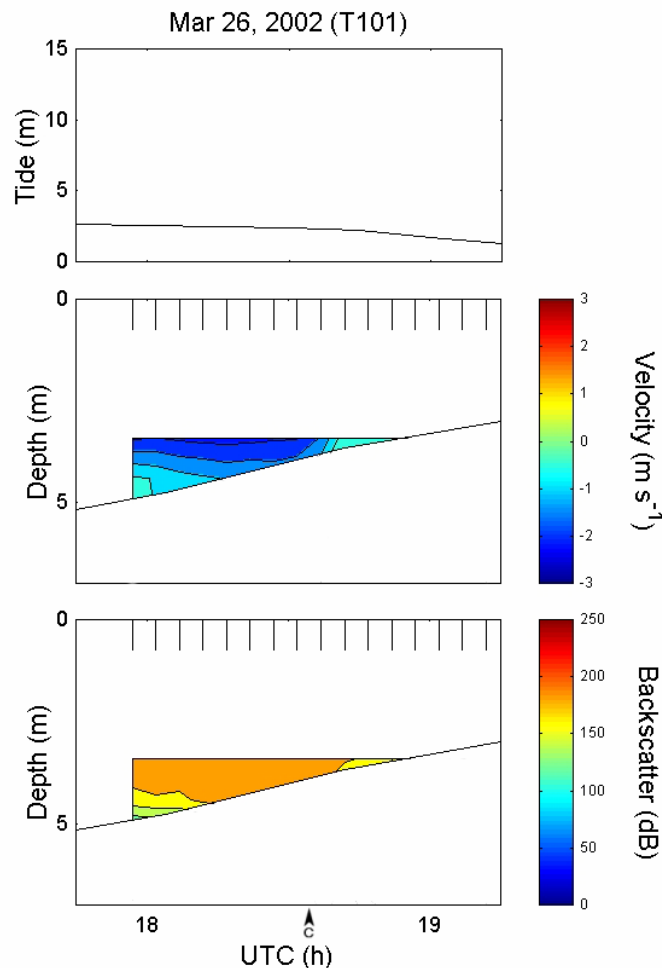


Figure 2. Velocity and backscatter versus time at the thalweg position of Transect 101, March 26, 2002. An extended tick indicates the time that an ADCP profile was collected. Positive velocity values represent upstream velocity and negative values downstream velocity. The black line represents the bottom depth estimated from CTD casts. Gate operations are indicated by the vertical arrows on the time axis: C=Closed, O=Open.

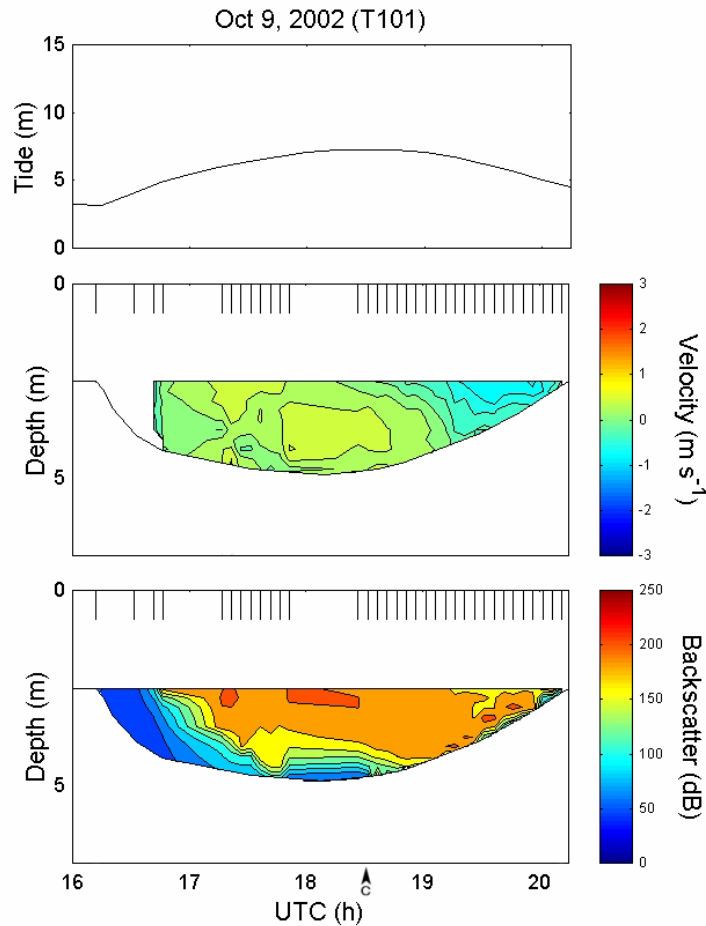


Figure 3. Velocity and backscatter versus time at the thalweg position of Transect 101, October 9, 2002. An extended tick indicates the time that an ADCP profile was collected. Positive velocity values represent upstream velocity and negative values downstream velocity. The black line represents the bottom depth estimated from CTD casts. Gate operations are indicated by the vertical arrows on the time axis: C=Closed, O=Open.

On March 20, 2003, one causeway gate was fully opened from 1326 – 1453 h during low tide. At 1237 h, the velocity at 2 m depth was 0 m s^{-1} during slack low tide (Figure 4). Following the causeway gate opening at 1326 h, the downstream velocity at 2 m depth increased to 2.4 m s^{-1} . Between 1444 – 1458 h the downstream velocity at 2 m depth decreased to 1 m s^{-1} following gate closure. The downstream velocity then decreased to 0.4 m s^{-1} by 1521 h. A similar pattern was observed at depth, although the magnitude of the velocity was lower. At 1627 h, the velocity at 2 m depth was 0.8 m s^{-1} upstream, following passage of the tidal bore at 1539 h. The upstream velocity then decreased to 0 m s^{-1} by 1647 h. At 1742 h, the velocity then increased downstream again, during the ebb tide. A maximum downstream velocity of 1.3 m s^{-1} was observed at 2 m depth during ebb tide, at 1953 h. The white areas on Figure 4 represent no data values, which are observed near the bottom during slack high tide. It is likely that regions of no data reflect extremely high sediment concentrations. The

backscatter at 2 m depth ranged from 13 – 90 dB between 1237 – 1242 h and then increased to 172 dB at 1343 h following gate opening (Figure 4). The backscatter remained high at 2 m water depth throughout the remainder of the survey, typically ranging from 170 – 225 dB. Backscatter decreased with depth, approaching values of 0 dB near the bottom, during slack high tide.

On May 14, 2003, one causeway gate was opened for fish passage from 1032 – 1339 h, during flood tide. The tidal bore was at 1222 h and slack high tide at 1430 h. Between 1254 – 1304 h during gate opening, the velocity throughout the water column was downstream, despite passage of the tidal bore (Figure 5). A maximum downstream velocity of 0.39 m s^{-1} was observed at 1.5 m. At 1309 h, the downstream velocity at 1.5 m depth decreased to 0.25 m s^{-1} , and an upstream velocity of 0.15 m s^{-1} was observed at 5 m depth. At 1339 h following gate closure, velocity throughout the water column was in an upstream direction, with the highest velocity observed near the bottom (Figure 5). At 1359 h, the velocity was approximately 0 m s^{-1} at 1.5 m depth, although a strong upstream velocity of 0.57 m s^{-1} was still observed at 5 m depth. By 1404 h, the surface velocity was in a downstream direction during ebb tide. The highest ebb velocity was 0.55 m s^{-1} at 1.5 m depth, observed at 1719 h. Velocities throughout the water column then approached 0 m s^{-1} during slack low tide. An elevated backscatter of 229 dB was observed at 1.5 m depth, following the passage of the tidal bore at 1254 h (Figure 5). Backscatter then decreased with depth and flood tide. At 1339 h following gate closure, backscatter was 163 dB at 5 m depth. Backscatter then increased throughout the water column during ebb tide (Figure 5). Figure 5 also demonstrates no data values (white areas) very near the bottom.

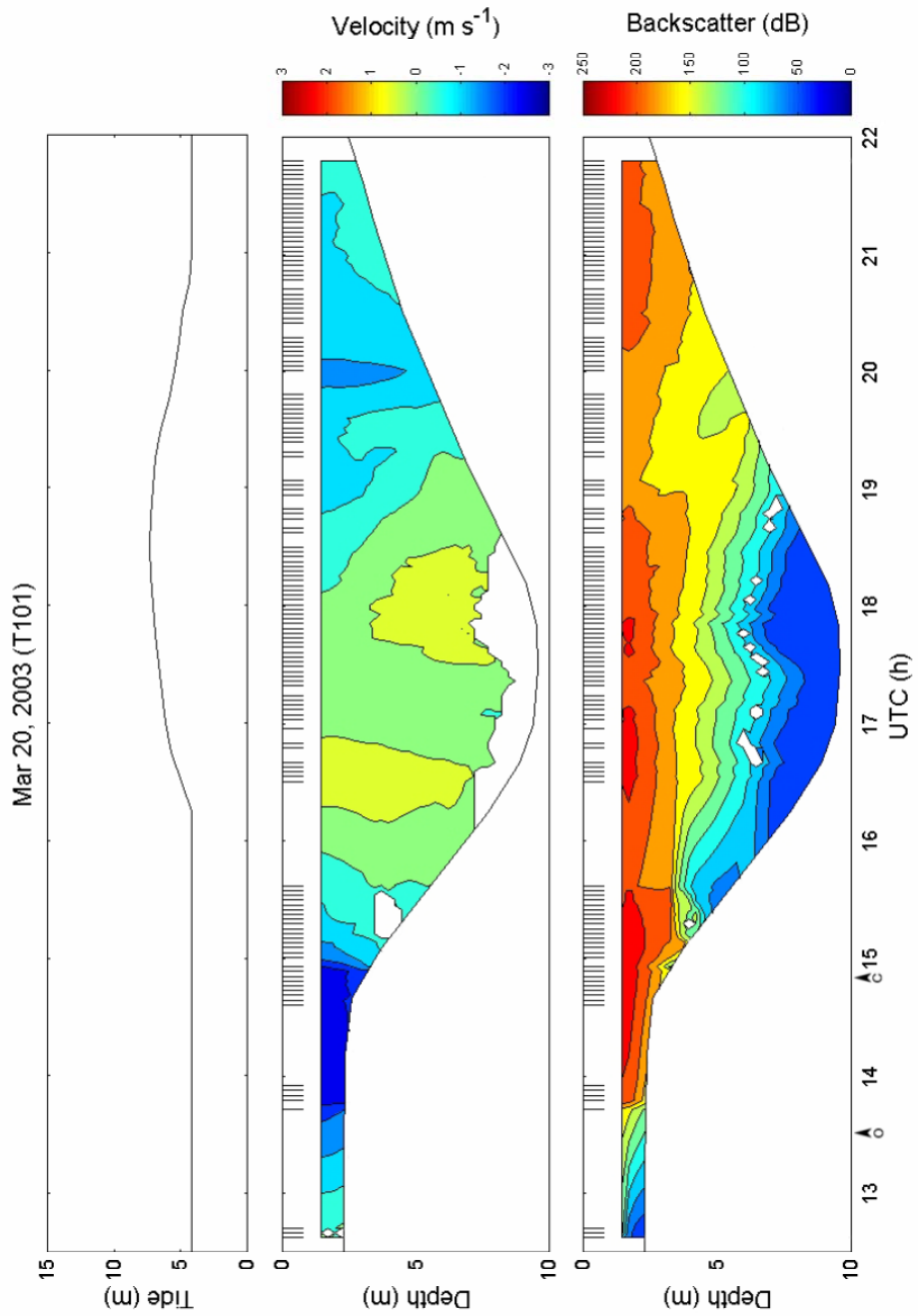


Figure 4. Velocity and backscatter versus time at the thalweg position of Transect 101, March 20, 2003. An extended tick indicates the time that an ADCP profile was collected. Positive velocity values represent upstream velocity and negative values downstream velocity. The black line represents the bottom depth estimated from CTD casts. Gate operations are indicated by the vertical arrows on the time axis: C=Closed, O=Open.

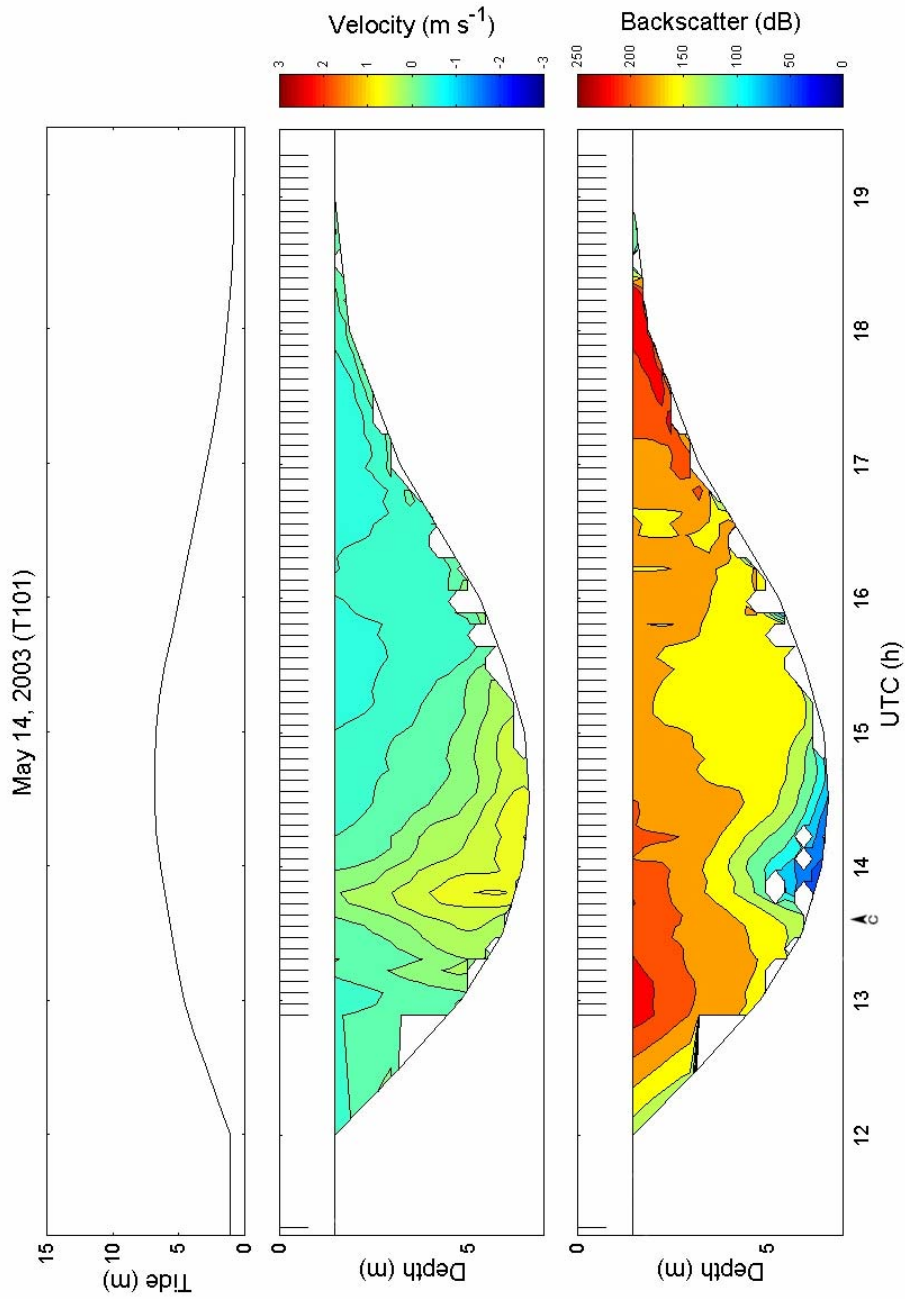


Figure 5. Velocity and backscatter versus time at the thalweg position of Transect 101, May 14, 2003. An extended tick indicates the time that an ADCP profile was collected. Positive velocity values represent upstream velocity and negative values downstream velocity. The black line represents the bottom depth estimated from CTD casts. Gate operations are indicated by the vertical arrows on the time axis: C=Closed, O=Open.

3.1.2 Salinity, temperature, and density profiles

Only one CTD cast was made on March 26 and March 27, 2002. The cast at 1923 h on March 26, 2002, shown in Figure 6, demonstrates that the water column at Transect 101 consisted primarily of freshwater. The salinity ranged from 0.1 to 0.3 between 1.3 and 3.5 m depths. The temperature and density ranged from 0.8 to 0.7°C and 0 to 0.2 kg m⁻³, respectively, between 1.3 m and 3.5 m depths (Figure 6). The cast was made 48 minutes after the closure of two causeway gates, during low slack tide.

The CTD cast at 1354 h on March 27, 2002, shown in Figure 7, exhibits an apparent density inversion with depth. The salinity decreased from 6.6 to 2.6 between 0.7 and 6 m depths. The temperature increased from -0.16 to 0.24°C and the density calculated using temperature and salinity only decreased from 5.2 to 2.0 kg m⁻³, between 0.7 m and 6 m. The surface SPM was observed to be 16.4 g l⁻¹. Assuming the density of the suspended material to be 2650 kg m⁻³ the effective bulk density of the fluid would have been approximately 15.6 kg m⁻³. An SPM concentration of about 22 g l⁻¹ at 6 m would have resulted in a neutrally stable water column. The CTD cast was made during flood tide, one hour following tidal bore passage. No causeway gates were opened during this cast, although the low salinity throughout the water column indicates that the river consisted primarily of freshwater. The low water temperatures on March 26 and March 27, 2002, reflect winter conditions.

On October 9, 2002, the opening of one causeway gate created a low salinity water column from 1717 – 1742 h. The salinity throughout the water column ranged from 0.2 to 0.5 during this time (Figure 8). Following passage of the tidal bore at 1740 h, there was an increase in the salinity below 1 m depth, associated with the flood tide. During high slack tide the salinity increased below 1.25 m depth and a maximum salinity of 19 was observed at 3.5 m depth. The surface freshwater observed from 1844 – 1949 h had an average salinity of 0.5. The water temperature ranged from 12 – 13°C throughout the survey, with slightly colder water observed at depth, associated with the flood tide (Figure 8). The warmer water temperatures compared to March 2002 reflect the mid-fall conditions in October 2002. The density during this survey exhibited similar behaviour to salinity (Figure 8). Between 1717 – 1742 h the average density was -0.3 kg m⁻³. Following passage of the tidal bore the density increased below 1 m depth, with a maximum density of 14.0 kg m⁻³ observed during high slack tide. The increased density at depth was associated with the flood tide water mass.

The survey on March 19, 2003, occurred during ebb tide. No causeway gates were opened during this survey, although the water column consisted of low salinity water. Throughout the survey the salinity remained uniform with depth, while the depth-averaged salinity decreased from 4.9 to 0.3 between 2019 – 2208 h (Figure 9). The temperature was approximately -0.1°C throughout the water column during this survey. A temperature of 2.1°C, however, was

observed at 1.25 m depth at 2139 h (Figure 9). The density remained uniform with depth, while the depth-averaged density decreased from 3.8 to 0 kg m⁻³ between 2019 – 2208 h (Figure 9).

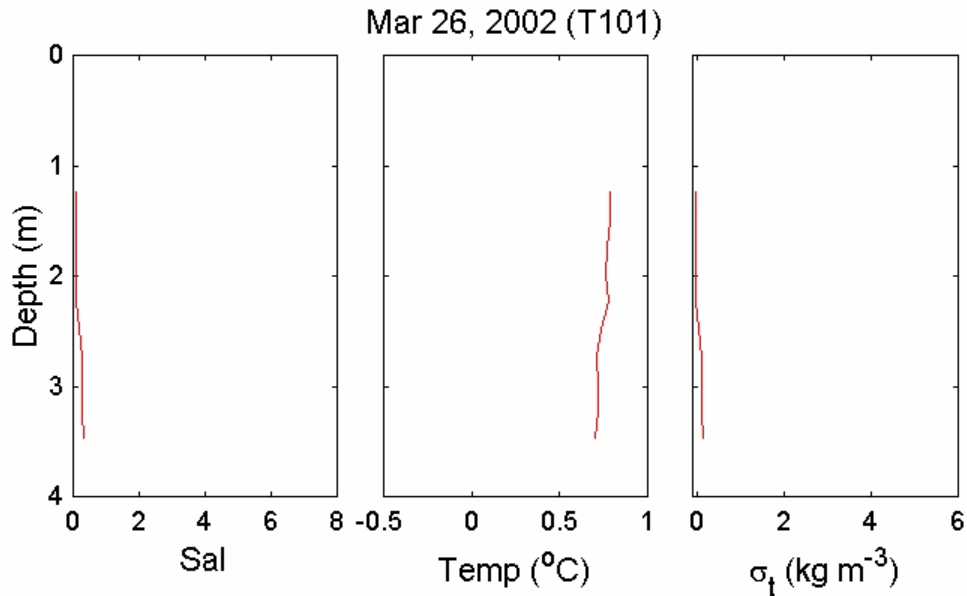


Figure 6. Salinity (Sal), temperature (Temp), and density (σ_t) versus depth at the thalweg position of Transect 101, March 26, 2002, at 1923 h.

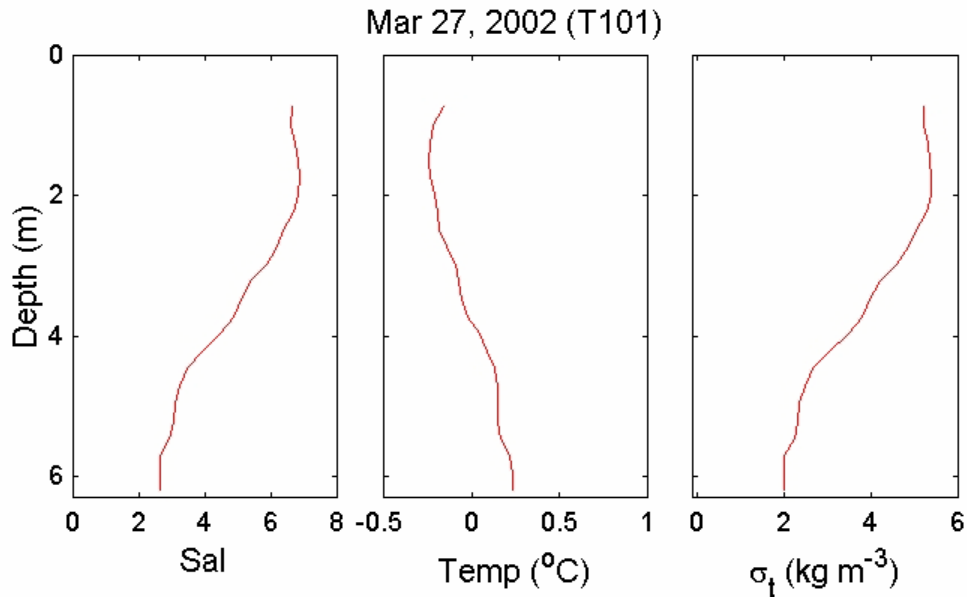


Figure 7. Salinity (Sal), temperature (Temp), and density (σ_t) versus depth at the thalweg position of Transect 101, March 27, 2003, at 1354 h.

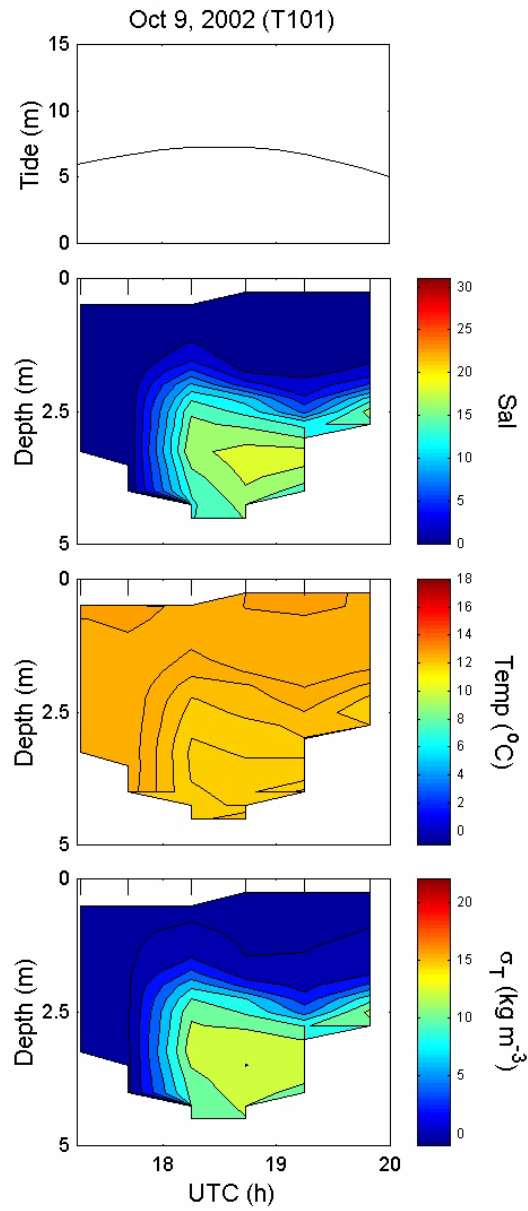


Figure 8. Salinity (Sal), temperature (Temp), and density (σ_T) versus time at the thalweg position of Transect 101, October 9, 2003. An extended tick indicates the time that a profile was collected.

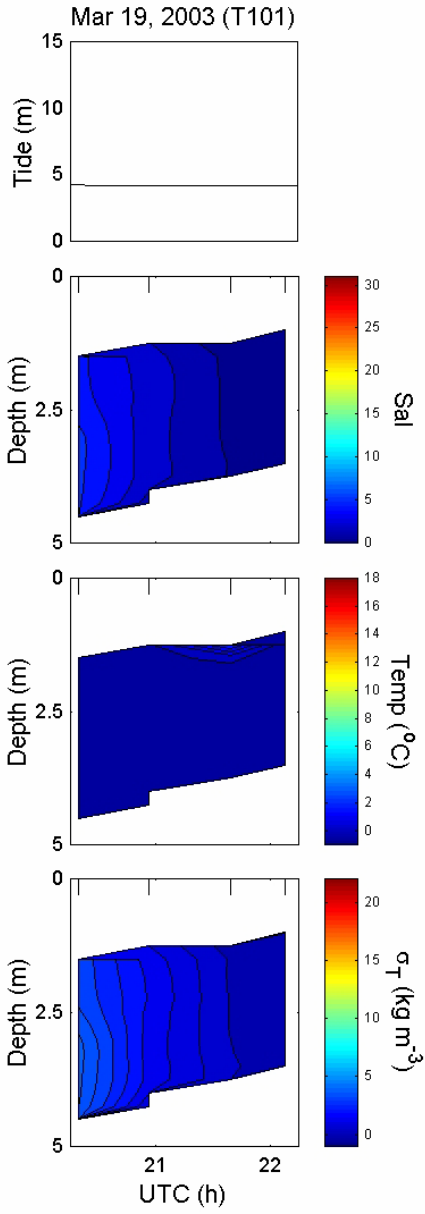


Figure 9. Salinity (Sal), temperature (Temp), and density (σ_T) versus time at the thalweg position of Transect 101, March 19, 2003. An extended tick indicates the time that a profile was collected.

On March 20, 2003, one causeway gate was opened from 1236 – 1453 h. During this survey the water column consisted of low salinity water. Between 1502 – 1728 h, the depth-averaged salinity only was 0.3, with a minimum and maximum salinity of 0.1 and 0.5, respectively (Figure 10). At 1812 h, the salinity increased at depth due to the flood tide. A maximum salinity of 7.8 was observed at 6 m depth during high slack tide, at 1843 h. Slightly increased salinity water was observed at depth throughout the remainder of the survey. The temperature was approximately 0°C throughout the survey, with the lowest temperature observed at 6 m depth during slack high tide (Figure 10). The density exhibited behaviour similar to salinity during the survey. The highest density of 5.9 kg m⁻³ was observed at 6.25 m depth during slack high tide (Figure 10). The lowest temperature and highest density were associated with the saltwater intrusion. The low temperatures during this survey are similar to those observed in March 2002, during winter conditions.

The CTD survey on May 14, 2003, was performed during one tidal period. During this survey one causeway gate was opened for fish passage between 1032 – 1339 h. Between 1226 – 1402 h, the depth-averaged salinity was 0.31 (Figure 11). As the flood tide progressed, higher salinity water was observed at depth, with a salinity of 5.0 observed at 6.5 m depth at 1504 h. This was the highest salinity observed during the survey and was observed during high slack tide. The depth-averaged water temperature during the survey was 7.4°C, with a minimum and maximum temperature of 6.9 and 7.7°C, respectively (Figure 11). The water temperatures during this survey were higher than those observed in March 2003. The density behaved similarly to salinity during this survey. Between 1226 – 1402 h, the depth-averaged density was 0.13 kg m⁻³ (Figure 11). A maximum density of 3.8 kg m⁻³ was observed at 6.5 m depth during slack high tide.

Last, the survey on September 12, 2003, reflects late-summer conditions. No causeway gates were opened prior to or during the survey. The CTD survey was carried out between 1727 – 1759 h, during slack high tide. During this time, an apparent density inversion was observed in the water column when the effect of the SPM concentration on the fluid density was not considered. The time-averaged salinity was 26.7 at 2 m depth and 25 at 3.75 m depth (Figure 12). The time-averaged density was 19.5 kg m⁻³ at 2 m depth and 18 kg m⁻³ at 3.75 m depth (Figure 12). The average temperature was 16.4°C, and remained uniform throughout the water column during the survey (Figure 12).

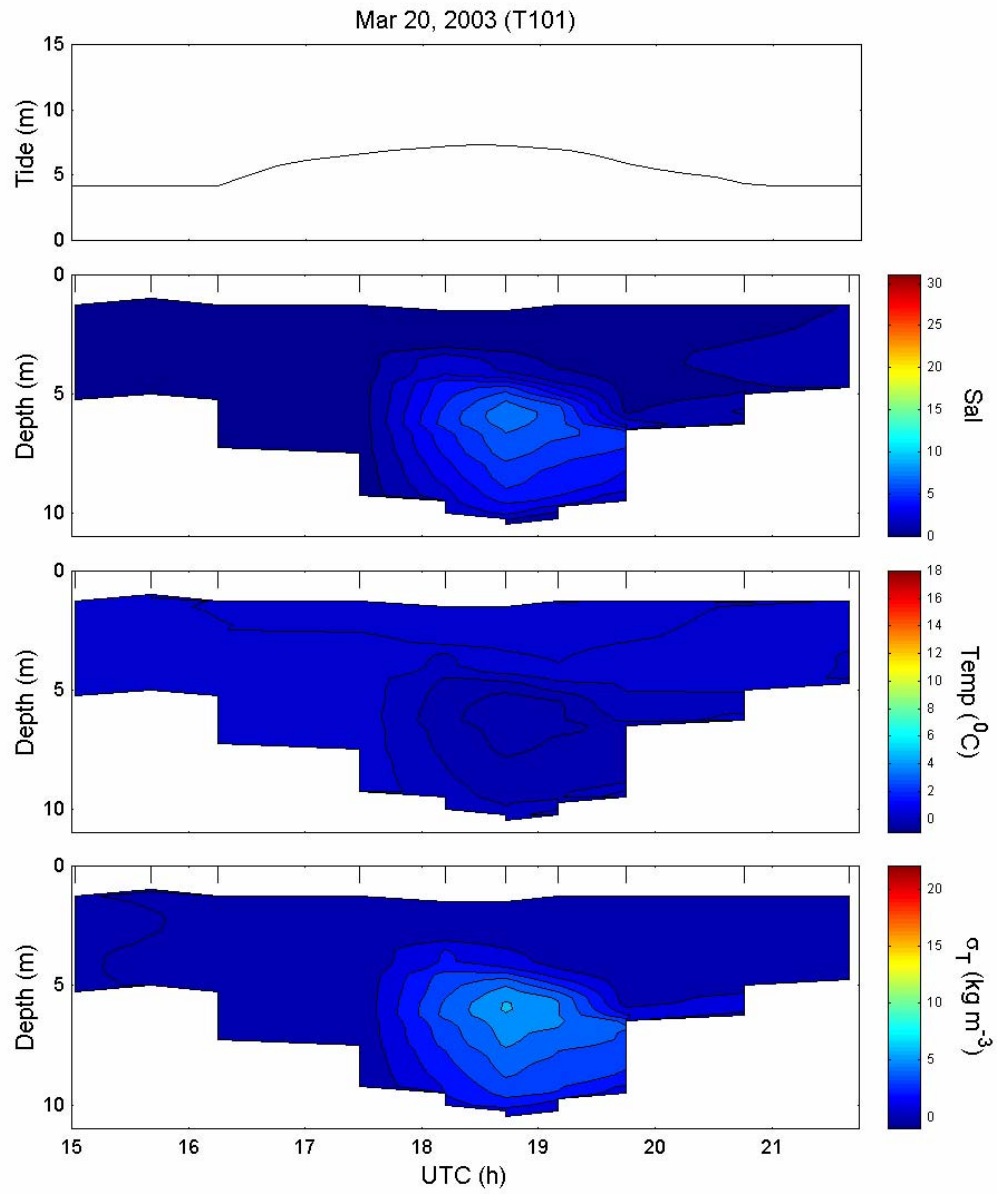


Figure 10. Salinity (Sal), temperature (Temp), and density (σ_T) versus time at the thalweg position of Transect 101, March 20, 2003. An extended tick indicates the time that a profile was collected.

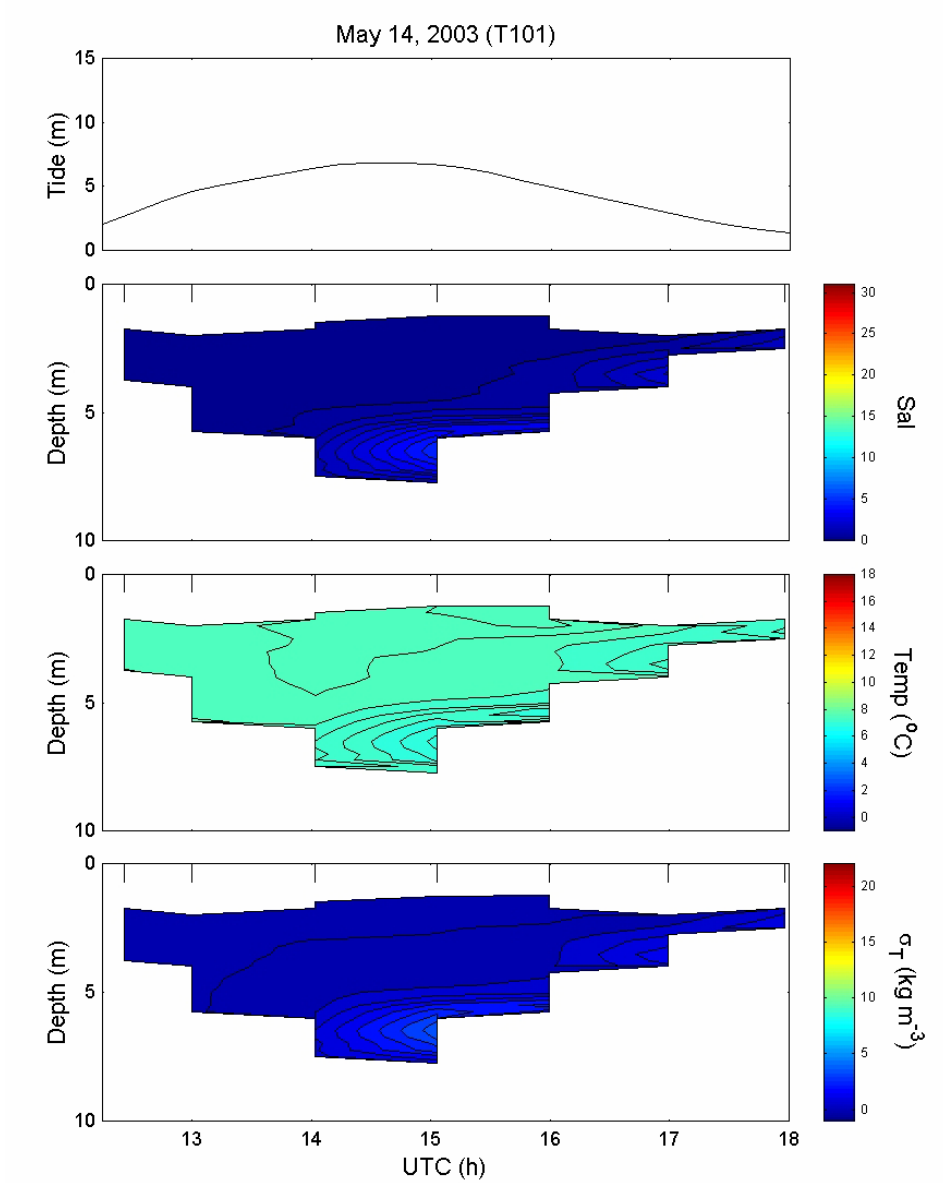


Figure 11. Salinity (Sal), temperature (Temp), and density (σ_t) versus time at the thalweg position of Transect 101, May 14, 2003. An extended tick indicates the time that a profile was collected.

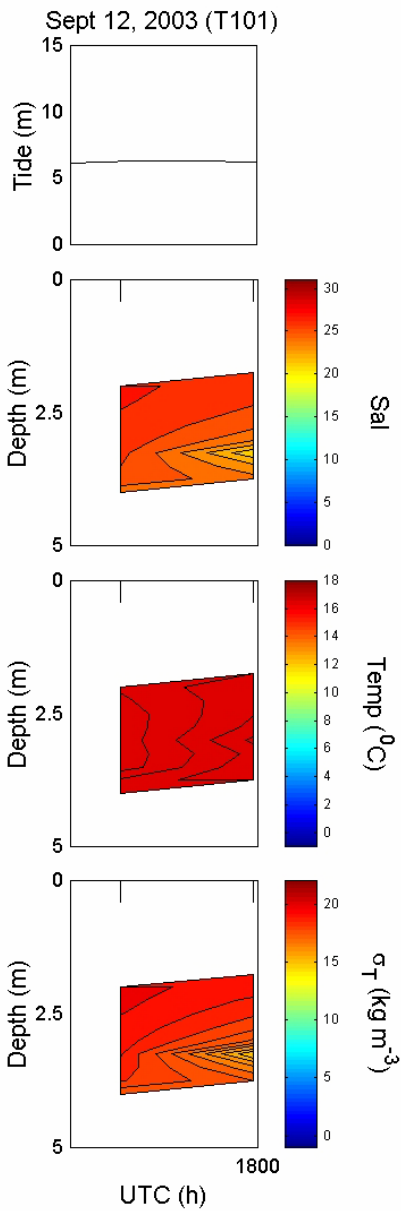


Figure 12. Salinity (Sal), temperature (Temp), and density (σ_t) versus time at the thalweg position of Transect 101, September 12, 2003. An extended tick indicates the time that a profile was collected.

3.1.3 Salinity, OBS, and dissolved oxygen profiles

The OBS voltage on March 26, 2002, at 1923 h, increased from 1.5 to 1.8 volts between 1.2 to 2 m depths, and then decreased to -0.01 volts at 3.5 m depth, suggesting the presence of a high sediment concentration at this depth (Figure 13). The dissolved oxygen concentration was approximately 7.1 ml l^{-1} between 1.2 to 2.5 m depths, and then increased to 7.5 ml l^{-1} at 3.5 m depth (Figure 13). Slack low tide was at 1852 h. At 1354 h on March 27, 2002, the OBS decreased from 0.2 to 0 volts between 1.2 and 6.2 m depths (Figure 14). The dissolved oxygen concentration increased from 5.7 to 7.0 ml l^{-1} between 1.2 to 5.7 m depths, then slightly decreased to 6.8 ml l^{-1} at 6.2 m depth (Figure 14). The survey was performed one hour after the passage of the tidal bore. An apparent density inversion was observed during this survey, which correlated with the rapid decrease in OBS towards the bottom and further supports the presence of high SPM concentrations (Figure 7). On October 9, 2002, the average dissolved oxygen concentration above 1.5 m depth increased from 4.7 to 5.3 ml l^{-1} during the survey (Figure 15). Between 1717 – 1815 h the average dissolved oxygen concentration below 1.5 m depth decreased from 4.9 to 4.3 ml l^{-1} , the 4.3 ml l^{-1} being observed during slack high tide. No OBS measurements were made during this survey (Figure 15).

On March 19, 2003, the OBS voltage remained almost uniform throughout the water column, although it slightly increased between 2.5 m depth and the surface at 2019 – 2139 h. At 2208 h, the OBS was -0.04 volts at 3.5 m depth (Figure 16). This was observed as the water level approached slack low tide. The depth-averaged dissolved oxygen concentration increased from 6.8 to 10.4 ml l^{-1} during this survey. The dissolved oxygen concentration value of 10.4 ml l^{-1} is high and perhaps reflects error associated with the uncalibrated DO sensor. The highest dissolved oxygen concentration of 11.7 ml l^{-1} was observed at 3.8 m, during ebb tide (Figure 16). On March 20, 2003, the time-averaged OBS in the upper 5 m was 1.5 volts, with a maximum OBS of 2.1 volts observed at 2.5 m depth, prior to high slack tide at 1730 h (Figure 17). Below 5 m depth the time-averaged OBS was 0.6 volts. The lowest OBS of -0.2 volts was observed near the bottom at 1615 h, approximately 30 minutes following the tidal bore passage. The dissolved oxygen exhibited a maximum depth-averaged concentration of 8.6 ml l^{-1} at 1541 h, which was associated with passage of the tidal bore (Figure 17). The depth-averaged dissolved oxygen concentration was approximately 7.0 ml l^{-1} for the remainder of the survey.

On May 14, 2003, OBS at or below 0 volts was observed near the bottom throughout the survey (Figure 18). At 1402 h, a low depth-averaged OBS of 0.07 volts was observed up to 3 m above the bottom. In addition, low OBS also was observed in surface waters during high slack tide. High slack tide was at 1430 h. At 2.3 m depth, the time-averaged OBS was 1.5 volts. The depth-averaged dissolved oxygen concentration in the upper 5 m was 7.1 ml l^{-1} , with the highest value of 7.9 ml l^{-1} observed at 1.8 m depth at 1402 h (Figure 18). The lowest

dissolved oxygen concentration of 4.5 ml l^{-1} was observed at 7.8 m depth during slack high tide.

Last, on September 12, 2003, the depth-averaged OBS increased from 0.01 to 2.0 volts in the upper 2 m during the survey (Figure 19). Below 2 m depth, the depth-averaged OBS only increased from 0.0 to 0.06 volts. Field surveyors noted high suspended sediment concentrations in the water column following passage of the tidal bore at 1616 h. Slack high tide was at 1728 h. The depth-averaged dissolved oxygen concentration increased from 1.8 to 2.9 ml l^{-1} during the survey (Figure 19). These were the lowest depth-averaged dissolved oxygen concentrations observed for all surveys at Transect 101.

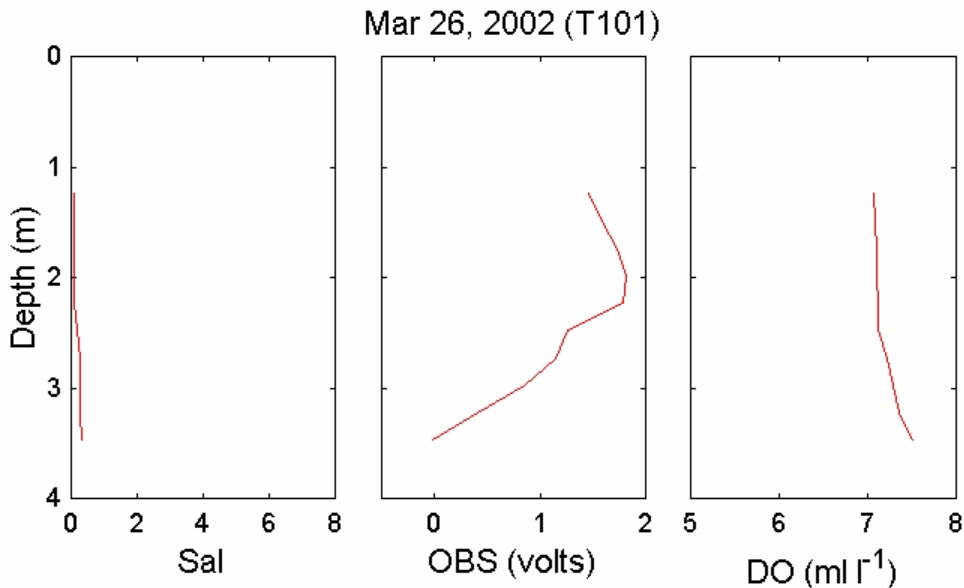


Figure 13. Salinity (Sal), optical backscatter (OBS), and dissolved oxygen concentration (DO) versus depth at the thalweg position of Transect 101, March 26, 2002, at 1923 h.

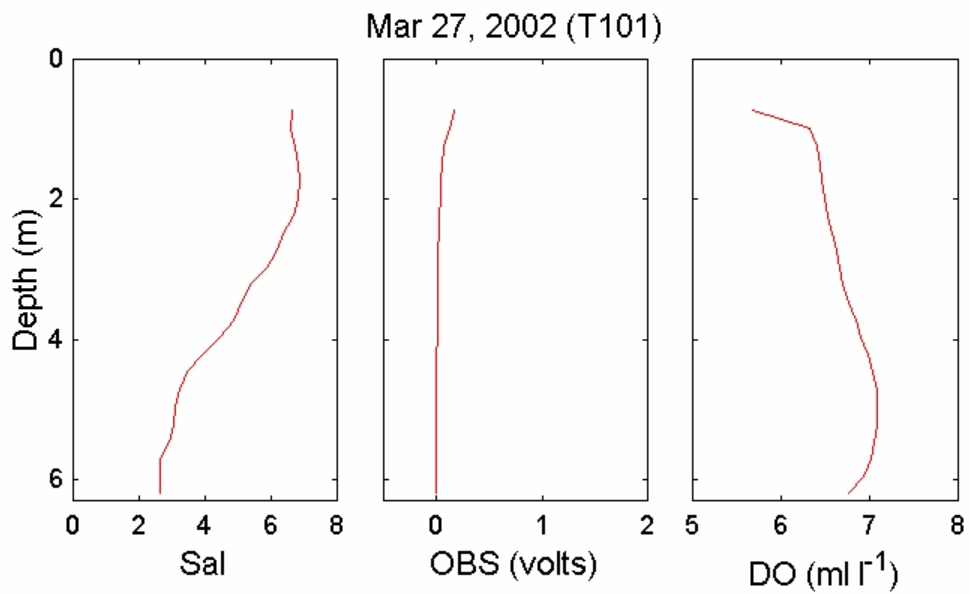


Figure 14. Salinity (Sal), optical backscatter (OBS), and dissolved oxygen concentration (DO) versus depth at the thalweg position of Transect 101, March 27, 2002, at 1354 h.

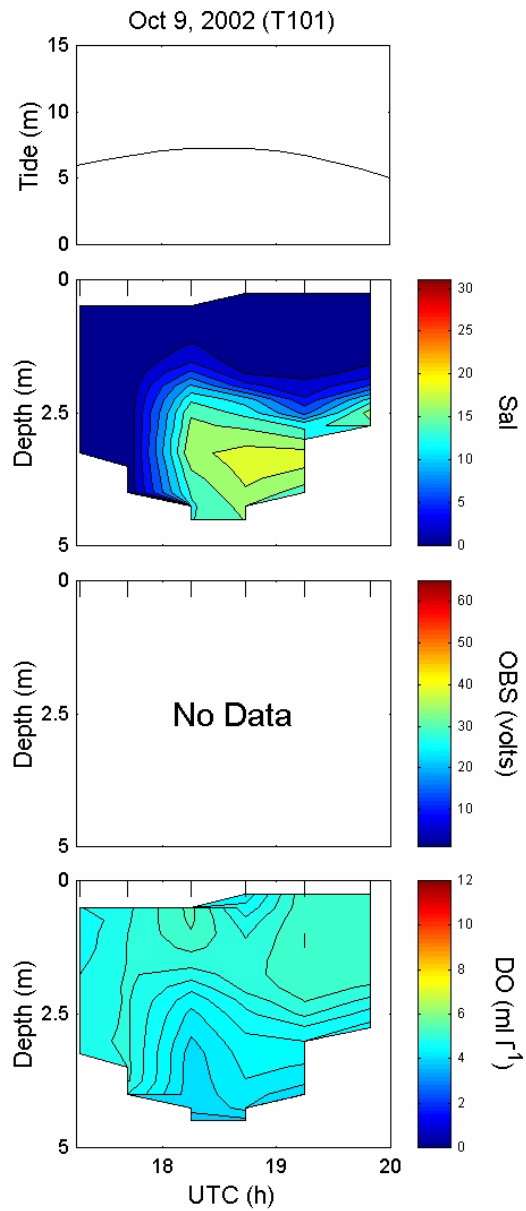


Figure 15. Salinity (Sal), optical backscatter (OBS), and dissolved oxygen concentration (DO) versus time at the thalweg position of Transect 101, October 9, 2002. An extended tick indicates the time that a profile was collected.

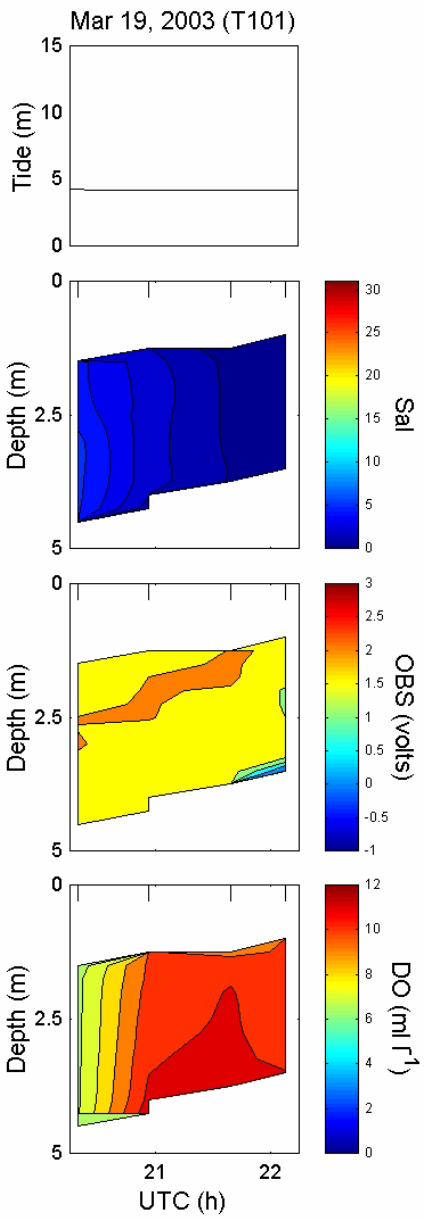


Figure 16. Salinity (Sal), optical backscatter (OBS), and dissolved oxygen concentration (DO) versus time at the thalweg position of Transect 101, March 19, 2003. An extended tick indicates the time that a profile was collected.

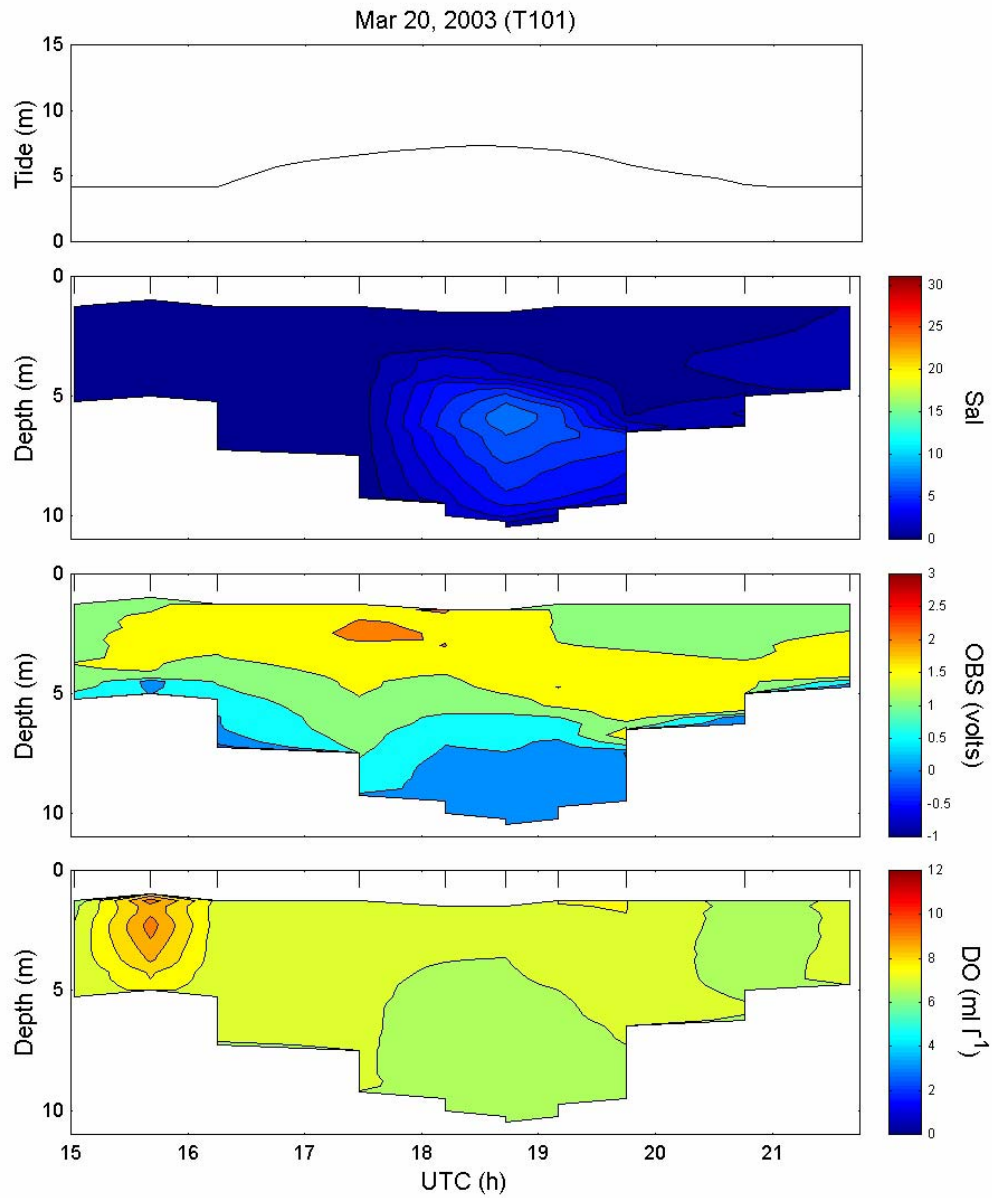


Figure 17. Salinity (Sal), optical backscatter (OBS), and dissolved oxygen concentration (DO) versus time at the thalweg position of Transect 101, March 20, 2003. An extended tick indicates the time that a profile was collected.

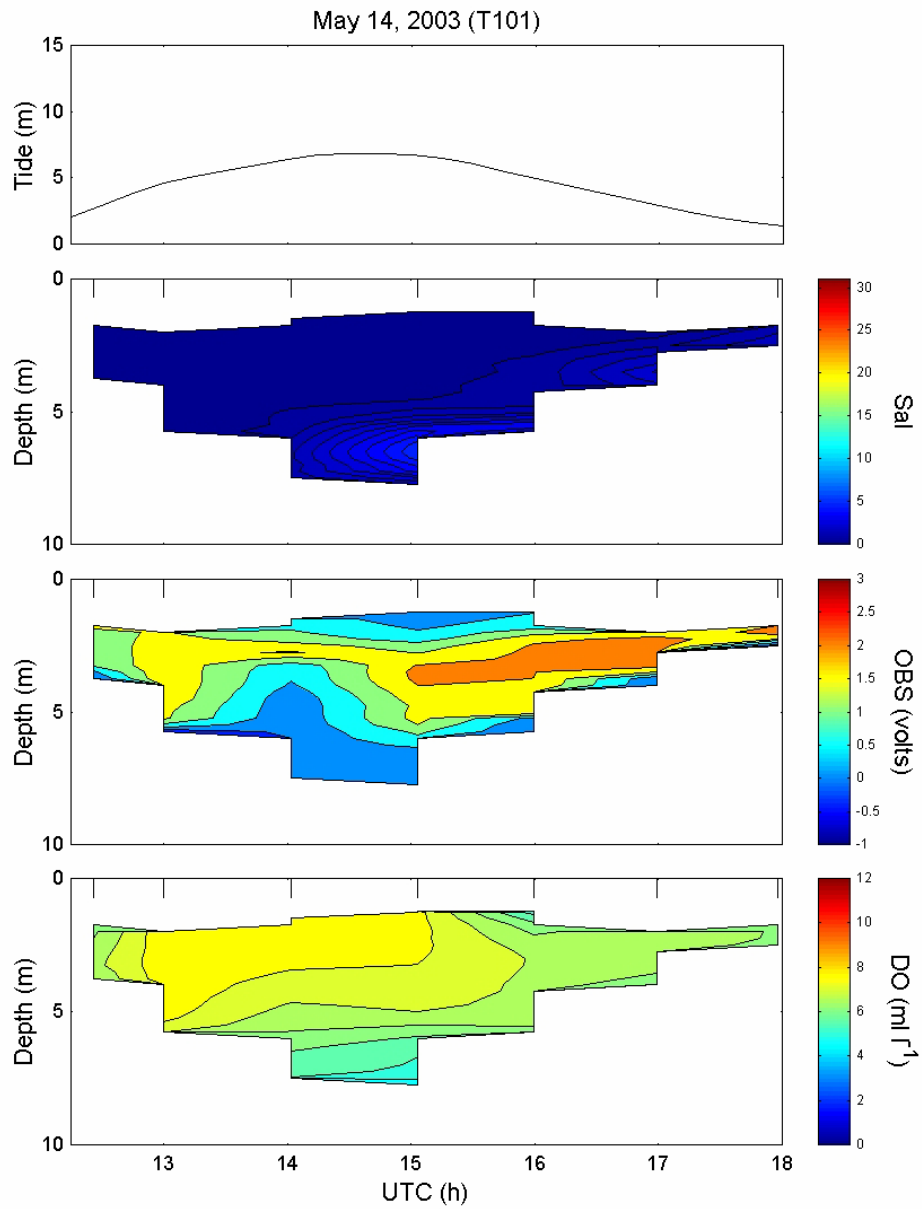


Figure 18. Salinity (Sal), optical backscatter (OBS), and dissolved oxygen concentration (DO) versus time at the thalweg position of Transect 101, May 14, 2003. An extended tick indicates the time that a profile was collected.

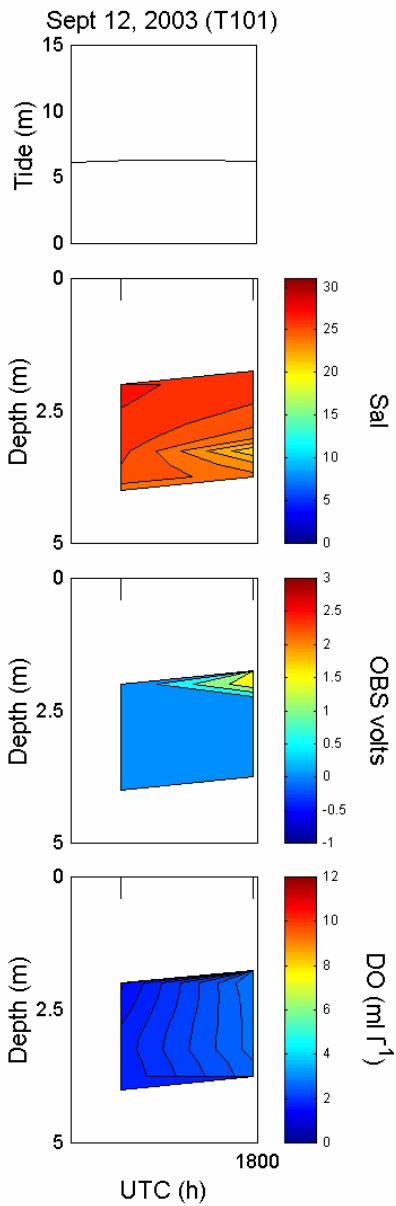


Figure 19. Salinity (Sal), optical backscatter (OBS), and dissolved oxygen concentration (DO) versus time at the thalweg position of Transect 101, September 12, 2003. An extended tick indicates the time that a profile was collected.

3.1.4 Discrete salinity, SPM, and velocity

The discrete physical measurements were used to support the observations made by the profiling instrumentation and permit inter-survey comparison at Transect 101 (Figure 20). On March 26, 2002, all measurements were made between 1651 – 1906 h, during ebb to low slack tide. The salinity at 0.5 m depth decreased from 0.8 to 0.1 during the survey. The causeway gates were opened from 1635 – 1835 h, while from 1651 – 1906 h the SPM at 0.5 m depth decreased from 37.3 to 1.8 g l⁻¹. The downstream velocity at 3.5 m depth reversed from 2.1 m s⁻¹ at 1756 h to an upstream velocity of 0.1 m s⁻¹ at 1911 h. Low slack tide was at 1852 h.

On March 27, 2002, discrete samples were collected between 1254 – 1354 h, during flood tide (Figure 20). The tidal bore passed at 1250 h, while causeway gates were not opened until 1710 h. As the flood tide progressed salinity at 0.5 m depth increased from 1.6 to 6.8. At 1254 h following tidal bore passage, SPM at 0.5 m depth was 67.8 g l⁻¹, which then decreased to 20.6 g l⁻¹ at 1305 h. At 1312 h, the near surface SPM was 80.2 g l⁻¹, which was the highest concentration observed during the survey. The SPM then decreased to 16.6 g l⁻¹ by 1354 h. The variable near surface SPM following tidal bore passage may reflect sediment heterogeneity due to turbulence associated with the tidal bore. No velocity measurements were made during this survey.

On October 9, 2002, salinity at 0.5 m depth increased from 3.9 to 6.1, between 1323 – 1502 h (Figure 20). At approximately 1500 h, two causeway gates were opened, which is reflected by the small increase in water level at this time. Following gate opening the near surface salinity decreased, ranging from 0.1 to 0.6, despite the saltwater intrusion associated with the flood tide. Prior to the causeway gate opening, SPM at 0.5 m depth ranged from 7.1 to 100.8 g l⁻¹. The highest SPM of 252.4 g l⁻¹ was observed following passage of a 0.25 m wave downstream, which was associated with freshwater discharged during gate opening. In contrast, only a slight increase in SPM, from 6.7 to 11.5 g l⁻¹, was observed following passage of the tidal bore at 1552 h. The SPM then decreased to 0.3 g l⁻¹ by 2000 h. The upstream velocity at 3.5 m depth ranged from 0.04 to 0.54 m s⁻¹ between 1647 – 1917 h, during flood tide. Slack high tide was at 1830 h. The causeway gates were closed at this time. On the ebb tide, the velocity increased downstream to a maximum of 0.87 m s⁻¹ at 2002 h.

On March 19, 2003, salinity at 0.5 m depth increased from 0.1 at 1215 h to a maximum of 8.4 at 1715 h (Figure 20). No causeway gates were opened during this survey. The highest salinity values were observed following passage of the tidal bore. The salinity then decreased during ebb tide to 4.2 by 2215 h. The SPM at 0.5 m depth increased from 2.1 g l⁻¹ at 1215 h to 36.3 g l⁻¹ after passage of the tidal bore at 1515 h. The maximum SPM of 45.8 g l⁻¹ was observed 30 mins. after tidal bore passage. The near surface SPM then decreased during ebb tide to 1.5 g l⁻¹ at 2215 h. The velocity at 0.5 m depth was 1 m s⁻¹

downstream at 1854 h, during ebb tide. The downstream velocity slowed to 0.4 m s^{-1} at 2148 h. Slack low tide was at 2330 h.

On March 20, 2003, the time-averaged salinity at 0.5 m depth was 4.1, prior to gate opening (Figure 20). One causeway gate was opened at 1236 h, which was marked by a decrease in salinity to 0.2 at 1345 h. Salinity at 0.5 m depth remained low during the next tidal cycle even though the gate was closed at 1453 h. The salinity 0.5 m above the bottom, however, increased to a maximum of 5.5, during the subsequent flood tide following gate closure. The SPM at 0.5 m depth increased to a maximum of 59.3 g l^{-1} following gate opening, then decreased to 3.5 g l^{-1} . The highest observed SPM concentration 0.5 m above the bottom was 12.2 g l^{-1} , which occurred during ebb tide. Passage of the tidal bore did not appear to increase the SPM concentration during this survey. The velocity at 0.5 m depth was 0.1 m s^{-1} downstream, during low slack tide. Following gate opening the downstream velocity increased to 3.1 m s^{-1} at 1251 h, then decreased to 2.4 m s^{-1} at 1547 h. During flood tide the surface velocity remained downstream at approximately 1 m s^{-1} , despite the gate being closed at this time. The downstream surface velocity then reversed to 0.3 m s^{-1} upstream during high slack tide, and then subsequently increased downstream again, to a maximum of 0.7 m s^{-1} during ebb tide. The downstream velocity at 3.5 m depth ranged from 1.2 to 1.8 m s^{-1} during the gate opening, and then decreased to 0.4 m s^{-1} downstream immediately following gate closure. The velocity at 3.5 m depth then increased in an upstream direction during flood tide, reaching a maximum of 0.94 m s^{-1} at 1533 h. The velocity at 3.5 m depth slowed to 0 m s^{-1} during slack high tide, then increased downstream during ebb tide to a maximum of 0.99 m s^{-1} at 2004 h.

On May 14, 2003, both surface and bottom salinity remained below 1 during the entire survey (Figure 20). One causeway gate was opened from 1032 – 1339 h. The maximum SPM at 0.5 m depth was 75.3 g l^{-1} following gate opening. The time-averaged SPM then decreased to 2.8 g l^{-1} throughout the water column. The tidal bore passage did not significantly increase SPM in the water column. The downstream velocity at 0.5 m depth was 2 m s^{-1} following gate opening, although the velocity direction reversed to 0.5 m s^{-1} upstream after passage of the tidal bore. The surface velocity then increased downstream to 0.6 m s^{-1} at 1713 h, during the ebb tide. The velocity at 3.5 m depth was 0.5 m s^{-1} upstream during flood tide, and then remained near 0 m s^{-1} upstream during slack high tide and ebb tide.

Last, on September 12, 2003, salinity at 0.5 m depth increased from 6.5 to 28 during flood tide. A maximum salinity at 0.5 m depth above the bottom of 27.9 was observed during slack high tide. The salinity subsequently decreased with the ebb tide. A maximum SPM at 0.5 m depth of 150.7 g l^{-1} was observed following tidal bore passage, then subsequently decreased towards slack high tide. At 1728 h, SPM at 0.5 m depth only was 11.7 g l^{-1} , while an SPM of 50 g l^{-1} was observed at 0.5 m depth above the bottom at 1737 h. The near surface

SPM decreased to 0.6 g l^{-1} during slack high tide, and then increased to 24.9 g l^{-1} during ebb tide. No velocity measurements were made during this survey.

3.1.5 Discrete salinity and nutrients

The silicate concentrations at 0.5 m depth ranged from 21.7 to $102.1 \mu\text{M}$, phosphate concentrations ranged from 0.1 to $2.8 \mu\text{M}$, nitrate concentrations ranged from 1.5 to $52.0 \mu\text{M}$, nitrite concentrations ranged from 0.1 to $2.7 \mu\text{M}$, and ammonia concentrations ranged from 0.3 to $50.5 \mu\text{M}$ (Figure 21). Ammonia levels often exceeded $20 \mu\text{M}$. On March 26, 2002, the ammonia sample at 1651 h was $23.8 \mu\text{M}$, following slack high. Two causeway gates were opened from 1635 – 1835 h. On March 27, 2002, there was an increase in the ammonia concentration from 24.5 to $45.3 \mu\text{M}$ following passage of the tidal bore at 1250 h. On October 9, 2002, all ammonia concentrations were less than $20 \mu\text{M}$. Two causeway gates were opened during flood tide. On March 19, 2003, an increase in the ammonia concentration was observed following passage of the tidal bore at 1500 h. In contrast, on March 20, 2003, ammonia concentrations were initially high and then decreased following opening of one causeway gate at 1239 h. Elevated ammonia concentrations in some samples also were observed following passage of the tidal bore at 1539 h. All ammonia concentrations were less than $20 \mu\text{M}$ on May 14, 2003. Last, ammonia concentrations were low on September 12, 2003, although elevated concentrations were observed immediately following passage of the tidal bore at 1616 h. The causeway gates were not opened until 1924 h during this survey.

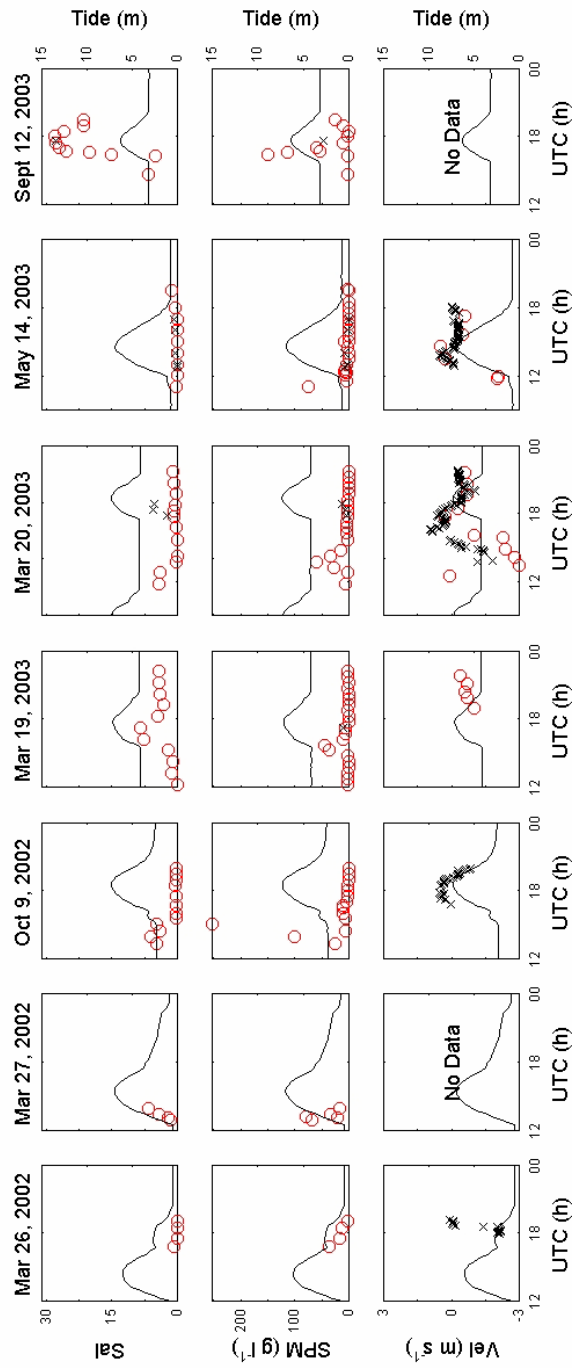


Figure 20. Salinity (Sal), suspended particulate matter concentration (SPM), and velocity (Vel) versus time at the thalweg position of Transect 101. Discrete salinity and SPM samples were collected at 0.5 m depth (o) and 0.5 m above the bottom (x). OTT current meter velocities were collected at 0.5 m depth (o) and ADCP velocities at 3.5 m depth (x). Positive velocity values represent upstream velocity and negative values downstream velocity.

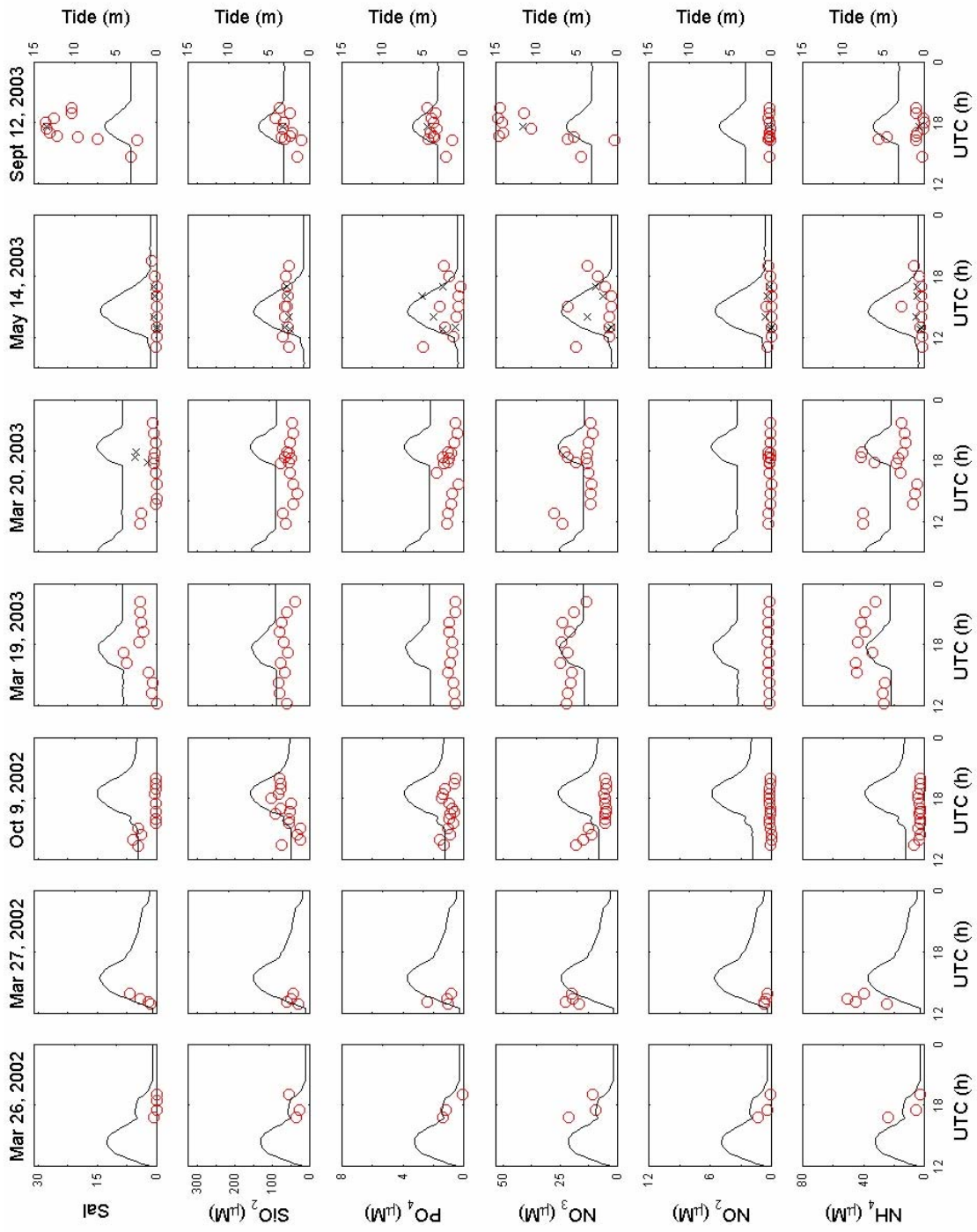


Figure 21. Salinity (Sal), silicate (SiO_2), phosphate (PO_4), nitrate (NO_3), nitrite (NO_2), and ammonia (NH_4) concentrations versus time at the thalweg position of Transect 101. Discrete nutrient samples were collected at 0.5 m depth (o) and 0.5 m above the bottom (x).

3.2 TRANSECT 21 (T21) NEAR OUTHOUSE POINT

One survey was performed at Transect 21 on May 15, 2003, between 1530 – 1700 h. During this survey, one causeway gate was opened from 0944 – 1525 h for fish passage. The tidal bore passed at 1205 h and slack high tide was at 1550 h. The survey was performed from slack high tide into the ebb tide.

3.2.1 ADCP velocity and backscatter profiles

On May 15, 2003, the downstream velocity at 1 m water depth was 0.90 m s^{-1} , 30 mins. following slack high tide and 1 h following causeway gate closure (Figure 22). The downstream velocity reached a maximum of 1.1 m s^{-1} during ebb tide, then decreased to 0.9 m s^{-1} downstream at 1654 h. At 1621 h, the downstream velocity at 5.5 m depth was 0.11 m s^{-1} , while near the bottom the downstream velocity reached a maximum of 0.69 m s^{-1} during ebb tide. The mean backscatter at 1 m depth was 101.5 dB during the survey (Figure 22). The backscatter decreased with depth, exhibiting a time-averaged value of 89.6 dB at 4 m depth. The white areas near the bottom on Figure 22 represent regions of no data collected by the ADCP instrument.

3.2.2 Salinity, temperature, and density profiles

During the May 15, 2003, CTD survey the water column consisted of low salinity water. Between 1456 – 1657 h, the salinity at 2.5 m depth decreased from 3.0 to 1.0 during ebb tide (Figure 23). The highest salinity was 9.0 at 4.25 m depth, during slack high tide. During the survey, lower salinity water was observed at the surface and at depth, compared to the salinity of the mid-water column. In contrast, warmer water was observed at the surface and bottom, with cooler temperatures observed in the mid-water column (Figure 23). This pattern also is reflected in the density structure of the water column, which exhibited a maximum of 7.0 kg m^{-3} at 4.25 m depth, during high slack tide (Figure 23). During the survey, the water column structure was dominated by the presence of freshwater discharged from behind the causeway during gate opening.

3.2.3 Salinity, OBS, and dissolved oxygen profiles

At 2.5 m depth, OBS increased from 0.8 to 2.1 volts between 1456 – 1657 h (Figure 24). The OBS was uniform to 5 m depth during the survey. Below 5 m depth, the time-averaged OBS was only 0.1 volts. The lowest OBS were observed at depth, where the ADCP instrument yielded no data (Figure 22). The time-averaged dissolved oxygen concentration increased from 5.8 to 7.5 ml l^{-1} during the survey (Figure 24). The dissolved oxygen concentration decreased with depth, while the concentration increased throughout the water column during ebb tide.

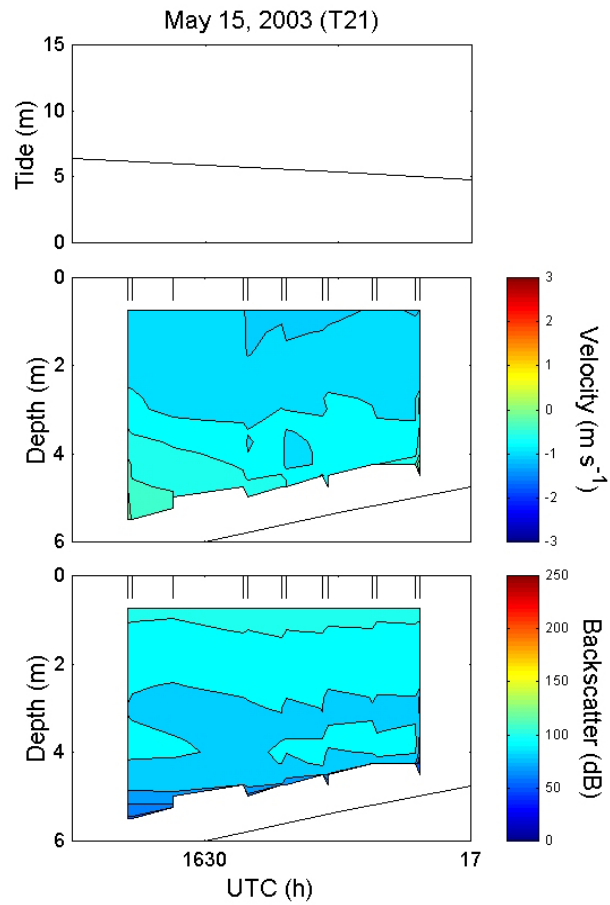


Figure 22. Velocity and backscatter versus time at the thalweg position of Transect 21, May 15, 2003. An extended tick indicates the time that an ADCP profile was collected. Positive velocity values represent upstream velocity and negative values downstream velocity. The black line represents the bottom depth estimated from CTD casts.

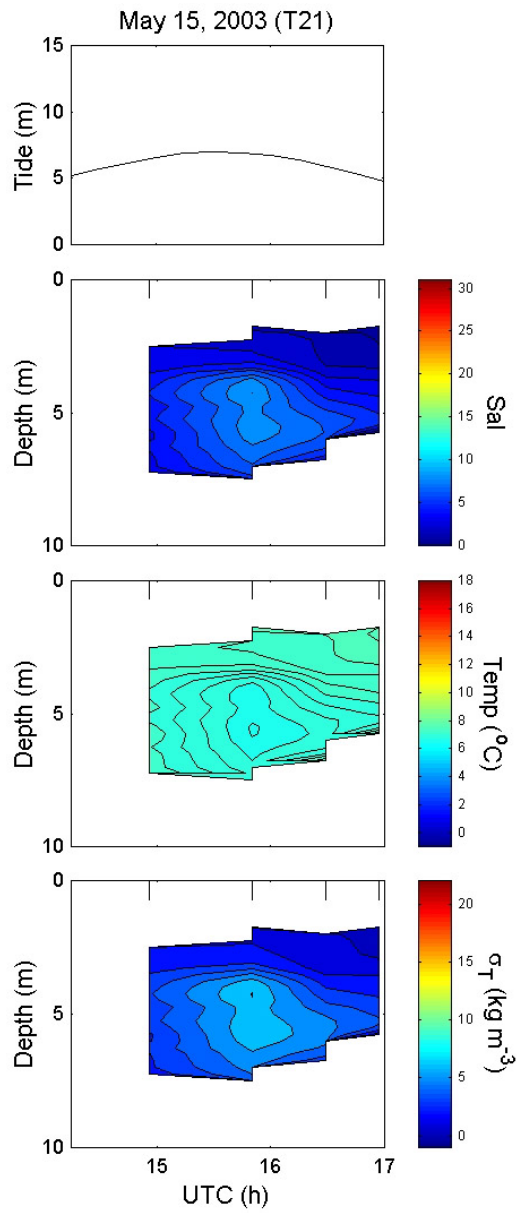


Figure 23. Salinity (Sal), temperature (Temp), and density (σ_T) versus time at the thalweg position of Transect 21, May 15, 2003. An extended tick indicates the time that a profile was collected.

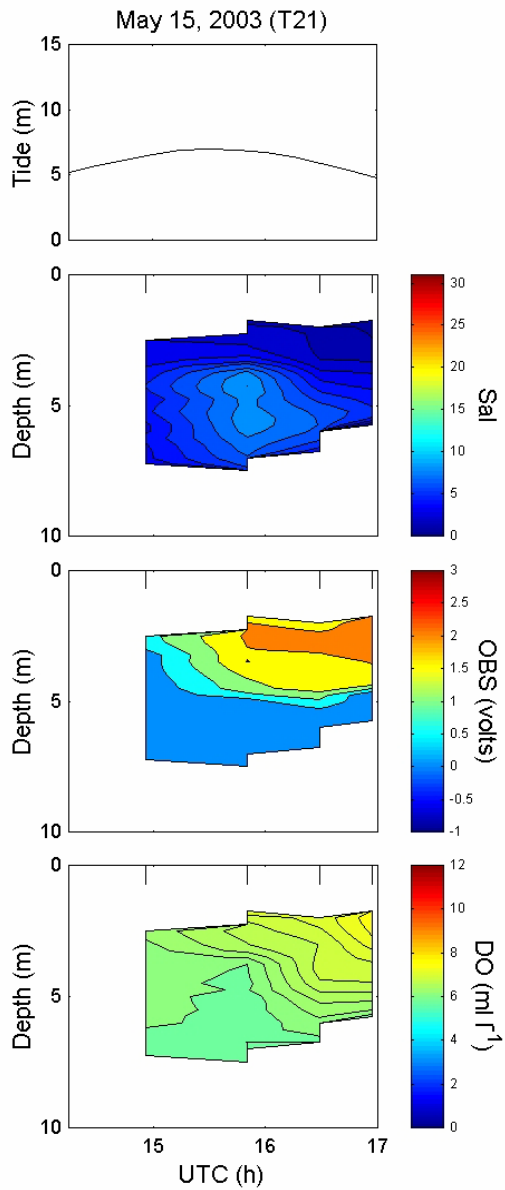


Figure 24. Salinity (Sal), optical backscatter (OBS), and dissolved oxygen concentration (DO) versus time at the thalweg position of Transect 21, May 15, 2003. An extended tick indicates the time that a profile was collected.

3.2.4 Discrete salinity, SPM, and velocity

The discrete physical measurements made on May 15, 2003, indicate that salinity slightly increased during flood tide, then decreased during high slack tide and ebb tide (Figure 25). A maximum salinity of 2.3 at 0.5 m depth was observed at 1538 h. The salinity at 0.5 m depth then decreased to 0.4 during ebb tide. The salinity 0.5 m above the bottom decreased from 8.0 to 7.2 between 1555 – 1630 h. The average SPM concentration at 0.5 m depth between 1555 – 1630 h was 1.8 g l^{-1} , and 20.0 g l^{-1} at 0.5 m depth above the bottom. The highest sediment concentrations were observed near the bottom (Figure 25). The downstream velocity was approximately 1 m s^{-1} at 0.5 m depth and 0.75 m s^{-1} at 0.5 m depth above the bottom (Figure 25). All measurements were made between slack high tide and ebb tide.

3.2.5 Discrete salinity and nutrients

For all nutrients, concentrations decreased from slack high tide to ebb tide (Figure 26). Silicate concentrations at 0.5 m depth decreased from 56.0 to 32.7 μM , phosphate concentrations decreased from 1.6 to 0.8 μM , nitrate concentrations decreased from 13.7 to 6.2 μM , nitrite concentrations decreased from 1.3 to 0.4 μM , and ammonia concentrations decreased from 7.6 to 3.8 μM . In general, nutrient concentrations at 0.5 m were similar to the concentrations measured at 0.5 m above the bottom. Nitrate concentrations, however, were approximately a factor of two higher than surface concentrations.

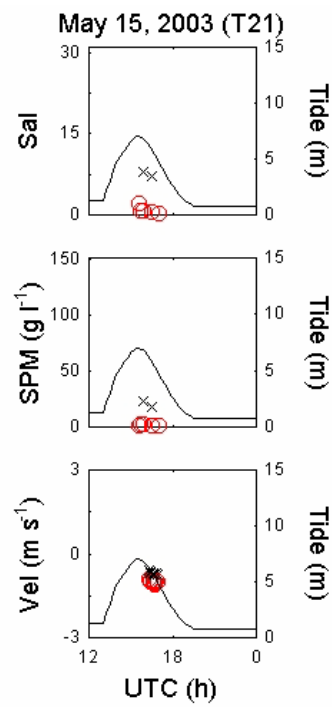


Figure 25. Salinity (Sal), suspended particulate matter concentration (SPM), and velocity (Vel) versus time at the thalweg position of Transect 21. Discrete salinity and SPM samples were collected at 0.5 m depth (o) and 0.5 m above the bottom (x). ADCP velocities were collected at 1 m depth (o) and 3.5 m depth (x).

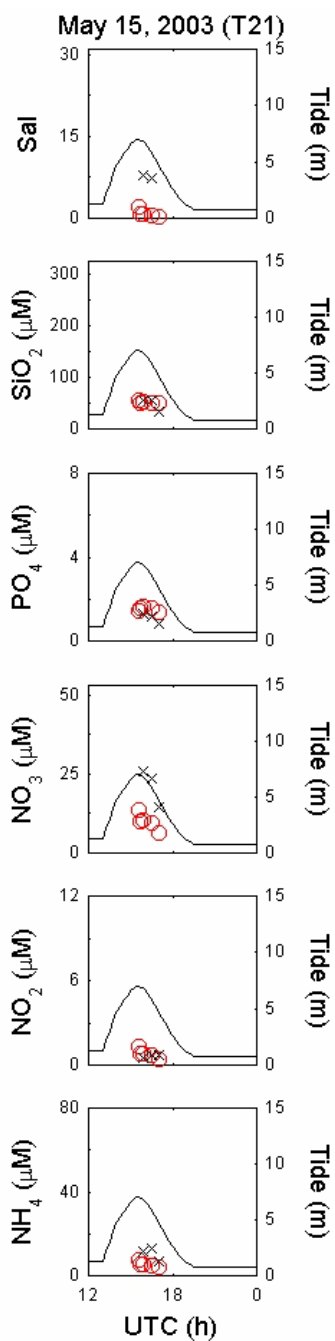


Figure 26. Salinity (Sal), silicate (SiO_2), phosphate (PO_4), nitrate (NO_3), nitrite (NO_2), and ammonia (NH_4) concentrations versus time at the thalweg position of Transect 21. Discrete samples were collected at 0.5 m depth (o) and 0.5 m above the bottom (x).

3.3 TRANSECT 11 (T11) NEAR DOVER

Two surveys were performed at Transect 11 in 2003, under different causeway gate operations. The survey on June 12, 2003, was performed from 1400 – 0300 h over one tidal period. During the survey one causeway gate was opened between 1004 – 1324 h for fish passage. Slack high tide was at 1500 h and slack low tide was at 2145 h. The tidal bore passed at 2244 h during the subsequent flood tide. The survey on September 9, 2003, was performed from 1430 – 0100 h, during similar tidal conditions to the survey on June 12. During the September 9 survey, one tidal gate was partially opened from 0959 – 1029 h, while two gates were partially opened from 1029 – 1117 h, following closure of the first gate. Slack high tide was at 1530 h and slack low tide was at 2230 h. The tidal bore passed at 2354 h, during the subsequent flood tide. On June 12, 2003, the single gate was fully opened for more than 4 h and was closed approximately 0.5 h prior to surveying. On September 9, 2003, the gates were partially opened for approximately 1.5 h, then closed more than 3 h prior to surveying.

3.3.1 ADCP velocity and backscatter profiles

On June 12, 2003, the downstream velocity remained uniform with depth during ebb tide from 1530 – 1900 h (Figure 27). During ebb tide, the maximum depth-averaged velocity was 2.3 m s^{-1} downstream, at 1724 h. The depth-averaged downstream velocity then decreased to 0.71 m s^{-1} at 1900 h. Between 2000 – 2300 h, the downstream velocity near the bottom approached 0 m s^{-1} . During slack low tide, a low downstream velocity was observed above the region of no data (Figure 27). Following tidal bore passage the depth-averaged upstream velocity was 2.6 m s^{-1} at 2323 h. The minimum backscatter during this survey was 40 dB at 2.2 m depth, during low slack tide (Figure 27). The maximum backscatter of 113 dB at 1 m depth was observed following passage of the tidal bore. In general, backscatter decreased with depth throughout the survey, while the highest backscatter at depth moved down through the water column during slack low tide. In addition, the region of no data increased in thickness above the bottom during ebb and flood tides, while the region of no data above the bottom also was thicker during slack low tide compared to slack high tide (Figure 27).

On September 9, 2003, the downstream velocity decreased with depth during ebb tide (Figure 28). Through time, the downstream velocity increased from 1.1 to 2.5 m s^{-1} at 1 m depth, between 1618 – 1731 h. The velocity also remained greater than 0 m s^{-1} above the region of no data. At 1945 h, the depth-averaged velocity was 0.13 m s^{-1} downstream, towards slack low tide. The region of no data was thickest during maximum ebb tide. The backscatter on September 9 was highest in the surface waters and decreased with depth during the survey. The maximum backscatter at 1 m depth was 116 dB at 1724 h (Figure 28). As the ebb tide approached slack low tide and the velocity decreased, the near bottom backscatter approached 0 dB. Backscatter less than 0 dB also was

observed and likely reflects error with the instrument due to extremely high sediment concentrations.

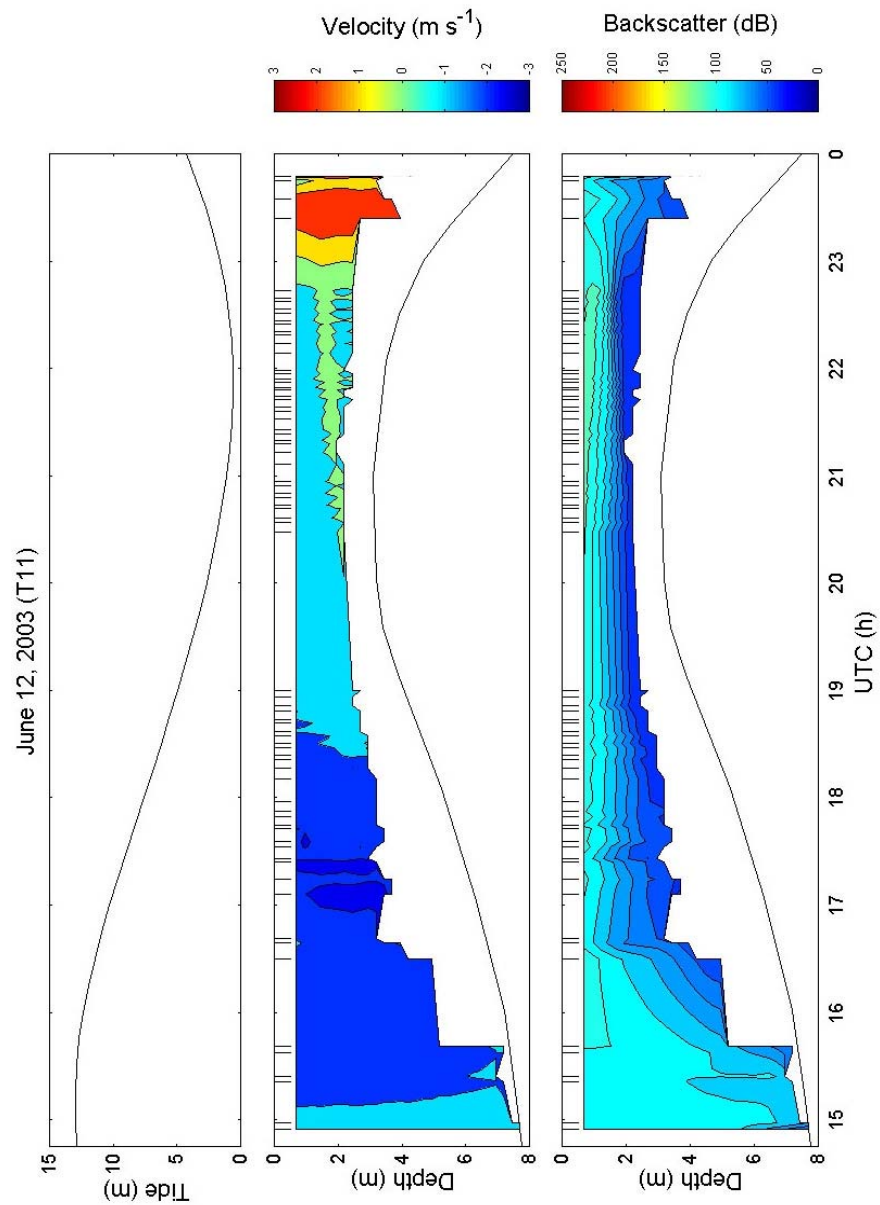


Figure 27. Velocity and backscatter versus time at the thalweg position of Transect 11, June 12, 2003. An extended tick indicates the time that an ADCP profile was collected. Positive velocity values represent upstream velocity and negative values downstream velocity. The black line represents the bottom depth estimated from CTD casts.

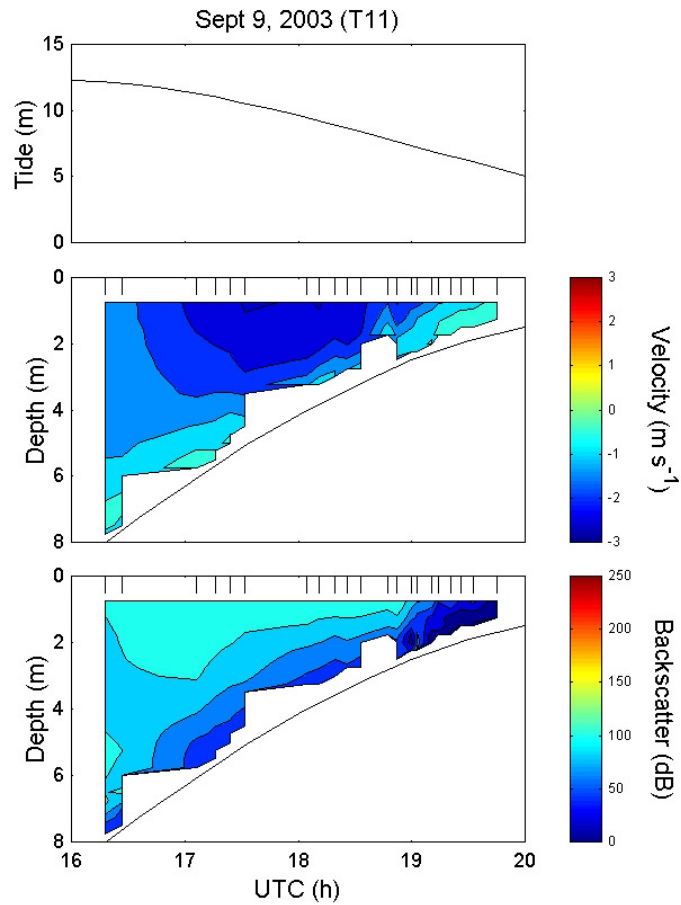


Figure 28. Velocity and backscatter versus time at the thalweg position of Transect 11, Sept. 9, 2003. An extended tick indicates the time that an ADCP profile was collected. Positive velocity values represent upstream velocity and negative values downstream velocity. The black line represents the bottom depth estimated from CTD casts.

3.3.2 Salinity, temperature, and density profiles

On June 12, 2003, the salinity, temperature, and density remained uniform with depth, but not with the water level. At 1411 h, prior to slack high tide, the depth-averaged salinity, temperature, and density were 23.6, 13.2°C, and 17.5 kg m⁻³, respectively (Figure 29). At 2204 h, following slack low tide, the depth-averaged salinity, temperature, and density were 5.7, 17.4°C, and 3.1 kg m⁻³, respectively. The decrease in salinity and density and increase in temperature between high and low tide reflect the presence of freshwater discharged during the causeway gate opening.

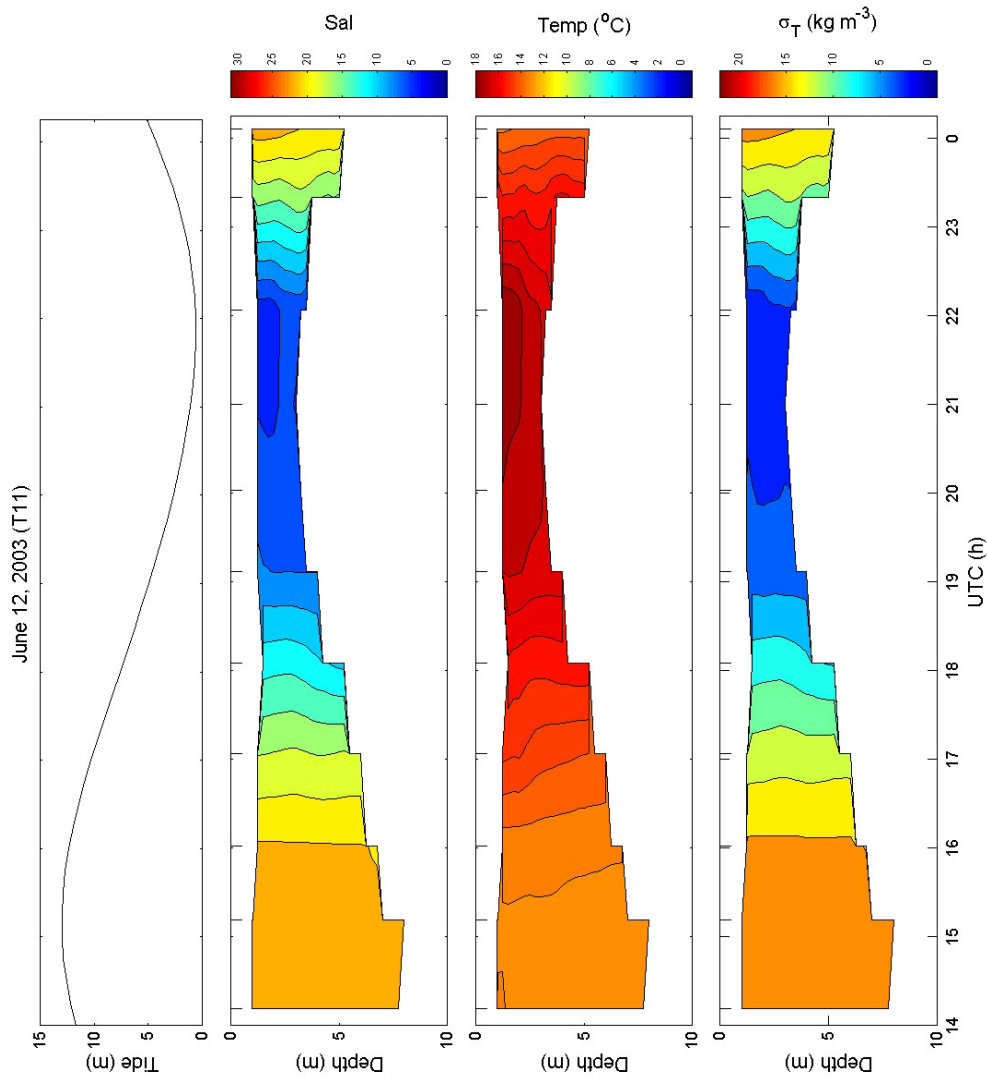


Figure 29. Salinity (Sal), temperature (Temp), and density (σ_T) versus time at the thalweg position of Transect 11, June 12, 2003. An extended tick indicates the time that a profile was collected.

On September 9, 2003, there was little variation in the water column salinity, temperature, and density structure during the survey (Figure 30). The time-averaged salinity, temperature, and density at all depths were 29.0, 16.7°C, and 20.2 kg m⁻³, respectively. Note the time that profiles were collected, as no data was collected between 1900 – 0000 h. A comparison of Figures 29 and 30 demonstrates the impact that the causeway gate opening has on water column properties at Transect 11, as causeway gates were closed more than three hours prior to surveying on September 9, 2003.

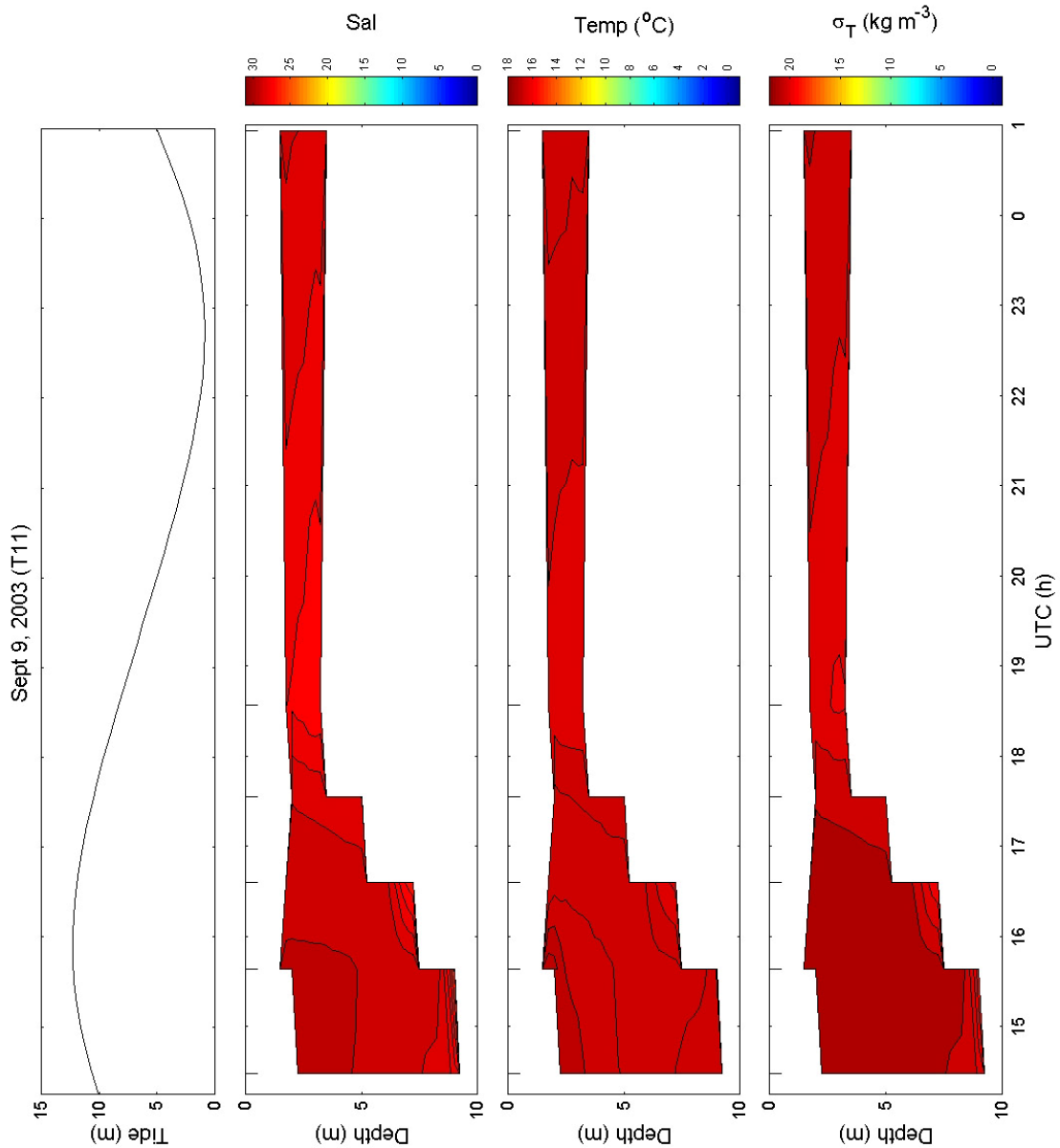


Figure 30. Salinity (Sal), temperature (Temp), and density (σ_T) versus time at the thalweg position of Transect 11, Sept. 9, 2003. An extended tick indicates the time that a profile was collected.

3.3.3 Salinity, optical backscatter, and dissolved oxygen profiles

On June 12, 2003, OBS increased towards the bottom during slack high tide (Figure 31). At 1511 h, OBS increased from 0.4 volts at 1 m depth to 1.9 volts at 6.5 m depth. The OBS then decreased to 0 volts between 6.5 to 8 m depth. During ebb tide, OBS was highest in the surface waters and decreased with depth. At 1601 h, OBS at 1.25 m depth was 1.8 volts. The OBS decreased to 0 volts at 6.75 m depth. Between 1800 – 2100 h, OBS was below 0.1 volts at all depths. Following passage of the tidal bore at 2244 h, OBS increased in the surface waters. At 2320 h, the OBS at 1.25 m depth was 2.2 volts, which was the highest value observed during the survey. Below 2.5 m depth, however, the OBS remained near 0 volts. High OBS values were observed near the surface for the remainder of the survey. The depth-averaged dissolved oxygen concentration decreased from 5.9 to 3.6 ml l⁻¹, between 1411 – 2204 h, during ebb tide (Figure 31). Following passage of the tidal bore, the depth-averaged dissolved oxygen concentration increased to 5.4 ml l⁻¹ at 0100 h.

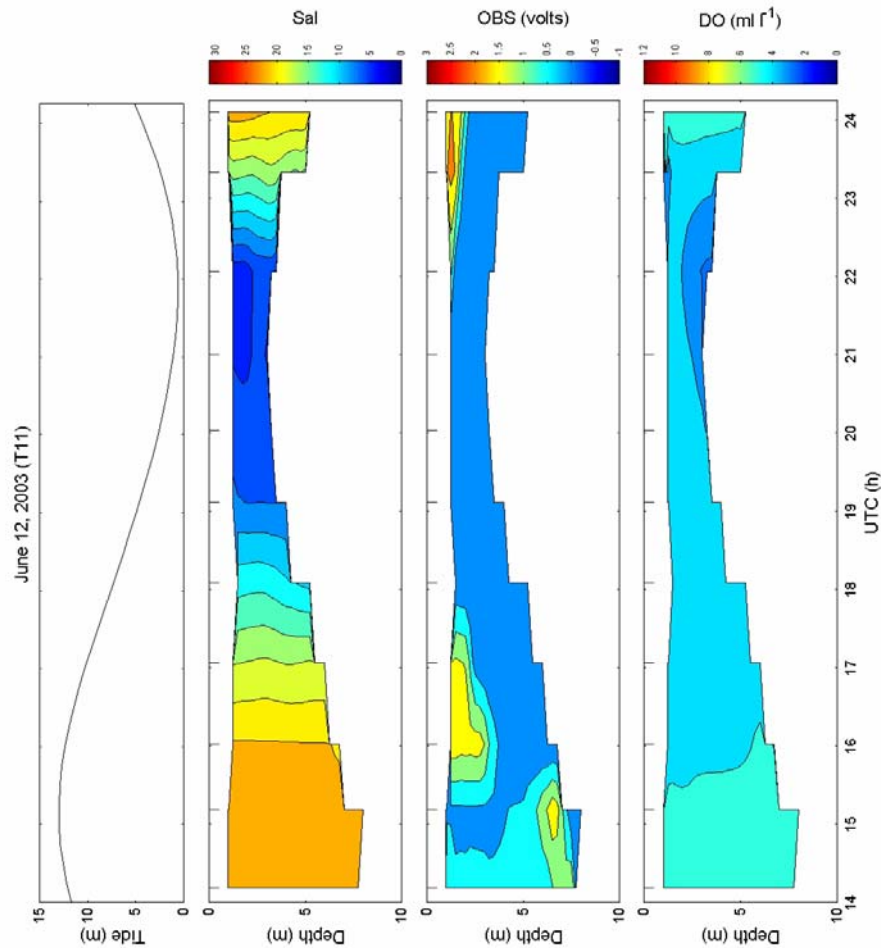


Figure 31. Salinity (Sal), optical backscatter (OBS), and dissolved oxygen concentration (DO) versus time at the thalweg position of Transect 11, June 12, 2003. An extended tick indicates the time that a profile was collected.

On September 9, 2003, OBS increased with depth during slack high tide to a maximum of approximately 1.8 volts at 6 m depth, and then decreased to 0 volts near the bottom (Figure 32). At 1834 h, OBS was approximately 0 volts throughout the water column. Following passage of the tidal bore at 2354 h, OBS of 1.8 volts was observed at 1.25 m depth, while OBS remained near 0 volts below 3 m depth. The depth-averaged dissolved oxygen concentration decreased from 4.0 to 3.4 ml l⁻¹, between 1538 – 1834 h, during ebb tide (Figure 32). Following passage of the tidal bore, the depth-averaged dissolved oxygen concentration increased to 3.8 ml l⁻¹ at 0560 h, with concentrations greater than 4 ml l⁻¹ observed near the surface.

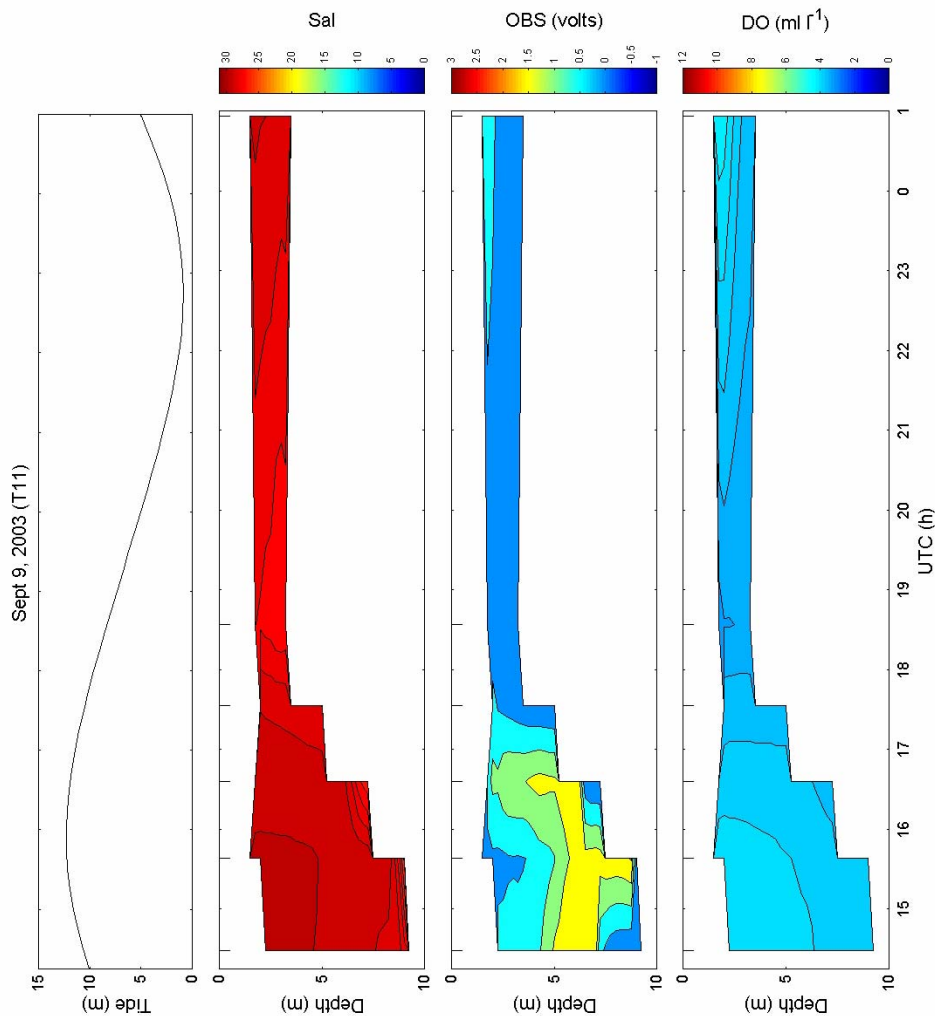


Figure 32. Salinity (Sal), optical backscatter (OBS), and dissolved oxygen concentration (DO) versus time at the thalweg position of Transect 11, Sept 9, 2003. An extended tick indicates the time that a CTD profile was collected.

3.3.4 Discrete salinity, SPM, and velocity

The discrete physical measurements made on June 12 and September 9, 2003, demonstrate the impact causeway gate opening has on the water column properties (Figure 33). During the survey on June 12, salinity at the surface and near the bottom decreased during ebb tide, then subsequently increased during flood tide. A maximum salinity of 23.8 was observed at 0.5 m depth, during slack high tide. A minimum salinity of 5.1 was observed at 0.5 m depth, during slack low tide. The highest SPM at 0.5 m depth was 41 g l^{-1} , at 1420 h before slack high tide. The near surface SPM then decreased between 1 to 10 g l^{-1} during ebb to slack low tide. Following passage of the tidal bore the near surface SPM increased to 17.4 g l^{-1} , then decreased to 1.5 g l^{-1} within 1.5 h. The SPM at 0.5 m above the bottom, however, were very high during this survey. Between slack high tide to slack low tide, near bottom SPM increased from 0.5 to 137.4 g l^{-1} . Following passage of the tidal bore the near bottom SPM concentration was 27 g l^{-1} , and then decreased to 15.9 g l^{-1} within 1.5 h. The downstream velocity at 1 m below the surface reached a maximum of 2.3 m s^{-1} , during ebb tide. During both high and low slack tide the velocity at 1 m depth remained downstream at approximately 0.3 m s^{-1} . Following passage of the tidal bore, the velocity reversed upstream to a maximum of 2.8 m s^{-1} . The velocity at 3.5 m depth behaved similar to the surface velocity, although the bottom velocity during slack high tide moved upstream at 0.6 m s^{-1} , while the near surface velocity remained downstream.

In contrast, both surface and bottom salinity remained greater than 20 throughout the survey on September 9, 2003 (Figure 33). The highest salinities were observed during slack high tide and following passage of the tidal bore. Both surface and bottom salinity slightly decreased during ebb tide and slack low tide. The average salinity during this survey was 28.5. The SPM at 0.5 m depth ranged between $0.2 - 7 \text{ g l}^{-1}$, although an SPM of 22.1 g l^{-1} was observed near the surface, prior to slack low tide. The SPM at 0.5 m above the bottom increased during ebb tide from $0.2 - 57.4 \text{ g l}^{-1}$. The near bottom SPM was 26.6 g l^{-1} following passage of the tidal bore. The downstream velocity at 1 m depth reached a maximum of 2.5 m s^{-1} during ebb tide. Both surface and bottom velocities approached 0 m s^{-1} during the high and low slack tides.

3.3.5 Discrete salinity and nutrients

For silicate, phosphate, nitrate, and ammonia, surface and bottom nutrient concentrations behaved similarly (Figure 34). The nitrate concentrations, however, showed large variability during each survey. The increase in all nutrient concentrations towards low slack tide suggests that the source of the nutrients was upstream of Transect 11. There was no significant difference in the nutrient concentrations or behaviour between the two surveys.

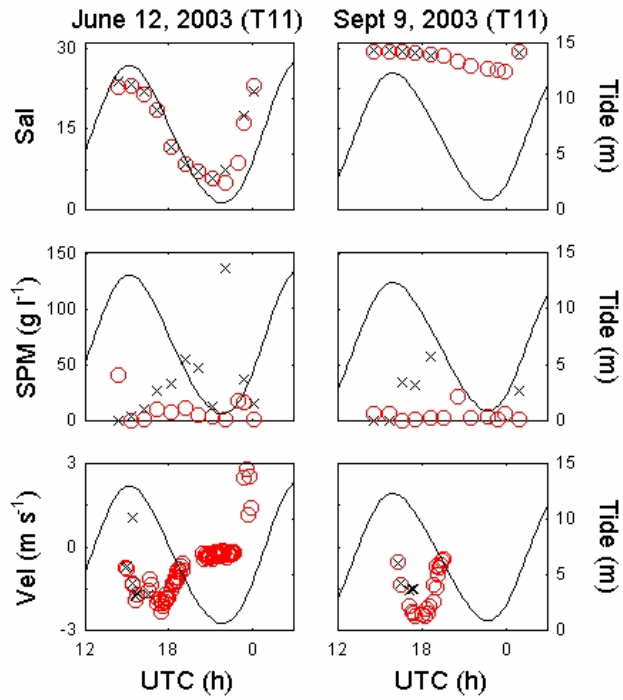


Figure 33. Salinity (Sal), suspended particulate matter concentration (SPM), and flow velocity (Vel) versus time at the thalweg position of Transect 11. Discrete salinity and SPM samples were collected at 0.5 m depth (o) and 0.5 m above the bottom (x). ADCP velocities were collected at 1 m depth (o) and 3.5 m below the surface (x).

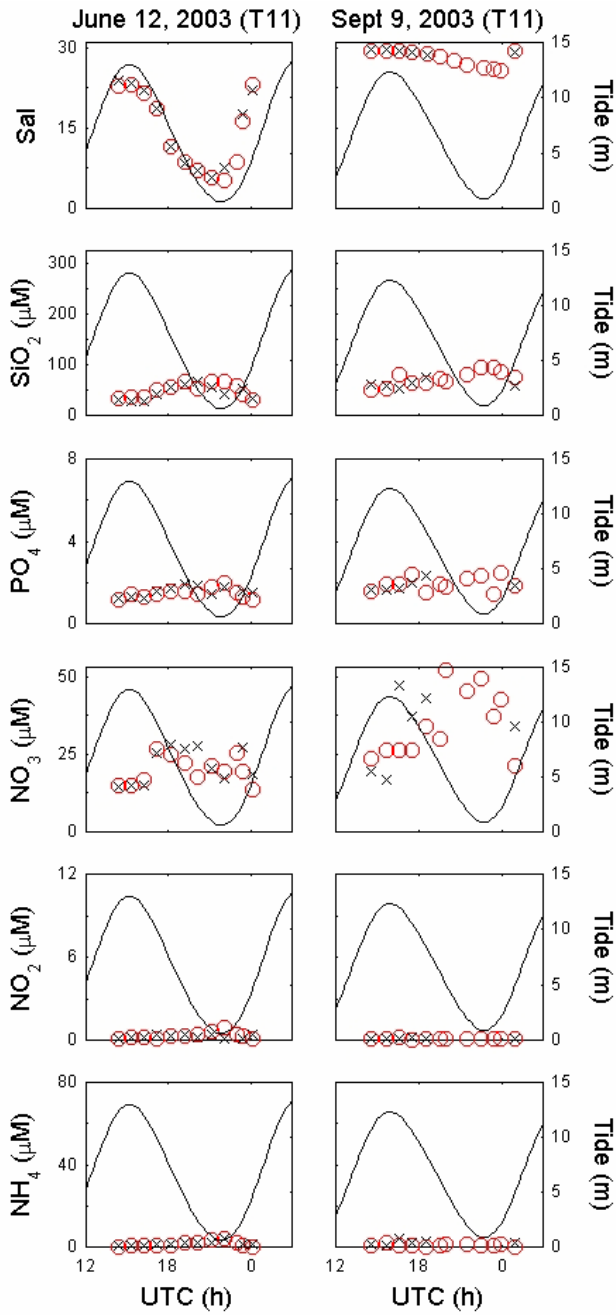


Figure 34. Salinity (Sal), silicate (SiO_2), phosphate (PO_4), nitrate (NO_3), nitrite (NO_2), and ammonia (NH_4) concentrations versus time at the thalweg position of Transect 21. Discrete samples were collected at 0.5 m depth (o) and 0.5 m above the bottom (x).

3.4 TRANSECT 1 (T1) NEAR HOPEWELL CAPE

Three surveys were performed at Transect 1 under different gate operations. The survey on June 13, 2003, was performed from 1400 – 0300 h, over one tidal period. One causeway gate was fully opened for fish passage between 1358 – 1424 h. High tide was at 1600 h and low tide at 2245 h. The tidal bore of the subsequent flood tide was at 2315 h. The survey on September 10, 2003, was performed from 1530 – 1700 h during slack high tide. No causeway gates were opened during this survey. The survey was cut short due to bad weather. Last, the survey on September 11, 2003, was performed from 1530 – 0300 h over one tidal period. No causeway gates were opened during this survey. Slack high tide was at 1715 h and slack low tide at 2302 h. The tidal bore of the subsequent flood tide was at 0245 h.

3.4.1 ADCP velocity and backscatter profiles

On June 13, 2003, the upstream velocity during flood tide decreased from 1 m s^{-1} to 0.6 m s^{-1} , between 1 and 17.5 m depth (Figure 35). At slack high tide, the velocity at 1 and 17.5 m depths reversed downstream to 0.29 and 0.21 m s^{-1} , respectively. During ebb tide, the downstream velocity increased to 1.4 and 0.6 m s^{-1} , at 1 and 13 m depths, respectively. The velocity then decreased and reversed upstream between 0.4 to 0.3 m s^{-1} , at 1 and 3 m depths by 2141 h. Following passage of the tidal bore, the velocity increased upstream at 2.4 and 1.8 m s^{-1} between 1 and 10 m depths, respectively. The maximum backscatter was 111 dB at the surface during slack low tide and 0 dB near the bottom (Figure 35). Typically, the backscatter ranged between 70 – 100 dB for most of the survey, decreasing from the surface to depth. The white area of no data near the bottom increased in thickness during ebb tide and reached a maximum thickness during slack low tide and following passage of the tidal bore.

On September 10, 2003, the upstream velocity prior to slack high tide was 0.7 m s^{-1} at 1 m depth, and then reversed downstream to 0.6 m s^{-1} following high tide (Figure 36). Throughout the survey the velocity decreased with depth and approached 0 m s^{-1} near the bottom. The backscatter was uniform during the survey, decreasing from approximately 100 dB at the surface to 80 dB near the bottom (Figure 36). During the survey, a white region of no data near the bottom was not observed.

Last, during the survey on September 11, 2003, the upstream velocity during flood tide decreased from 0.8 m s^{-1} to 0.6 m s^{-1} , between 1 and 18.5 m depths, respectively (Figure 37). At slack high tide the velocity at 1 m depth was downstream at 0.1 m s^{-1} , while at 18.5 m depth the velocity was upstream at 0.3 m s^{-1} . During ebb tide, the downstream velocity increased to 0.9 and 0.2 m s^{-1} , at 1 and 16.5 m depths, respectively, while the velocity at 17 m depth was upstream at 0.4 m s^{-1} . The velocity then reversed upstream from 0.2 to 0 m s^{-1} at 1 and 3.7 m depths, at 2242 h. Following passage of the tidal bore, the velocity increased

upstream to 2.1 and 0.6 m s⁻¹ between 1 and 9.5 m depths, respectively. The maximum backscatter was 107 dB at the surface during ebb tide (Figure 37). Backscatter less than 0 dB were observed throughout the water column during slack low tide. The white area of no data near the bottom was only present during slack low tide and following passage of the tidal bore.

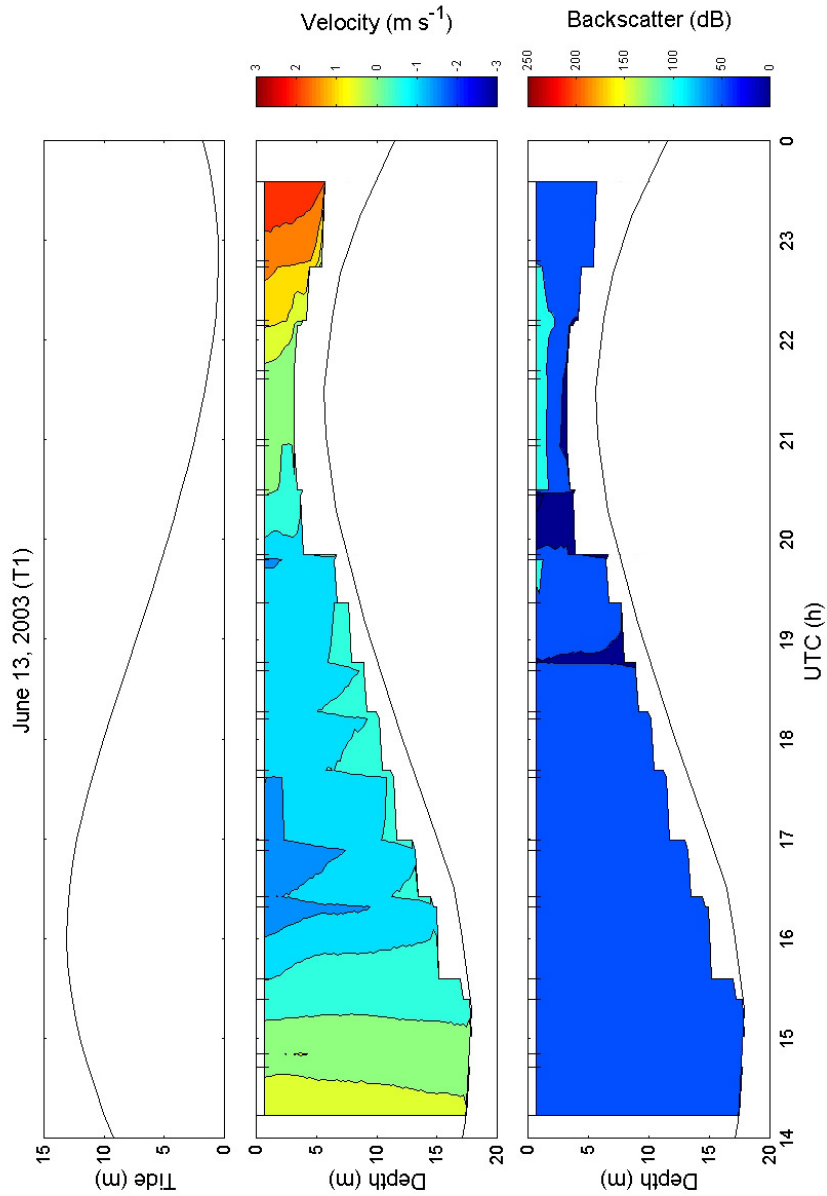


Figure 35. Velocity and backscatter versus time at the thalweg position of Transect 1, June 13, 2003. An extended tick indicates the time that an ADCP profile was collected. Positive velocity values represent upstream velocity and negative values downstream velocity. The black line represents the bottom depth estimated from CTD casts.

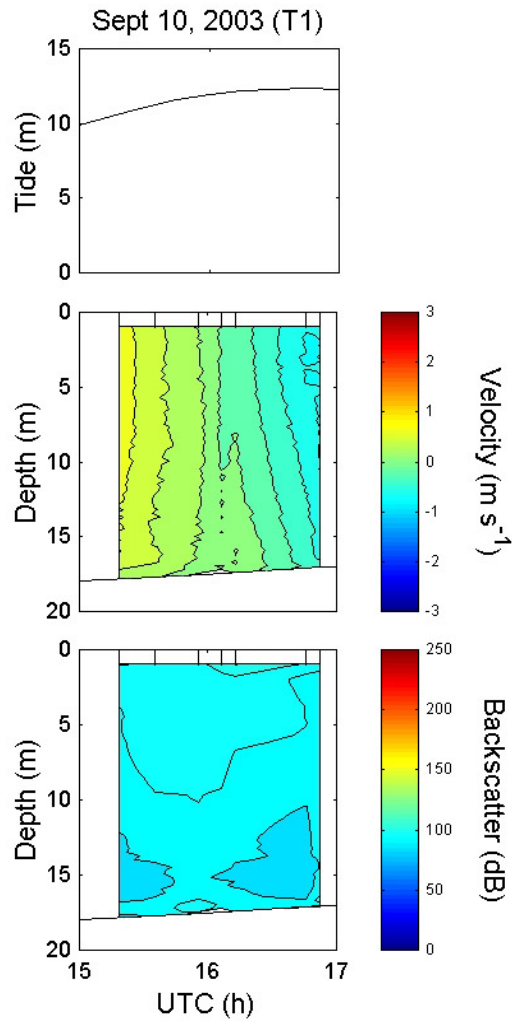


Figure 36. Velocity and backscatter versus time at the thalweg position of Transect 1, Sept. 10, 2003. An extended tick indicates the time that an ADCP profile was collected. Positive velocity values represent upstream velocity and negative values downstream velocity. The black line represents the bottom depth estimated from CTD casts.

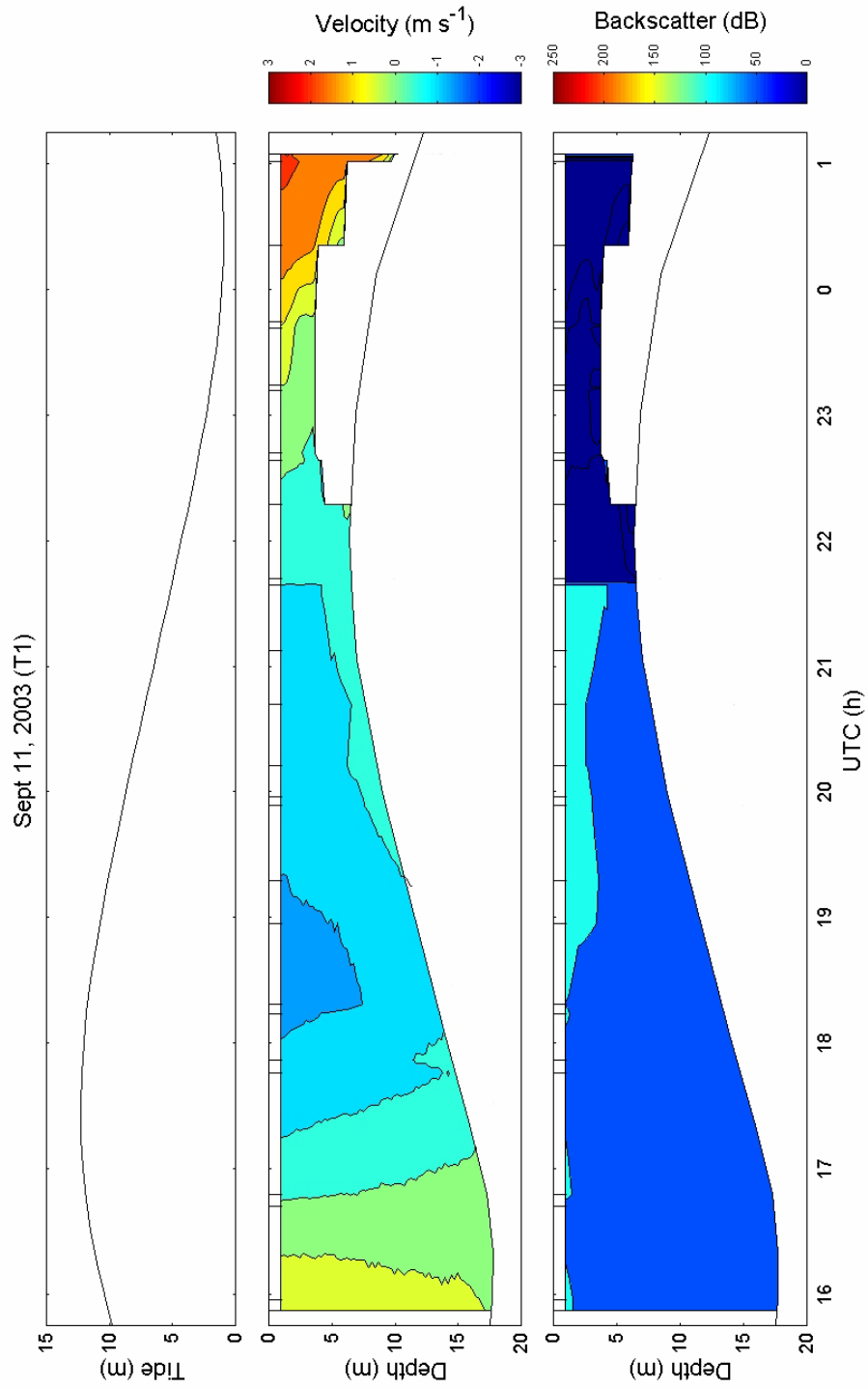


Figure 37. Velocity and backscatter versus time at the thalweg position of Transect 1, Sept. 11, 2003. An extended tick indicates the time that an ADCP profile was collected. Positive velocity values represent upstream velocity and negative values downstream velocity. The black line represents the bottom depth estimated from CTD casts.

3.4.2 Salinity, temperature, and density profiles

On June 13, 2003, the salinity, temperature, and density remained uniform with depth, but not with the water level. At 1356 h, prior to slack high tide, the depth-averaged salinity, temperature, and density were 27.6, 11.5°C, and 20.9 kg m⁻³, respectively (Figure 38). The density slightly increased near the bottom. At 2213 h during slack low tide, the depth-averaged salinity, temperature, and density were 20.9, 14.6°C, and 15.2 kg m⁻³, respectively. The decrease in salinity and density and increase in temperature between high and low tide reflect the presence of freshwater discharged during the causeway gate opening. As well, note the apparent density inversion at slack low tide, as higher density water is observed near the surface and lower density water at depth.

On September 10, 2003, there was little variation in the water column salinity, temperature, and density structure during the survey (Figure 39). The time-averaged salinity, temperature, and density for all depths were 30.2, 16.7°C, and 21.9 kg m⁻³, respectively. Similarly, on September 11, 2003, there also was little variation in the water column salinity, temperature, and density structure during the survey (Figure 40). At 1558 h, prior to slack high tide, the depth-averaged salinity, temperature, and density were 30.3, 16.4°C, and 22.0 kg m⁻³, respectively. At 0001 h during slack low tide, the depth-averaged salinity, temperature, and density were 28.3, 16.3°C, and 20.5 kg m⁻³, respectively. The slight decrease in salinity and density and increase in temperature between high and low tide may reflect the presence of freshwater discharged from upstream tributaries, although the change in salinity, temperature, and density is less obvious than occurred when the causeway gates were opened on June 13, 2003 (Figure 38). Again, note the apparent density inversion at slack low tide, as higher density water is observed near the surface and lower density water at depth (Figure 40).

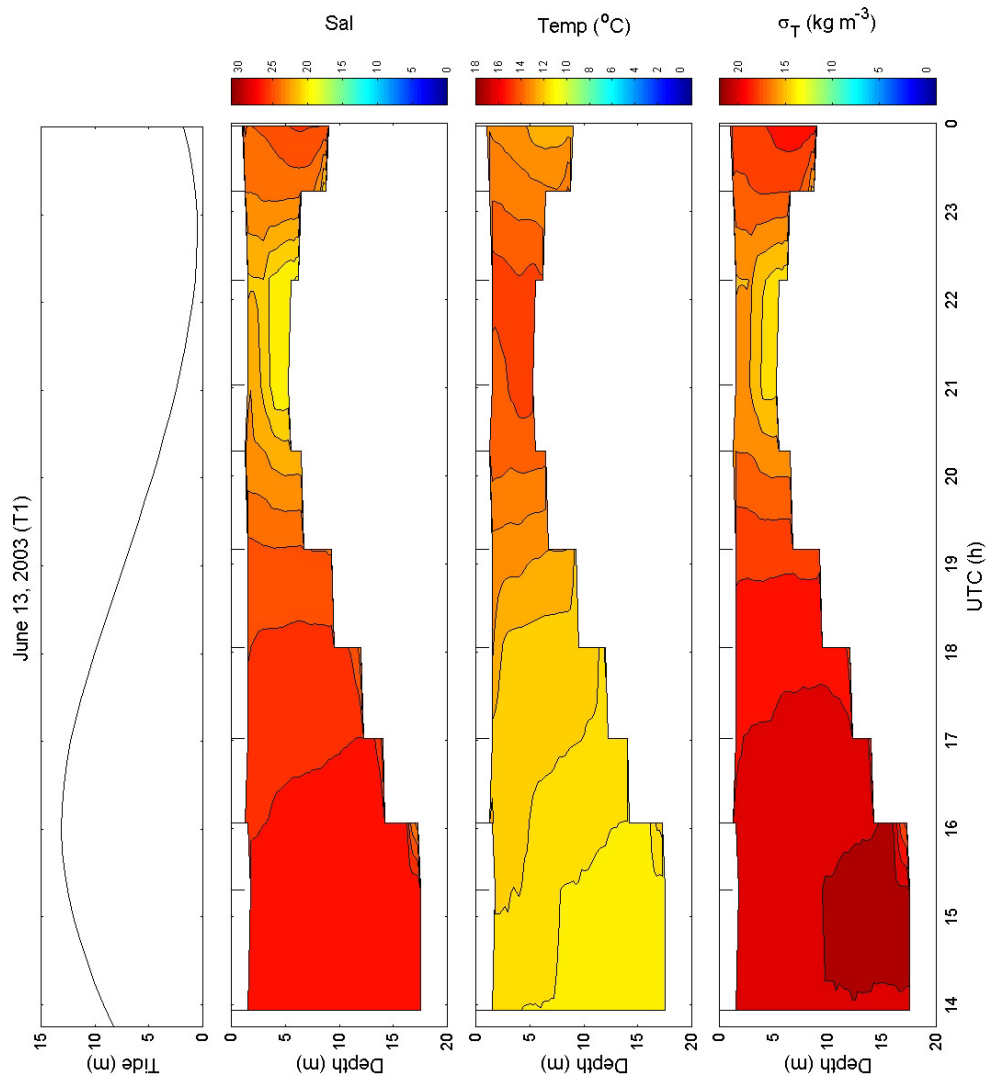


Figure 38. Salinity (Sal), temperature (Temp), and density (σ_T) versus time at the thalweg position of Transect 1, June 13, 2003. An extended tick indicates the time that a profile was collected.

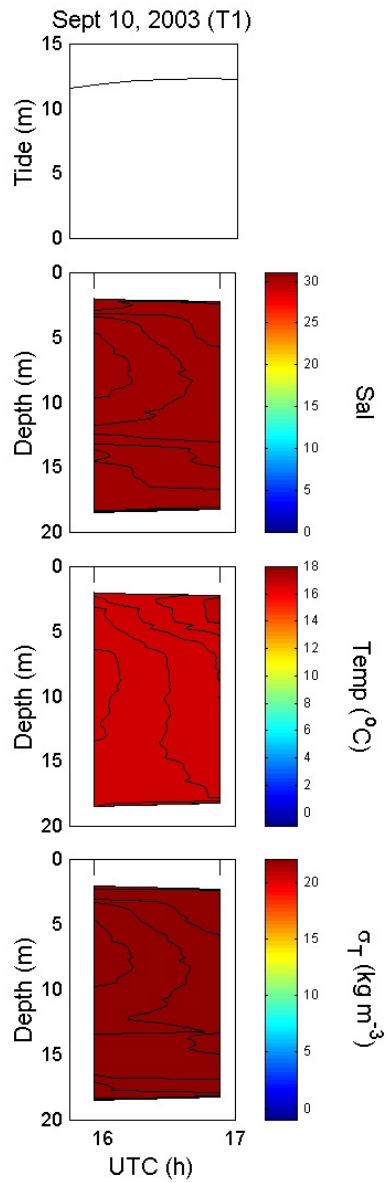


Figure 39. Salinity (Sal), temperature (Temp), and density (σ_T) versus time at the thalweg position of Transect 1, Sept. 10, 2003. An extended tick indicates the time that a profile was collected.

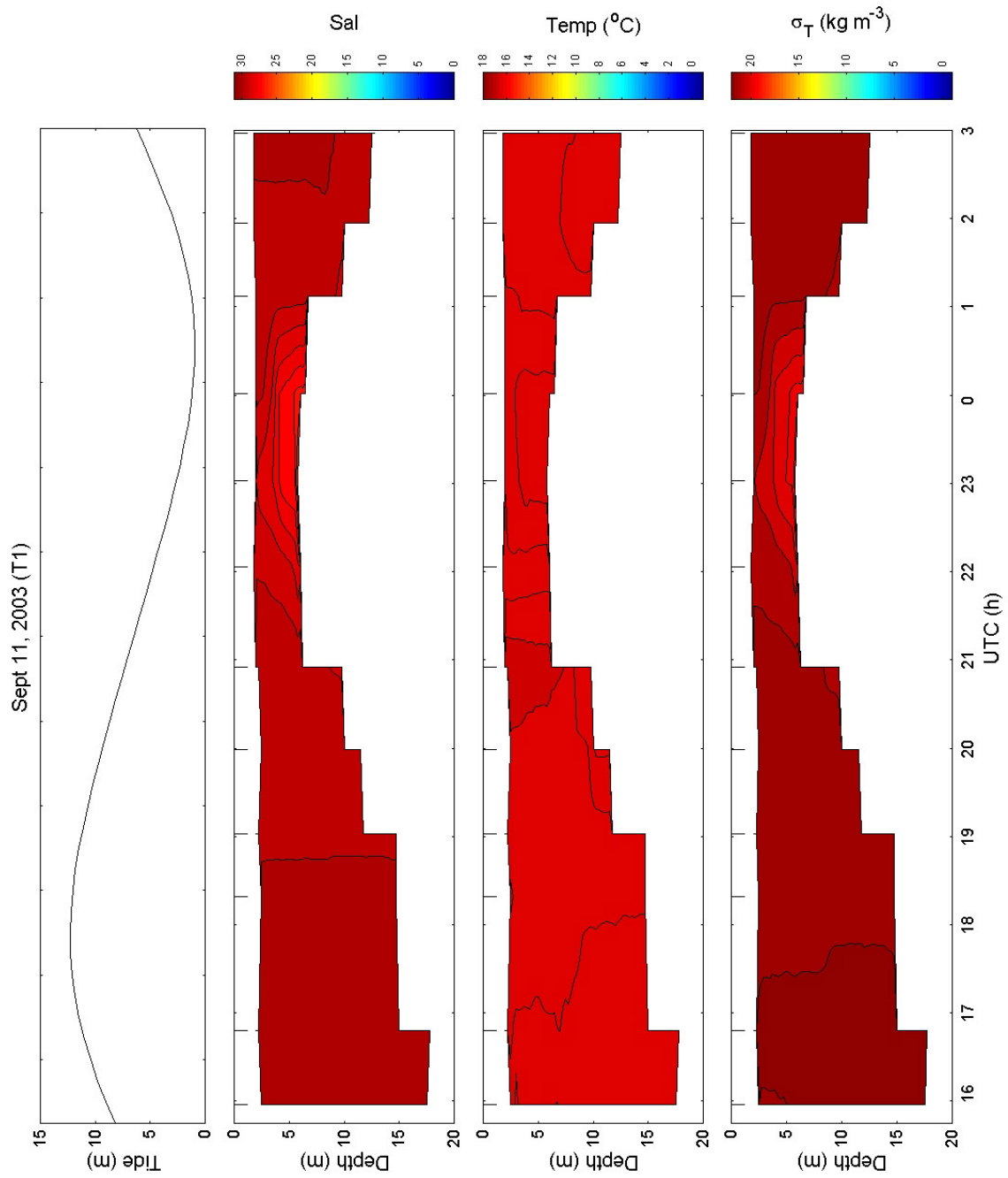


Figure 40. Salinity (Sal), temperature (Temp), and density (σ_T) versus time at the thalweg position of Transect 1, Sept. 11, 2003. An extended tick indicates the time that a profile was collected.

3.4.3 Salinity, optical backscatter, and dissolved oxygen profiles

On June 13, 2003, OBS increased from 0.3 to 1.0 volts between 1.5 and 17.5 m depths, prior to slack high tide (Figure 41). During slack high tide OBS decreased throughout the water column, exhibiting a depth-averaged value of 0.3 volts. During ebb tide, OBS slightly increased in surface waters, while OBS increased above the bottom as the ebb tide progressed. The OBS very near the bottom, however, remained approximately 0 volts during ebb to slack low tide. During slack low tide, OBS throughout the water column was near 0 volts. Following passage of the tidal bore, OBS in surface waters was greater than 1.5 volts, then decreased in the surface waters and increased at depth through time. During passage of the tidal bore, OBS very near the bottom was approximately 0 volts. The depth-averaged dissolved oxygen concentration decreased from 6.9 to 4.8 ml l⁻¹ between high and low slack tide (Figure 41). The lowest dissolved oxygen concentration of 4.7 ml l⁻¹ was observed near the bottom during slack low tide. The depth-averaged concentration then increased to 5.7 ml l⁻¹ following passage of the tidal bore.

On September 10, 2003, the time-averaged OBS increased from 0.2 to 0.9 volts between 2.5 and 18 m depths (Figure 42). The dissolved oxygen concentration only slightly decreased with depth during the survey (Figure 42). The average dissolved oxygen concentration was 4.6 ml l⁻¹. Last, on September 11, 2003, OBS increased from 0.2 to 0.5 volts between 2.5 and 17.5 m depths, prior to slack high tide (Figure 43). During slack high tide OBS decreased throughout the water column, exhibiting a depth-averaged OBS of 0.2 volts. During ebb tide, OBS slightly increased in surface waters, while the OBS increased above the bottom as the ebb tide progressed. The OBS very near the bottom, however, remained approximately 0 volts during ebb to slack low tide. During slack low tide, OBS throughout the water column was near 0 volts. Following passage of the tidal bore, OBS in surface waters was greater than 1.5 volts, which then decreased in the surface waters and increased at depth through time. During passage of the tidal bore, OBS very near the bottom was approximately 0 volts. The depth-averaged dissolved oxygen concentration decreased from 4.6 to 3.8 ml l⁻¹ between high and low slack tide (Figure 43). The lowest dissolved oxygen concentration of 3.5 ml l⁻¹ was observed near the bottom during slack low tide. The depth-averaged concentration then increased to 4.5 ml l⁻¹ following passage of the tidal bore.

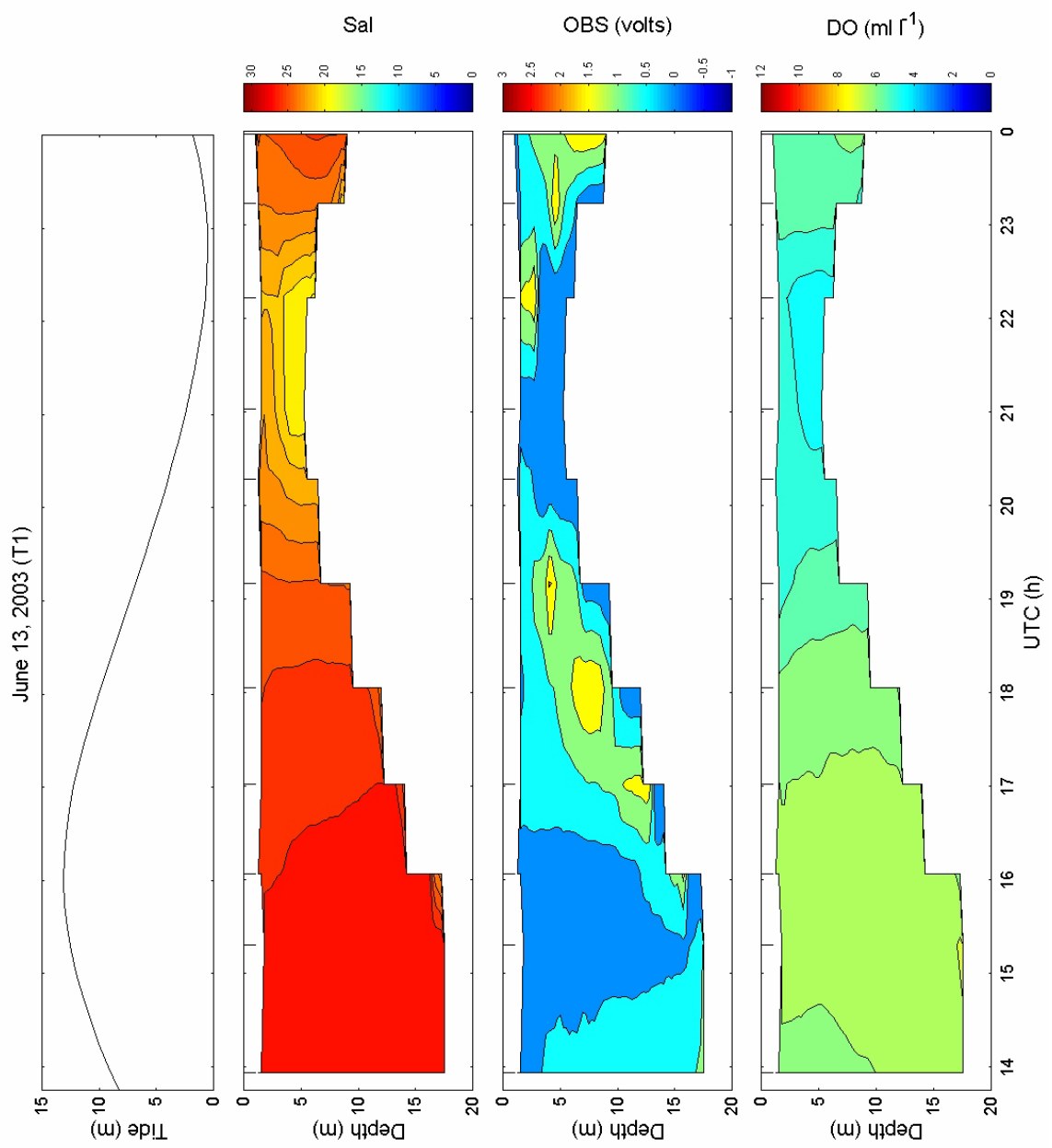


Figure 41. Salinity (Sal), optical backscatter (OBS), and dissolved oxygen concentration (DO) versus time at the thalweg position of Transect 1, June 13, 2003. An extended tick indicates the time that a profile was collected.

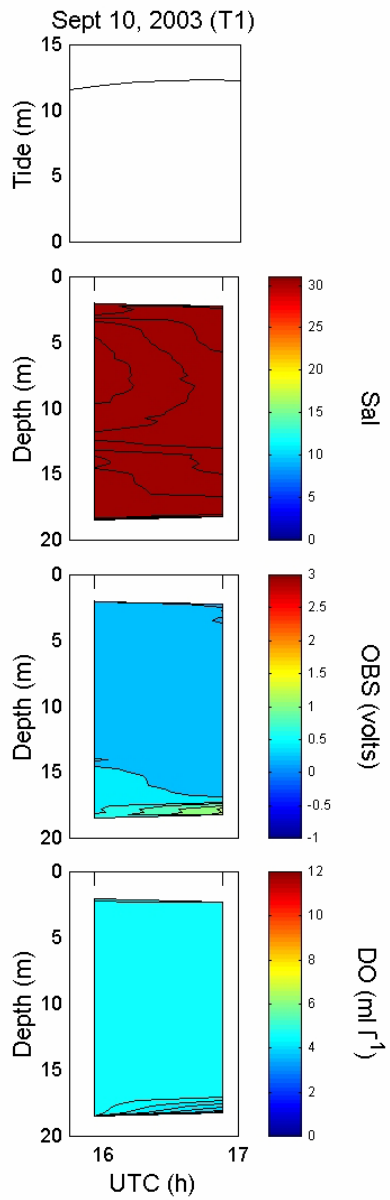


Figure 42. Salinity (Sal), optical backscatter (OBS), and dissolved oxygen concentration (DO) versus time at the thalweg position of Transect 1, Sept. 10, 2003. An extended tick indicates the time that that a profile was collected.

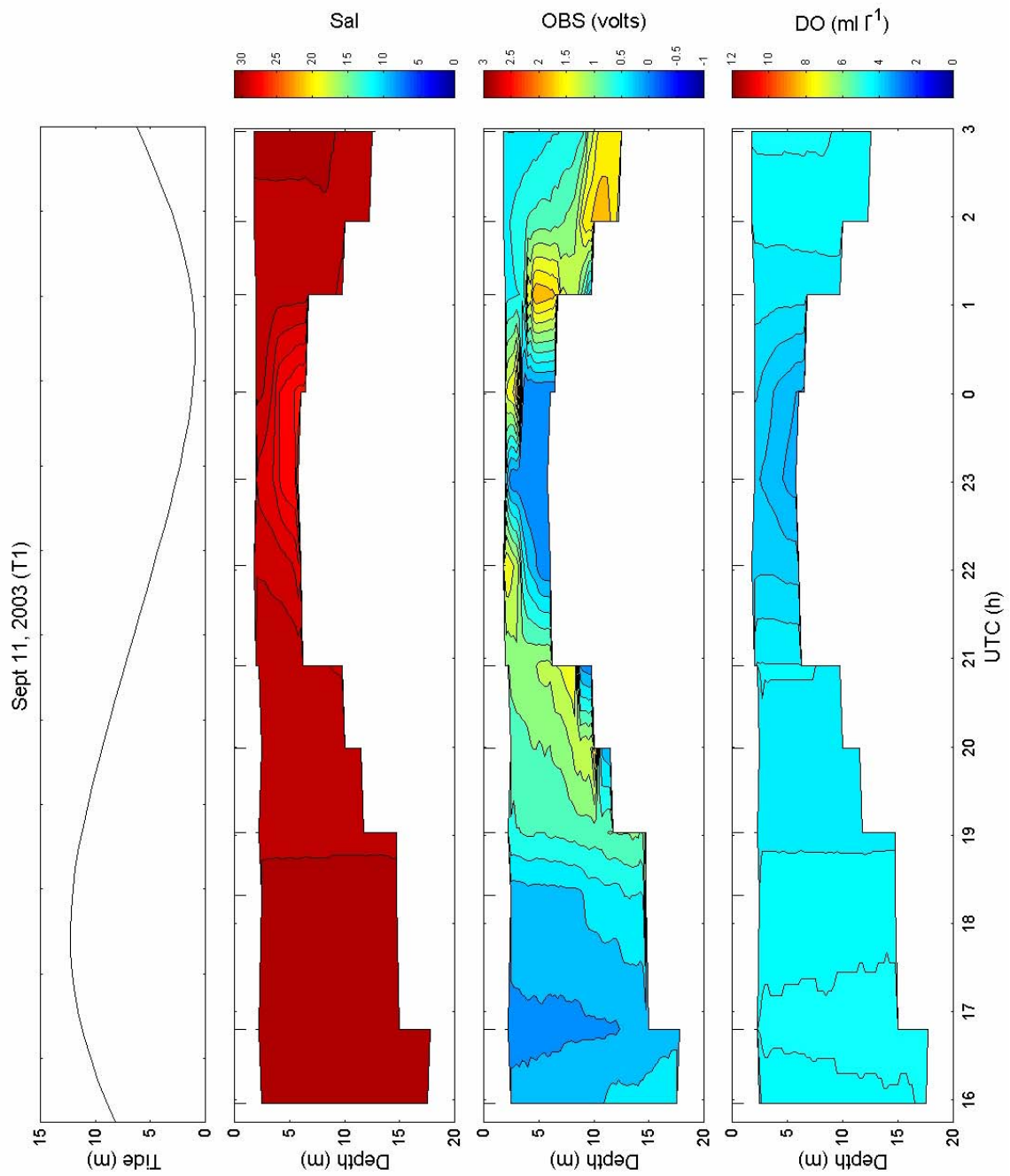


Figure 43. Salinity (Sal), optical backscatter (OBS), and dissolved oxygen concentration (DO) versus time at the thalweg position of Transect 1, Sept. 11, 2003. An extended tick indicates the time that a profile was collected.

3.4.4 Discrete salinity, SPM, and velocity

The discrete physical measurements at Transect 1 demonstrate the impact causeway gate opening has on the water column properties (Figure 44). During the survey on June 13 (causeway gates open), salinity at the surface and near the bottom decreased during ebb tide, then subsequently increased during flood tide. A maximum salinity of 27.9 was observed 0.5 above the bottom at 1523 h, during slack high tide. A minimum salinity of 24.1 was observed at 0.5 m depth, during slack low tide. The highest SPM at 0.5 m depth was 13.7 g l^{-1} , prior to slack low tide. The surface SPM ranged between $0.1 - 1.7 \text{ g l}^{-1}$. The SPM at 0.5 m above the bottom, however, were very high during this survey. Between slack high tide to slack low tide, bottom SPM increased from 0.6 to 79.5 g l^{-1} . Following passage of the tidal bore the near bottom SPM concentration was 21.7 g l^{-1} , which decreased to 6.7 g l^{-1} within 45 mins. The downstream velocity at 1 m depth reached a maximum of 1.4 m s^{-1} , during ebb tide. During both high and low slack tide the velocity at 1 m depth remained downstream at approximately 0.3 m s^{-1} . Following passage of the tidal bore the velocity reversed upstream, reaching a maximum of 2.5 m s^{-1} at 2335 h. Velocity at 3.5 m depth behaved similar to the surface velocity. On September 10, 2003 (causeway gates closed), the surface and bottom salinity were 30, while SPM at the surface and depth were less than 0.3 g l^{-1} (Figure 44). The average velocity at 1 m below the surface during slack high tide was 0.5 m s^{-1} . The velocity at 3.5 m depth reversed during slack high tide from upstream at 0.7 m s^{-1} to downstream at 0.6 m s^{-1} , between 1518 – 1651 h.

Similar to September 10, 2003, both surface and bottom salinity remained high throughout the survey on September 11, 2003 (causeway gates closed) (Figure 44). The highest salinities were observed during slack high tide and following passage of the tidal bore. Both surface and bottom salinity slightly decreased during ebb tide and slack low tide. The average salinity during this survey was 29.9. The SPM at 0.5 m depth ranged between $0.1 - 0.5 \text{ g l}^{-1}$. The SPM at 0.5 m above the bottom increased during ebb tide from $0.3 - 51.0 \text{ g l}^{-1}$, then subsequently decreased. There was no obvious effect of the tidal bore passage on the bottom SPM concentration. The downstream velocity at 1 m depth reached a maximum of 1.3 m s^{-1} during ebb tide. Both surface and bottom velocities approached 0 m s^{-1} during high and low slack tide. The maximum upstream velocity at 1 m depth following passage of the tidal bore was 2.1 m s^{-1} .

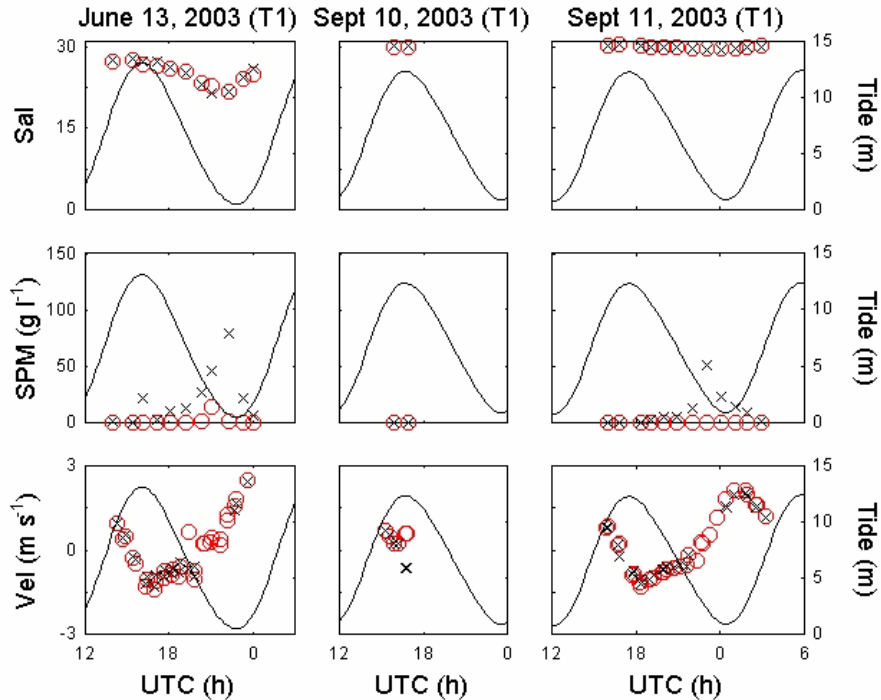


Figure 44. Salinity (Sal), suspended particulate mass (SPM), and flow velocity (Vel) versus time at the thalweg position of Transect 1. Discrete salinity and SPM samples were collected at 0.5 m depth (o) and 0.5 m above the bottom (x). ADCP velocities were collected at 1 m depth (o) and 3.5 m below the surface (x).

3.4.5 Discrete salinity and nutrients

For the surveys on June 13 and September 10, 2003, all surface and bottom nutrient concentrations behaved similarly (Figure 45). The nitrate concentrations, however, showed large variability during each survey. In contrast, bottom concentrations for nutrients often were higher than surface concentrations during the September 11, 2003, survey. The silicate, phosphate, and nitrate concentrations also were variable during this survey. Typically, nutrient concentrations were observed to increase at Transect 1 towards slack low tide, which suggests that the source of the nutrients was upstream of this location.

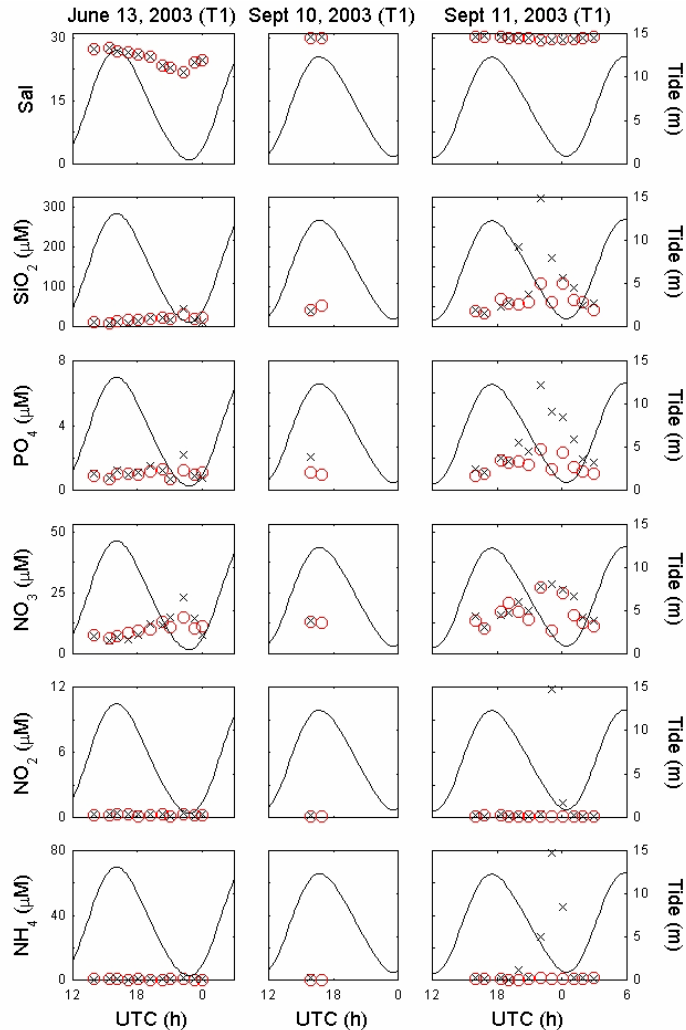


Figure 45. Salinity (Sal), silicate (SiO₂), phosphate (PO₄), nitrate (NO₃), nitrite (NO₂), and ammonia (NH₄) concentrations versus time at the thalweg position of Transect 1. Discrete samples were collected at 0.5 m depth (o) and 0.5 m above the bottom (x).

4.0 DISCUSSION

Comparison of surveys yields insight into the river's variable hydrodynamic and physical properties under different causeway gate manipulation scenarios. The causeway gate management strategy, the opening or closing of the gates, has two objectives: 1) to protect local infrastructure from flooding; and 2) to permit fish passage. Typically, the causeway gates are opened preceding precipitation events to decrease the water level in the headpond behind the causeway, flush mud that has accumulated near the gates, and permit fish passage. The strategy depends on several factors such as water levels in the river below the causeway and fish spawning periods.

4.1 RIVER VELOCITY AND FLOW DYNAMICS

The most apparent impacts of gate manipulation on the river's velocity and flow direction are observed at Transect 101 located 3-km downstream of the causeway. On March 26, 2002, two causeway gates were opened during ebb tide. During gate opening, the downstream velocity at 3.5 m depth was 2 m s^{-1} throughout ebb tide, while no gradual increase and subsequent decrease in velocity was observed (Figure 2). Within 6 mins. of gate closure, the downstream velocity at 3.5 m depth decreased to 0.2 m s^{-1} . Similarly, at the beginning of the survey on March 20, 2003, one causeway gate was opened during slack low tide. The downstream velocity was 2.4 m s^{-1} at 2 m depth, compared to an anticipated velocity of 0 m s^{-1} that should be expected during slack low tide (Figure 4). The subsequent ebb tide during this survey was 3.5 h after the causeway gate had been closed. During the ebb tide, the downstream velocity at 1.5 m depth gradually increased towards mid-tide, reaching a maximum of 1.3 m s^{-1} (Figure 4). The maximum downstream velocity at 3.5 m depth during this survey was 1.2 m s^{-1} .

If it is assumed that the river at Transect 101 restores its tidally-driven flow characteristics immediately following causeway gate closure (as demonstrated on March 26, 2002), then the ebb tide velocities from other surveys at Transect 101 also can be compared. On October 9, 2002, one causeway gate was closed 30 mins. prior to ebb tide. During this survey the downstream velocity gradually increased to a maximum velocity of 0.9 m s^{-1} at 2 m depth, during mid-tide (Figure 3). The maximum velocity at 3.5 m depth was 0.8 m s^{-1} . On May 14, 2003, one causeway gate was closed 1.5 h prior to ebb tide. During this survey, the downstream velocity also gradually increased during ebb tide, reaching a maximum of 0.5 and 0.4 m s^{-1} at 1.5 and 3.5 m depths, respectively (Figure 5). Comparison of the ebb tide velocities between surveys demonstrates that during gate opened surveys the downstream, ebb tide velocity is dominated by the freshwater discharge from the causeway. As well, during gate opened events the ebb velocity does not vary during the ebb tide, compared to the gradually increasing velocity observed when the causeway gates were closed. The maximum ebb velocity observed during gate opened surveys also was up to an order-of-magnitude greater than the maximum ebb velocity observed during the gate closed events.

No surveys were performed at Transect 101 when the causeway gates were closed throughout flood tide. The causeway gates, however, were closed at different times during flood tide for different surveys, which permits comparison of the effects of gate manipulation on the river's velocity and flow direction during flood tide. On October 9, 2002, one causeway gate remained opened throughout flood tide. One hour following passage of the tidal bore the river velocity remained downstream at 0.3 m s^{-1} , at 1.5 and 3.5 m depths (Figure 3). At mid-tide, the flood tide velocity overtook the downstream freshwater flow from the opened gate, as the flow reversed in the upstream direction reaching a maximum

velocity of 0.5 m s^{-1} , at 2.5 and 3.5 m depths. At slack high tide, the surface flow was 0 m s^{-1} , but remained upstream at 0.5 m s^{-1} at depth.

On March 20, 2003, the causeway gate was closed 1 h prior to tidal bore passage. Immediately before passage of the tidal bore the flow was downstream at 0.4 and 0 m s^{-1} , at 1.5 and 3.5 m depths, respectively (Figure 4). Following passage of the tidal bore the flow reversed in the upstream direction at 0.8 m s^{-1} , at both 1.5 and 3.5 m depths. At slack high tide, the velocity at 1.5 m depth was 0 m s^{-1} , while the flow at 3.5 m depth remained upstream at 0.2 m s^{-1} . Last, on May 14, 2003, the causeway gate also was closed 1 h prior to slack high tide. Following tidal bore passage, the flow remained in the downstream direction at 0.4 and 0.1 m s^{-1} , at 1.5 and 3.5 m depths, respectively (Figure 5). By mid-tide, the flow reversed to the upstream direction at 0.2 and 0.5 m s^{-1} , at 1.5 and 3.5 m depths, respectively. At slack high tide, the velocity at 1.5 m depth was 0 m s^{-1} , while the flow at 3.5 m depth remained upstream at 0.4 m s^{-1} .

During flood tide at Transect 101, the freshwater discharge from the opened causeway gates overtook the upstream flow associated with the incoming tide, even after passage of the tidal bore. Similarly, closure of the causeway gates up to one hour before flood tide also impacted the incoming tidal velocity and flow direction. With gate closure, surface velocities were 0 m s^{-1} during slack high tide, while the velocity at depth did not reach 0 m s^{-1} until 1 h following high tide. Clearly, gate manipulation influences the river velocity and flow direction at Transect 101. In general, opened causeway gates accelerated downstream flow during ebb tide and impeded the upstream flow during flood tide. It is believed that causeway gate openings also would accelerate flow in the downstream direction during slack tides.

At Transect 21 on May 15, 2003, one causeway gate was opened during flood tide and closed 30 mins. before slack high tide. At slack high tide, the river's flow remained downstream at 0.9 and 0.6 m s^{-1} , at 1.5 and 3.5 m depths, respectively (Figure 22). With the onset of ebb tide, downstream velocities of 1 and 0.8 m s^{-1} , at 1.5 and 3.5 m depths, respectively, were observed. These were comparable to the maximum ebb tide velocities observed at Transect 101 when the causeway gates were closed. From this single survey, it is apparent that the gate opening increased the downstream velocity and altered the river's flow direction up to 5.5-km from the causeway.

In contrast, gate manipulation did not appear to affect the river's velocity or flow direction at Transect 11, located 16-km from the causeway. On June 12, 2003, one causeway gate was opened for 3.5 h for fish passage, and then closed 20 mins. prior to the survey. On September 9, 2003, a maximum of two causeway gates were partially-opened for 1.25 h and closed 3.25 h prior to the survey. On June 12, 2003, the maximum depth-averaged downstream velocity during ebb tide was 2.3 m s^{-1} (Figure 27). During slack low tide, the velocity throughout the water column was downstream at 0.15 and 0 m s^{-1} , at the surface and bottom

respectively. On September 9, 2003, the maximum downstream velocity observed during ebb tide was 2.1 m s^{-1} (Figure 28). During slack low tide, the depth-averaged downstream velocity was 0.13 m s^{-1} throughout the water column. The highest depth-averaged velocity of 2.6 m s^{-1} at Transect 11 flowed upstream, following passage of the tidal bore on June 12, 2003. Comparable flow dynamics between the two surveys performed at Transect 11 suggested that causeway gate manipulation did not affect the river's velocity or flow direction at this location.

Causeway gate manipulation also did not affect the river's velocity or flow direction at Transect 1, located 34-km from the causeway. On June 13, 2003, one causeway gate was fully opened for fish passage during the first half-hour of the survey. On September 10, 2003, and September 11, 2003, no causeway gates were opened. The upstream velocity during mid-flood tide, on June 13, 2003, was 1 m s^{-1} , at 1 m depth (Figure 35). Similarly, the velocities at 1 m depth during late-flood tide on September 10, 2003, and September 11, 2003, were 0.7 and 0.8 m s^{-1} , respectively (Figures 36 and 37). During ebb tide on June 13, 2003, the maximum downstream velocity at 1 m depth was 1.4 m s^{-1} , compared to 0.9 m s^{-1} on September 11, 2003. Following passage of the tidal bore, the maximum upstream velocity at 1 m depth was 2.4 m s^{-1} and 2.1 m s^{-1} , on these dates respectively. Similar velocities and flow directions between all three surveys were observed at depth over their respective tidal periods. The slightly higher velocities observed on June 13, 2003, compared to September 10, 2003, and September 11, 2003, likely were due to the larger tidal amplitude observed during this survey.

In general, gate manipulation was observed to influence river velocity and flow direction up to 5.5-km from the causeway. During gate opened events, the river velocity within 5.5-km of the causeway was accelerated downstream during ebb tide by up to an order-of-magnitude, compared to the ebb tide velocity observed during gate closed events. In addition, the incoming flow velocity during flood tide was impeded by the downstream discharge of freshwater observed during gate opened events. At 16-km and 34-km from the causeway, however, gate manipulation was not observed to affect the river velocity or flow direction. This suggests that gate manipulation only amplifies/suppresses river velocity and alters flow direction in the upper reaches of the Petitcodiac River estuary, proximal to the causeway.

4.2 SALINITY, TEMPERATURE, AND DENSITY

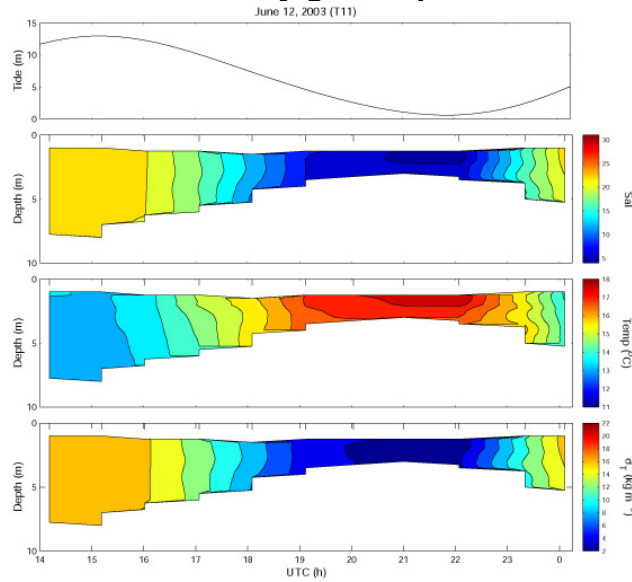
The gate manipulation has an effect on the river's salinity, temperature, and density structure up to 34-km from the causeway. At Transect 101, the causeway gate manipulation influenced the salinity, temperature, and density of the water column. In March 2002 and March 2003, the water column primarily consisted of low salinity water during both gate opened and closed events. On March 26, 2002, March 20, 2003, and May 14, 2003, causeway gates were

opened prior to CTD sampling. For these surveys, the water column consisted of low salinity water, while the maximum density associated with flood tide water was 5.9 and 3.8 kg m⁻³, on March 20, 2002, and May 14, 2003, respectively (Figures 6, 10, and 11). On March 27, 2002, and March 19, 2003, the causeway gates were closed prior to and throughout the surveys. During these surveys the water column salinity, temperature, and density remained low despite gate closure, suggesting that significant volumes of freshwater were discharged into the upper reaches of the Petitcodiac River estuary from other sources during the winter and spring season (Figures 7 and 9). Freshwater sources may include snowmelt and rainwater discharged from Petitcodiac River tributaries below the causeway, such as Hall's Creek.

On September 12, 2003, the causeway gates were closed prior to and throughout the survey. During this survey the water salinity, temperature, and density were much higher than those observed in March and May, 2002 and 2003, as the maximum density during high slack tide was 20 kg m⁻³ (Figure 12). The lower volume of freshwater in the system at Transect 101 during this survey likely reflects the late-summer season when precipitation was low. On October 9, 2003, one causeway gate was opened during the survey, reflected by the low salinity water throughout the water column during flood tide and at the surface during slack high tide (Figure 8). During this survey, however, higher salinity water associated with the flood tide was observed at depth, suggesting that gate opening during the early fall, which also is typically a dry season, does not overwhelm the upper reaches of the river estuary with freshwater throughout the entire tidal period.

On May 15, 2003, one causeway gate was opened prior to and during the survey at Transect 21. During this survey, the river consisted of low salinity, low temperature, and low density water. Similar to the gate opened surveys in March and May, 2002 and 2003, at Transect 101, the survey at Transect 21 also demonstrated that the river is dominated by freshwater, as the maximum density during slack high tide only was 7.4 kg m⁻³ (Figure 24). Many variables appear to affect the water column salinity, temperature, and density at Transect 101 and Transect 21, including the time of year, antecedent conditions preceding surveying, and the number and length of time that causeway gates were opened or closed prior to or during surveying.

Causeway gates opened



Causeway gates closed

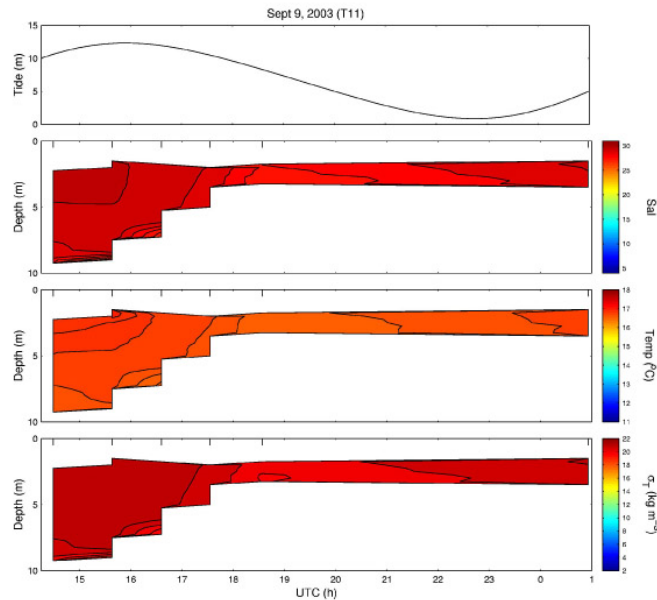


Figure 46. The effect of gate manipulation on the water column salinity, temperature, and density structure at Transect 11, located 16-km downstream of the causeway.

The surveys performed in June 2003 and September 2003 at Transect 11 and Transect 1 demonstrated that gate manipulation also affects the water column salinity, temperature, and density structure at 16-km and 34-km from the causeway, during the summer and fall seasons. At transect 11, on June 12, 2003, one causeway gate was opened for 3.5 h and was closed 30 mins. prior to the survey. During ebb tide the water column salinity and density decreased, while the temperature increased (Figure 29). This is due to warm, freshwater

discharged downstream from behind the causeway during the gate opened event prior to the survey. In contrast, two causeway gates only were partially opened for 1.5 h and closed more than 5 h prior to the survey on September 9, 2003. During this survey the water column salinity, temperature, and density did not change significantly over the tidal period (Figure 30). The effect of gate manipulation on the water column structure at Transect 11 is observed in Figure 46. Similarly, at Transect 1, on June 13, 2003, one causeway gate was opened for 0.5 h and closed 30 mins. after the survey began. During this survey the water column salinity and density slightly decreased during ebb tide, while the temperature slightly increased (Figure 38). In contrast, no causeway gates were opened prior to or during the surveys on September 10 and September 11, 2003 (Figures 39 and 40). During these surveys the water column salinity, temperature, and density did not change significantly over the tidal period, suggesting that gate opened events affect the water column structure up to 34-km from the causeway.

It has been observed that gate manipulation significantly influences the water column salinity, temperature, and density structure up to 16-km downstream of the causeway, while also influences the water column structure up to 34-km downstream of the causeway. During selected surveys an inverted salinity, temperature, and density water column structure were observed at slack tide. The likely cause of the water column inversion is high suspended sediment concentrations observed in the Petitcodiac River.

4.3 SUSPENDED SEDIMENTS

High concentrations of suspended sediments may influence water column optical and acoustical properties (Lynch et al., 1994), contaminant and nutrient fluxes (Fowler and Knauer, 1986), and alter aquatic organism community structure health (Parkhill and Gulliver, 2002). In the Petitcodiac River, high SPM concentrations were observed for most discrete samples. Calibration of the ADCP backscatter and OBS, however, was not possible due to the limited number of discrete SPM samples collected. Calibration of the ADCP backscatter and OBS instruments would permit estimation of the mass flux of sediment throughout the river estuary during entire tidal periods. For future studies in such extreme SPM environments, calibration of these instruments should be a requirement.

At Transect 101, the SPM concentration varied with causeway gate manipulation and the tide. Following gate opening there was an increase in SPM throughout the water column with passage of the freshwater wave downstream. This may in part be the result of bottom sediment resuspension, but also may result from the flushing of sediment that accumulates near the causeway gates. An increase in SPM at 0.5 m depth following gate opening was observed on October 9, 2002. Figure 20 indicates a slight increase in water level prior to the flood tide, which was associated with the downstream passage of the freshwater wave following

gate opening. At this time, the surface SPM increased to 252.4 g l^{-1} (Figure 20). Recall that flushing of accumulated mud is part of the causeway gate management strategy. Following passage of the freshwater wave on October 9, 2002, the near surface SPM rapidly decreased through time. In contrast, following passage of the tidal bore the near surface SPM only slightly increased, then decreased through time to a background concentration of order $1 - 10 \text{ g l}^{-1}$ (Figure 20). The causeway gates were still open at this time. An increase in SPM associated with gate opening also was observed on March 20, 2003, and May 14, 2003. Similarly, the surface SPM did not significantly increase following passage of the tidal bore during these surveys (Figure 20).

On March 27, 2002, March 19, 2003, and September 12, 2003, at Transect 101, the causeway gates were closed. Following passage of the tidal bore the SPM at 0.5 m depth increased from order $1 - 10 \text{ g l}^{-1}$ to order of $10 - 100 \text{ g l}^{-1}$. This suggests that when the causeway gates were opened, passage of the tidal bore does not substantially increase SPM throughout the water column, as compared to gate closed events. This may be due to the altered flow velocities at Transect 101 during gate opened events (discussed in previous section), while the discharge of lower SPM concentrated waters during gate opened events also may dilute the high SPM concentrations associated with incoming Bay of Fundy water during flood tide. At Transect 21, the SPM remained high during flood tide, on May 15, 2003, suggesting that gate opened events also affects suspended sediment dynamics associated with the tidal bore at this location (Figure 25).

At Transect 11, SPM at 0.5 m depth increased following passage of the tidal bore on June 12, 2003, while the surface SPM did not significantly increase following passage of the tidal bore on September 9, 2003. One causeway gate was opened prior to surveying on June 12, 2003, although the limited data makes difficult the ability to infer the impact of gate manipulation on tidal bore sediment resuspension at this location. For both surveys, the near surface SPM slightly increased during ebb to low tide, while SPM at 0.5 m above the bottom significantly increased during this time (Figure 33). The increased bottom SPM during ebb to low tide also was observed during surveys at Transect 1 (Figure 44). This suggests that suspended sediment at 16-km and 34-km from the causeway was not significantly impacted by causeway gate manipulation, rather were influenced by the ebb tide.

The effective, or bulk mean, clearance rate (w_e) is the settling velocity required to explain the sediment clearance rate from the water column at 0.5 m depth. The effective clearance rate of the disaggregated inorganic grain sizes (DIGS) is given by $w_e(i)$ where i represents the grain size diameter. The effective clearance rate is

$$C(t) = C_0 e^{-(w_e/h)t}, \quad (1)$$

where $C(t)$ is the observed concentration (g l^{-1}) at time t (s), C_0 is the concentration (g l^{-1}) at time $t=0$, w_e is the effective clearance rate (m s^{-1}), and h is the SPM sample depth (m). The parameters w_e and $w_e(i)$ assume that the water column is well-mixed through time. In this study, the near surface suspended sediment effective clearance rates were of order 0.1 mm s^{-1} at Transect 101, Transect 11, and Transect 1, during slack low tide when the causeway gates were closed. No SPM or DIGS data was available for Transect 21 during slack low tide. Figure 47 outlines the near surface SPM effective clearance rate observed at Transect 11 during slack low tide, on September 9, 2003.

Fine-grained sediment is that size fraction $<63 \mu\text{m}$ in diameter (McCave et al., 1995). In aquatic environments the deposition of fine-grained sediment can occur by gravitational settling of single grains or within flocs (Kranck and Milligan, 1991; Droppo and Ongley, 1994). As such, the size-dependent removal of fine-grained sediment can be explained by assuming that suspensions consist of single discrete particles and flocs (Curran et al., 2002a). Single grain settling assuming Stokes' Law results in the progressive fining of the DIGS in suspension through time, as larger grains deposit more quickly than smaller grains. In contrast, floc deposition results in the loss of all DIGS at a rate proportional to the floc settling velocity, assuming that flocs are unbiased samplers of the single grains in suspension (Kranck and Milligan, 1991). Figure 47 demonstrates that the shape of the DIGS distribution is preserved through time during slack low tide at Transect 11, which suggests that near surface sediment deposited primarily as flocs (Figure 47). The effective settling velocity of DIGS also supports floc-dominated deposition, as a $1\text{-}\mu\text{m}$ grain is observed to deposit at a rate similar to a $10\text{-}\mu\text{m}$ grain. The slight increase in the effective settling velocity of the larger single grains indicate that the relative proportion of single grain settling increases with increasing particle sizes (Figure 47).

In suspension, floc formation scales with the square of concentration, while floc breakup only scales linearly with concentration (Dyer et al., 1996; Hill, 1998; Curran et al., 2002a). In several different marine environments, flocs are observed to deposit on order of 1 mm s^{-1} (Alldredge and Gotschalk, 1989; van Leussen and Cornelisse, 1993; ten Brinke, 1994; Hill et al., 1998; Sternberg et al., 1999; Hill et al., 2000; Curran et al., 2003). In the high sediment, low energy waters of the Petitcodiac River during slack tide, it is expected that large flocs should readily form. Unfortunately, the turbid conditions of the Petitcodiac River prevented direct measurement of floc size using *in situ* cameras. Because conditions that promote large floc formation exist and the evolution in DIGS support floc-dominated deposition, it is expected that Petitcodiac River water column should clear of sediment of order 1 mm s^{-1} . The clearance rates of order 0.1 mm s^{-1} , however, raise questions over the mechanisms that influence the deposition of 1 mm s^{-1} flocs in this system.

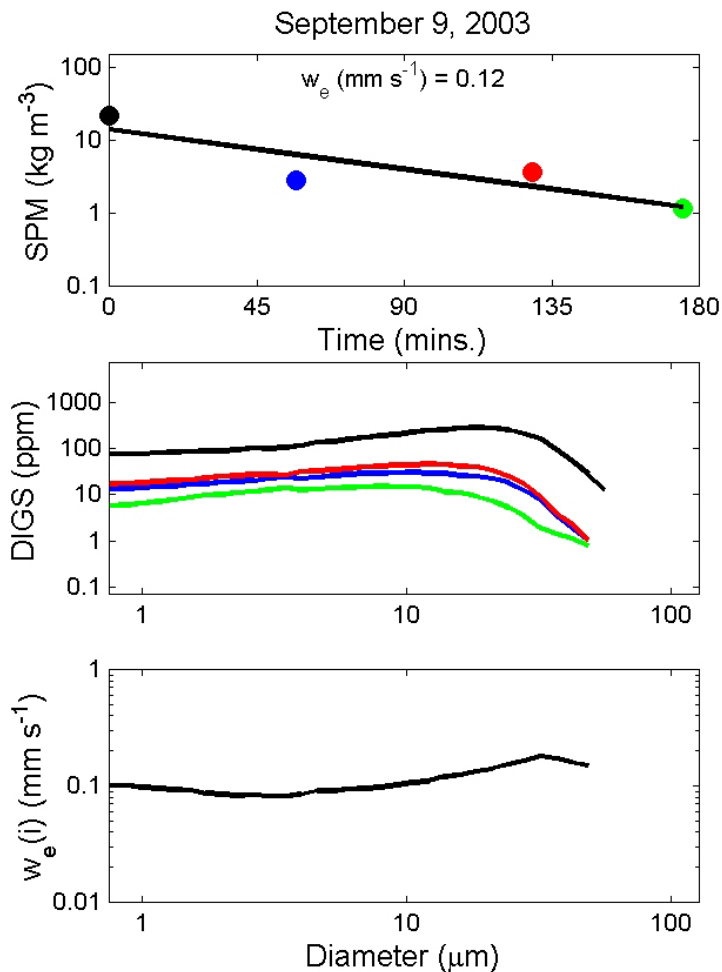


Figure 47. Suspended particulate matter concentration versus time at Transect 11. The near surface suspended SPM effective clearance rate is 0.12 mm s^{-1} , which is lower than expected for floc deposition. The preserved disaggregated inorganic grain sizes through time during slack low tide suggest that the suspended sediment is deposited primarily as flocs. This is supported by the effective clearance rate of DIGS, as a $1\text{-}\mu\text{m}$ grain deposits at a rate similar to a $10\text{-}\mu\text{m}$ grain.

If it is assumed that the Petitcodiac River suspension is fully-flocculated and consists of mature flocs but is not clearing on order of 1 mm s^{-1} , then some other mechanism may be controlling the suspended sediment clearance rate. Four alternative explanations exist (Hill et al., 2000; Curran et al. 2002b).

The first alternative explanation is that the plume is dominated by a population of small flocs that settle at rates of order 0.1 mm s^{-1} . Considering the high SPM concentrations in the Petitcodiac River, however, it is unlikely that flocs only reach small sizes during slack tide. The second alternative explanation is the resupply of sediment from elsewhere in the river (e.g. advection or bed resuspension). To understand this conceptually, consider the deposition of ten flocs from suspension. If nine of these flocs are replaced by flocs from

elsewhere in the river, the net clearance rate of flocs is perceived to be less than the actual clearance rate. This gives the impression that flocs are depositing much slower than reality. Since the measurements for clearance rate were made during slack water it is unlikely that sediment resupply from elsewhere in the river can explain the lower than expected clearance rates observed in this study. The third alternative explanation is that the suspension between the surface and 0.5 m depth is not well-mixed. If the plume were not well-mixed, however, the suspension would maintain a constant concentration at 0.5 m depth until the surface was completely devoid of sediment. This condition would not result in the exponential decay of sediment observed in Figure 47.

The fourth alternative explanation is hindered settling. Mehta (1989) indicated that at sediment concentrations of order $0.1 - 1 \text{ g l}^{-1}$, the formation of flocs accelerates the deposition of the suspension. At concentrations greater than 1 g l^{-1} , however, the clearance rate begins to decrease to order 0.1 mm s^{-1} due to inter-particle hindrance, or hindered settling. Hindered settling occurs in concentrated suspensions, as water must move upward, out of the way of depositing particles to make room for settling, thus slowing the suspension's clearance rate. At suspended concentrations greater than 10 g l^{-1} the clearance rate decreases to order 0.01 mm s^{-1} (Mehta, 1989). Since the near surface concentrations in the Petitcodiac River were typically of order $1 - 100 \text{ g l}^{-1}$, hindered settling is the likely explanation for the lower than expected clearance rates observed during slack low tide, throughout the river. The presence of apparent density inversions also supports the occurrence of hindered settling, as freshwater may be trapped within the settling suspension and is brought to the river bottom (Figure 48). Since the estimate of density only is a function of salinity and temperature, and not sediment concentration, apparent density inversions were observed (e.g. March 27, 2002, at Transect 101 – Figure 7).

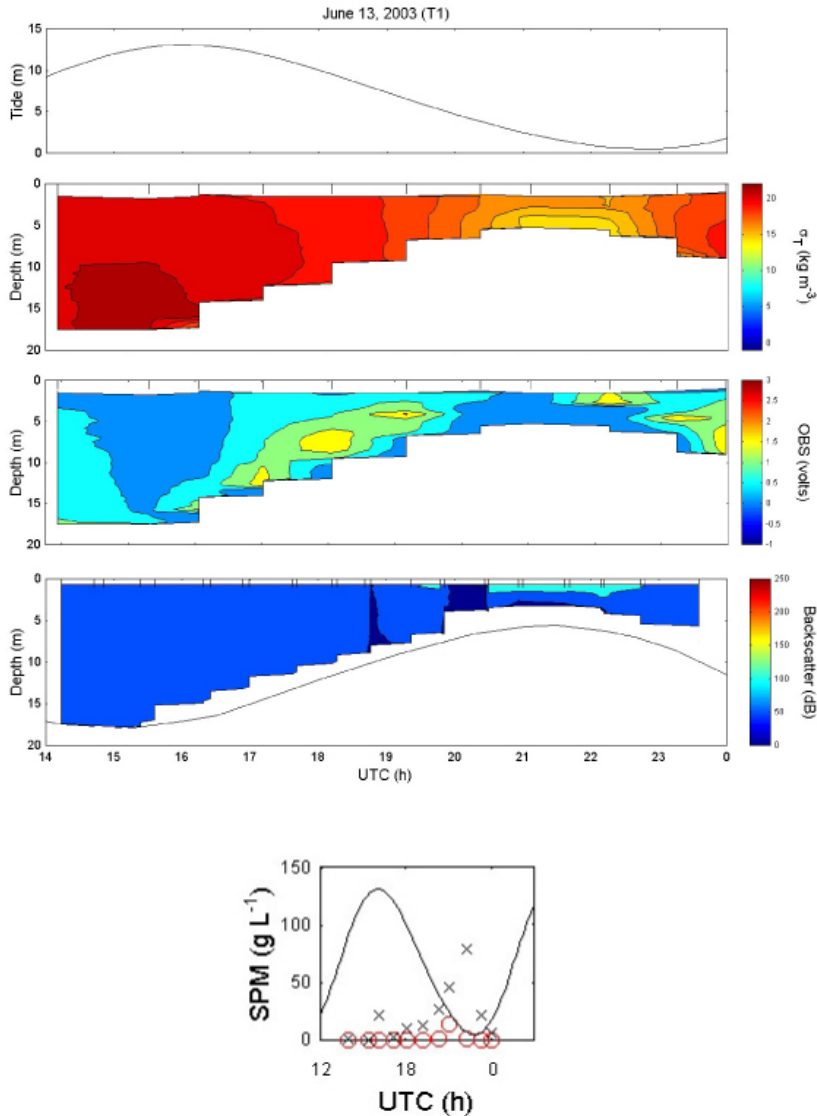


Figure 48. Density, optical backscatter, acoustical backscatter, and SPM versus time at Transect 1, June 13, 2003. The density demonstrates an inversion at low tide. The OBS demonstrates values near 0 volts at low tide, while the ADCP backscatter demonstrates decreasing values with depth at low tide and values of 0 dB at the bottom. Discrete bottom SPM concentrations at low tide are of order $10 - 100 \text{ g l}^{-1}$ (x), while discrete surface SPM concentrations are much lower (o).

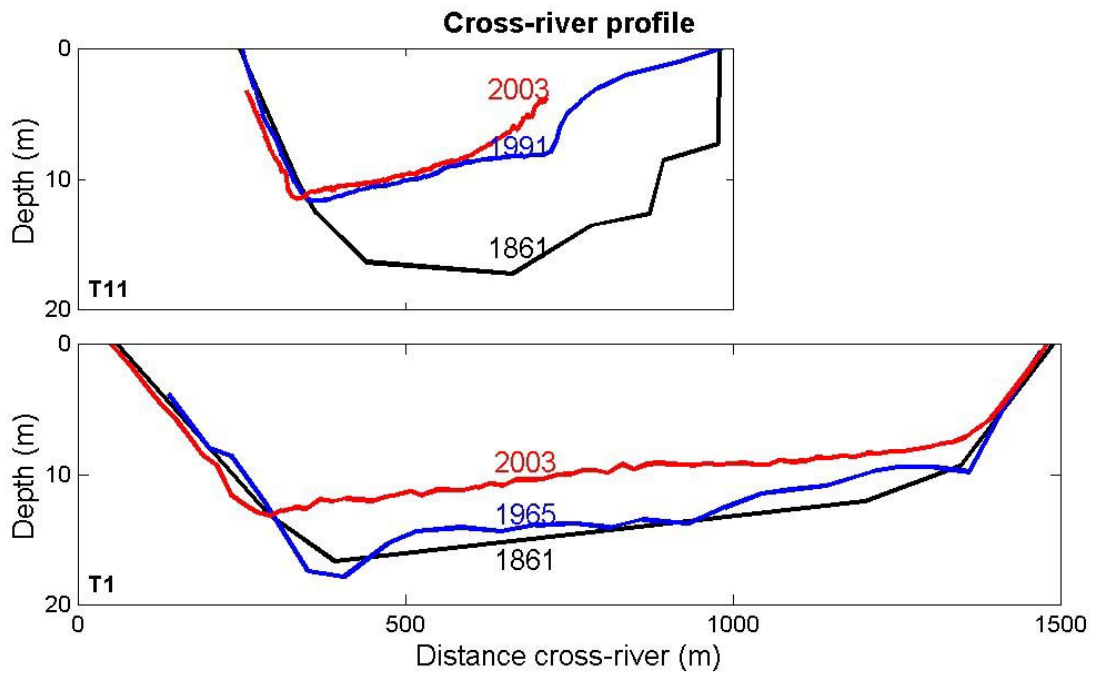
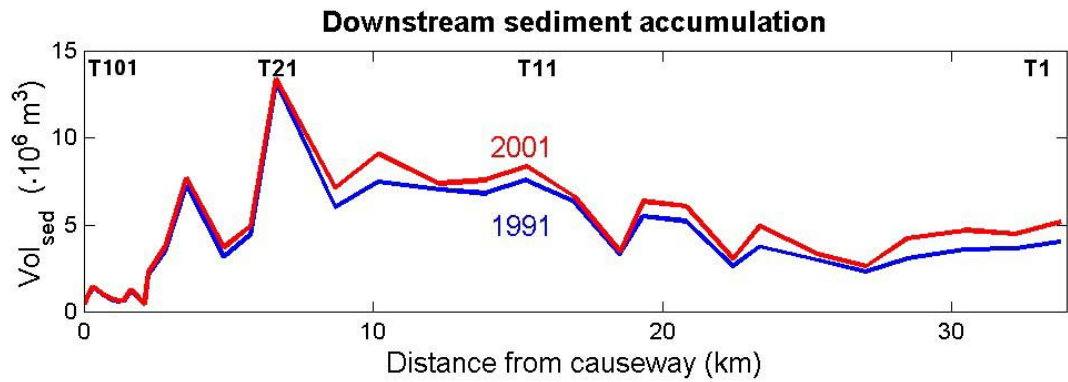
Sediment concentrations in the Petitcodiac River of order $10 - 100 \text{ g l}^{-1}$ also suggest the presence of fluid mud. Fluid mud is defined as concentrations in excess of 10 g l^{-1} (Kineke et al., 1996; Ross and Mehta, 1989). It is described as a high density layer of mud and water that exhibits low shear strengths and unintuitive behaviour (Wells, 1983). Its bulk density may be slightly higher than seawater (1030 kg m^{-3}) up to a yogurt-like consistency (1300 kg m^{-3}) (Wells, 1983). Thick layers of fluid mud were observed over the inner Amazon continental shelf, in regions of strong tidal flow and salinity fronts (Trowbridge and Kineke, 1994). Fluid mud on the Amazon continental shelf also corresponded with vertical structure inversions in salinity and temperature,

similar to those in the Petitcodiac River, which would be statically unstable in the absence of high sediment concentrations (Trowbridge and Kineke, 1994). In addition, regions of fluid mud on the Amazon continental shelf often resulted in OBS measurements approaching zero or negative values, which may explain similar observations in the Petitcodiac River (Kineke and Sternberg, 1992).

In the Petitcodiac River, it is believed that fluid mud may occur near the bottom, with the thickness of the fluid mud layer increasing towards slack low tide (Figure 48). Despite advancement in the understanding of fluid mud on the near bottom velocity field, however, several questions still remain including the affect of fluid mud on the overlying velocity, salinity, and temperature fields (Trowbridge and Kineke, 1994). As such, the presence of hindered settling, and likely fluid mud, in the Petitcodiac River requires some consideration in the prediction of river processes and flow dynamics, compared to a relatively simpler river system that would exist in the absence of such high sediment concentrations.

The source of sediment for most rivers characterized by fluid mud is the upstream watershed. In contrast, the source of sediment in the Petitcodiac River is downstream from the Upper Bay of Fundy. Typically, the locus of fluid muds changes rapidly in space and time, as suspended sediment and river processes change (Wells, 1983). In the Petitcodiac River, the presence of fluid mud and a prograding wedge of bottom sediment downstream of the causeway, reflect the dynamic nature of the river system. Figure 49 demonstrates the continued accumulation of sediment in the Petitcodiac River since construction of the causeway. Despite the rapid in-fill of sediment that coincided with causeway construction in the upper reaches of the estuary (Bray et al., 1982; Galay, 1983), sediment continues to accumulate in the Petitcodiac River up to 34-km downstream of the causeway (Figure 49). This indicates that the sediment dynamics in the Petitcodiac River still have not reached equilibrium despite completion of the causeway more than 3 decades ago. Thus, potential impacts caused by the accumulation of sediment remain uncertain, and the downstream extent of the prograding sediment wedge remains unknown.

Although the impacts of the causeway are not fully-understood, it is clear from the results of this study that causeway gate manipulation affects the Petitcodiac River hydrodynamics and suspended sediment properties up to 34-km from the causeway. Considering the sedimentary conditions of the river system still are not in equilibrium, the long-term effects of the causeway on the river system remain uncertain.



Data courtesy of GEMTEC Limited, Fredericton, New Brunswick

Figure 49. Downstream and cross-sectional surveys demonstrate on-going accumulation of sediment up to 34-km from the causeway and indicate that the sediment wedge is prograding downstream towards the Bay of Fundy. This suggests that the Petitcodiac River has not reached sediment accumulation equilibrium.

4.4 WATER QUALITY

In the Petitcodiac River during the field surveys, ammonia concentrations at Transect 101 increased following passage of the tidal bore and during flood tide, suggesting that the source of ammonia is downstream of the Gunningsville Bridge. The effect of gate manipulation on ammonia concentrations is best demonstrated on March 20, 2003, where the ammonia concentration dramatically decreased during gate opening at 1326 - 1453 h, then subsequently increased following gate closure then passage of the tidal bore. They data suggest that gate opened events may dilute elevated ammonia concentrations downstream of the causeway.

At Transect 101, the average dissolved oxygen concentrations for the survey on September 12, 2003, was 2.4 ml l^{-1} (Figure 19). The low dissolved oxygen concentrations observed during this survey were correlated with suspended solid concentrations at 0.5 m depth of order $10 - 100 \text{ g l}^{-1}$ (Figure 20). During other surveys performed at Transect 101, the dissolved oxygen concentrations were high when the suspended solid concentrations were of order $0.1 - 1 \text{ g l}^{-1}$. Low dissolved oxygen concentrations were not observed on May 15, 2003, at Transect 21 (Figure 24).

Low dissolved oxygen concentrations also were observed at Transect 11 and Transect 1 in June 2003 and September 2003, during ebb and low tide. At Transect 11, the depth-averaged dissolved oxygen concentration decreased to 3.6 and 3.4 ml l^{-1} at low tide, on June 12, 2003, and September 9, 2003, respectively (Figures 31 and 32). The near bottom dissolved oxygen concentrations on these days were 2.8 and 3.2 ml l^{-1} , respectively. The low dissolved oxygen concentrations during these surveys were correlated with near bottom sediment concentrations of order $10 - 100 \text{ g l}^{-1}$ (Figure 33). Similar observations were made at Transect 1 in June 2003 and September 2003. During these surveys the dissolved oxygen concentration also decreased during ebb to low tide. The low dissolved oxygen concentrations again were correlated with near bottom suspended sediment concentrations of order 10 g l^{-1} (Figure 44). Typically, the lowest dissolved oxygen concentrations were correlated with the highest suspended sediment concentrations. Dissolved oxygen concentrations, however, also may vary with water temperature, as warmer waters in summer and fall have a lower oxygen carrying-capacity. Because the temperature during these surveys did not vary significantly when low dissolved oxygen was observed, it is believed that low dissolved oxygen concentrations in the Petitcodiac River may be due to increased sediment from bed resuspension and not a change in the oxygen carrying-capacity due to water temperature fluctuations.

The relationship between decreased dissolved oxygen concentrations and increased suspended solid concentrations due to bed resuspension has been observed in other aquatic environments. Irvine et al. (1997) observed that

increased turbidity due to bed resuspension caused by ship passage in shallow regions of Hamilton Harbour, Ontario, created an oxygen demand that reduced the dissolved oxygen in the water column. It has been suggested that dissolved oxygen concentrations in the water column decrease due to increased organic material associated with suspended bed sediments, which require oxygen for decomposition (Barton and Taylor, 1996). The potential effects of highly concentrated sediment resuspension on dissolved oxygen, particularly in the context of sediment resuspension should be considered in the Petitcodiac River management strategy.

5.0 CONCLUSIONS

The primary goal of this study was to address “the enormous deficiency in very basic information [that] exists [for the Petitcodiac River]”, identified at the Petitcodiac River/Estuary Modelling Workshop held in March 2002. The objectives of the study were to: 1) test instrumentation and develop sampling strategies for data collection in the unique conditions found within the Petitcodiac River System; 2) provide data in support of predictive modelling studies being conducted by proponents as part of the EIA; and 3) provide data that would permit the conclusions of the EIA to be evaluated by Fisheries and Oceans Canada in a scientifically-defensible manner. First, the 13 field surveys performed during 2002 – 2003 permitted refinement of sampling techniques that can be used to observe complex systems such as the Petitcodiac River, while techniques also can be applied to similar environments such as the Avon River in Nova Scotia, Canada. Second, data that was collected during this study was forwarded to the EIA proponent in a digital format suitable to their needs, in a timely manner. Last, the data that was collected will permit DFO to undertake a more informed review of the EIA.

The data acquired during this study, however, does not provide a detailed analysis of river processes at a specified location rather they provide an overview of river processes that reflect conditions throughout the Petitcodiac River under different causeway gate operations, tidal conditions, and seasons. In this study, it was observed that causeway gate manipulation affects the river velocity and flow direction up to 5-km from the causeway, while salinity and temperature effects were observed up to 34-km from the causeway. Together these may alter the flow conditions and magnitude of the saltwater intrusion on a daily basis. In addition, elevated ammonia concentrations and low dissolved oxygen concentrations in the presence of high suspended sediment concentrations also was observed.

The high concentrations of sediment in the Petitcodiac River result in physical processes such as hindered settling and may support fluid mud. The apparent density inversions, low clearance rates, and anomalous behaviour of the optical and acoustical backscatter instruments reflect the extreme conditions of the Petitcodiac River, which suggests that consideration of these properties is

required in attempts to predict the river's dynamics. Last, the presence of the sediment prograding wedge indicates that the river system has not reached equilibrium even 36 years after causeway construction. Although deposition of large amounts of sediment have been observed up to 34-km from the causeway, the distal extent of the sediment prograding wedge remains unknown, as does the affects this may have on downstream river processes.

ACKNOWLEDGEMENTS

Sincere appreciation to Hughes Surveying, Saint John, New Brunswick, GEMTEC Limited, Fredericton, New Brunswick, and Environment Canada, Atlantic Region, for their support with field initiatives and their contribution of data to this study. Special thanks also to Paul MacPherson (Particle Dynamics Laboratory, BIO) and Carol Anstey (Nutrients Laboratory, BIO) for providing support with sample analysis and to Ole Mikkelsen (Particle Dynamics Laboratory, BIO) for a very helpful review of this technical report.

BIBLIOGRAPHY

Allredge, A.L. and Gotschalk, C.C. 1989. Direct observations of the mass flocculation of diatom blooms: characteristics, settling velocities and formation of diatom aggregates. *Deep-Sea Research*. 36:159-171.

Armstrong, F.A.J., Sterns, C.R., and Strickland, J.D.H. 1967. The measurement of upwelling and subsequent biological processes by means of the Technicon AutoAnalyzer and associated equipment. *Deep-Sea Research*. 14:381-389.

Barton, B.A. and Taylor, B.R. 1996. Oxygen requirements of fishes in northern Alberta rivers with a general review of the adverse effects of low dissolved oxygen. *Water Quality Research Journal of Canada*. 31:361-409.

Bray, D.I., DeMerchant, D.P., and Sullivan, D.L. 1982. Some hydrotechnical problems related to the construction of a causeway in the estuary of the Petitcodiac River, New Brunswick. *Canadian Journal of Civil Engineering*. 9:296-312.

Butler, R.L. 1969. 1968 Petitcodiac River Estuary Causeway, Dam, Fishway. Unpublished report to the Regional Director, Department of Fisheries. 4pp. In Locke, A. and Bernier, R. 2000. Annotated Bibliography of Aquatic Biology and Habitat of the Petitcodiac River system, New Brunswick. Canadian Manuscript Report of Fisheries and Aquatic Sciences No. 2518, Fisheries and Oceans Canada, Moncton, New Brunswick. 162pp.

Curran, K.J., Hill, P.S., and Milligan, T.G. 2002a. The role of particle aggregation in size-dependent deposition of drill mud. *Continental Shelf Research*. 22:405-416.

Curran, K.J., Hill, P.S., and Milligan, T.G. 2002b. Fine-grained suspended sediment dynamics in the Eel River flood plume. *Continental Shelf Research*. 22:2537-2550.

Curran, K.J., Hill, P.S., and Milligan, T.G. 2003. Time variation of floc properties in a settling column. *Journal of Sea Research*. 49:1-9.

Droppo, I.G. and Ongley, E.D. 1994. Flocculation of suspended sediment in rivers of Southeastern Canada. *Water Research*. 28:1799-1809.

Dyer, K.R., Cornelisse, J., Dearnaley, M.P., Fennessy, M.J., Jones, S.E., Kappenberg, J., McCave, I.N., Pejrup, M., Puls, W., van Leussen, W., and Wolfstein, K. 1996. A comparison of in situ techniques for estuarine floc settling velocity measurements. *Journal of Sea Research*. 36:15-29.

Fowler, S.W. and Knauer, G.A. 1986. Role of large particles in the transport of elements and organic compounds through the oceanic water column. *Progress in Oceanography*. 16:147-194.

Galay, V.J. 1983. Some hydrotechnical problems related to the construction of a causeway in the estuary of the Petitcodiac River, New Brunswick: Discussion. *Canadian Journal of Civil Engineering*. 10:169-170.

Grasshoff, K. 1969. Technicon International Congress, June 1969.

Hill, P.S., Syvitski, J.P.M., Cowan, E.A., and Powell, R.D. 1998. In situ observations of floc settling velocities in Glacier Bay, Alaska. *Marine Geology*. 145:85-94.

Hill, P.S., Milligan, T.G., and Geyer, W.R. 2000. Controls on effective settling velocity of suspended sediment in the Eel River flood plume. *Continental Shelf Research*. 20:2095-2111.

Irvine, K.N., Droppo, I.G., Murphy, T.P., and Lawson, A. 1997. Sediment resuspension and dissolved oxygen levels with ship traffic: implications for habitat remediation. *Canadian Water Quality Research Journal of Canada*. 32:421-437.

K erouel, R. and Aminot, A. 1997. Fluorometric determination of ammonia in sea and estuarine waters directed by segmented flow analysis. *Marine Chemistry*. 57:265-275.

Kineke, G.C. and Sternberg, R.W. 1992. Measurements of high concentration suspended sediments using the optical backscatterance sensor. *Marine Geology*. 108:253-258.

Kineke, G.C., Sternberg, R.W., Trowbridge, J.H., and Geyer, W.R. 1996. Fluid-mud processes on the Amazon continental shelf. *Continental Shelf Research*. 16:667-696.

Kranck, K. and Milligan, T.G. 1991. Grain size in oceanography. In Principles, Methods, and Applications of Particle Size Analyzers, Syvitski, J.P.M. (ed.). Cambridge University Press: New York. 332-345.

Kranck, K. and Milligan, T.G. 1992. Characteristics of suspended particles at an 11-hour anchor station in San Francisco Bay, California. *Journal of Geophysical Research*. 97:11373-11382.

Locke, A., Hanson, M.J., Klassen, G.J., Richardson, S.M., and Aub e, I.C. 2003. The damming of the Petitcodiac River: Species, populations, and habitat loss. *Northeastern Naturalist*. 10:39-54.

- Lynch, J.F., Irish, J.D., Sherwood, C.R., and Agrawal, Y.C. 1994. Determining suspended sediment particle size information from acoustical and optical backscatter measurements. *Continental Shelf Research*. 14:1139-1166.
- McCave, I.N., Manighetti, B., and Robinson, S.G. 1995. Sortable silt and fine sediment size/composition: parameters for paleocurrent speed and paleoceanography. *Paleoceanography*. 10:593-610.
- Mehta, A.J. 1989. On estuarine cohesive sediment suspension behavior. *Journal of Geophysical Research*. 94:14303-14314.
- Milligan, T.G. and Kranck, K. 1991. Electro-resistance particle size analyzers. In Principles, Methods, and Applications of Particle Size Analyzers, Syvitski, J.P.M. (ed.). Cambridge University Press: New York. 109-118.
- Murphy, J. and Riley, J.P. 1962. A modified single solution method for the determination of phosphate in natural waters. *Analytica Chimica Acta*. 27:30.
- New Brunswick Department of Supply and Services. 2002. Petitcodiac River/Estuary Modelling Workshop Summary of a workshop held in Moncton, New Brunswick, Canada March 3 to 5, 2002. LeBlanc, C., Bliss, D., and Burrell, B. (eds.). <<http://www.petitcodiac.com/model-e.html>> (cited 7 January 2004).
- Parkhill, K.L. and Gulliver, J.S. 2002. Effect of inorganic sediment on whole-stream productivity. *Hydrobiologia*. 472:5-17.
- Richardson, S.M., Hanson, M.J., and Locke, A. 2002. Effects of impoundment and water-level fluctuations on macrophyte and macroinvertebrate communities of a dammed tidal river. *Aquatic Ecology*. 36:493-510.
- Ross, M.A. and Mehta, A. 1989. On the mechanics of lutoclines and fluid mud. *Journal of Coastal Research*, special issue. 5:51-61.
- Schell, T.M. 1998. Compilation of suspended particulate matter (SPM) recorded in the Shepody Bay/Petitcodiac River System. Canadian Technical Report of Fisheries and Aquatic Sciences No. 2246, Fisheries and Oceans Canada, Dartmouth, Nova Scotia. 29pp.
- Sheldon, R.W. 1972. Size separation of marine seston by membrane and glass-fibre filters. *Limnology and Oceanography*. 17:494-498
- Sternberg, R.W., Berhane, I., and Ogston, A.S. 1999. Measurement of size and settling velocity of suspended aggregates on the northern California continental shelf. *Marine Geology*. 154:43-54.

Strickland, J.D.H. and Parsons, T.R. 1972. A practical handbook of seawater analysis. Fisheries Research Board of Canada Bulletin 167 (2nd edition): Ottawa. 310pp.

ten Brinke, W.B.M. 1994. Settling velocity of mud aggregates in the Oosterschelde tidal basin (the Netherlands), determined by a submersible video system. *Estuarine Coastal and Shelf Science*. 39:549-564.

Traykovski, P., Geyer, R.W., Irish, J.D., and Lynch, J.F. 2000. The role of wave-induced density-driven fluid mud flows for cross-shelf transport on the Eel River continental shelf. *Continental Shelf Research*. 20:2113-2140.

Trowbridge, J.H. and Kineke, G.C. 1994. Structure and dynamics of fluid muds on the Amazon continental shelf. *Journal of Geophysical Research*. 99:865-874

van Leussen, W. and Cornelisse, J.M. 1993. The role of large aggregates in estuarine fine-grained sediment dynamics. In *Nearshore and Estuarine Cohesive Sediment Transport*. Mehta, A.J. (ed.). American Geophysical Union, Washington, D.C. 75-91.

Wells, J.T. 1983. Dynamics of coastal fluid mud in low, moderate, and high-tide range environments. *Canadian Journal of Fisheries and Aquatic Sciences*, supplement (Proceedings of the Symposium on the Dynamics of Turbid Coastal Environments). 40:130-142.

Wells, P.G. 1999. Environmental Impacts of Barriers on Rivers Entering the Bay of Fundy: Report on an ad-hoc Environment Canada Working Group Technical Report Series No. 334, Canadian Wildlife Service, Environment Canada, Ottawa, Ontario. 43pp.

ADDITIONAL REFERENCES

Conservation Council of New Brunswick. 1999. Tidal barriers in the inner Bay of Fundy: ecosystem impacts and restoration opportunities. Percy, J. and Harvey, J. (eds.). Proceedings of a Workshop, April 14th and 15th, 1999, Moncton, NB. 133pp.

Environmental Monitoring Working Group. 1998. Petitcodiac River trial gate opening project: environmental monitoring of the Petitcodiac River system 1997. Moncton, New Brunswick.

Environmental Monitoring Working Group. 1999. Petitcodiac River trial gate opening project: environmental monitoring of the Petitcodiac River system 1998. Moncton, New Brunswick.

Locke, A. and Bernier, R. 2000. Annotated bibliography of aquatic biology and habitat of the Petitcodiac River system, New Brunswick. Canadian Manuscript Report of Fisheries and Aquatic Sciences, No. 2246, Fisheries and Oceans Canada, Dartmouth, Nova Scotia. 162pp.

Locke, A. 2001. Annotated bibliography of aquatic biology and habitat of the Petitcodiac River system, New Brunswick, Part 2. Canadian Manuscript Report of Fisheries and Aquatic Sciences, No. 2561, Fisheries and Oceans Canada, Dartmouth, Nova Scotia. 62pp.